THE SYNTHESIS AND PROPERTIES OF SELECTED TRANSITION METAL-PYRAZOLE COMPLEXES AND THEIR APPLICATION TOWARDS HOMOGENEOUS CATALYSIS

WYNNE EVANS, B. Sc., A. R. C. S.

A THESIS SUBMITTED TO THE COUNCIL FOR NATIONAL ACADEMIC AWARDS

FOR THE DEGREE OF DOCTOR OF PHILOSOPHY

DEPARTMENT OF SCIENCE AND CHEMICAL ENGINEERING

THE POLYTECHNIC OF WALES

JUNE 1991

ABSTRACT

The literature shows that μ^2-pyrazolyl bridged complexes may find useful application in the field of homogeneous catalysis. Metal-containing, chelating ligands can theoretically be generated by deprotonation of transition metal complexes containing η^1-pyrazole ligands. Reaction of such species with other metal complexes containing labile groups, should provide a route to the synthesis of homobimetallic or heterobimetallic complexes containing the bridging ligand.

This study describes the preparation of Ni(II) and Ru(II) pyrazole and 3,5-dimethyl pyrazole complexes by reaction of the pyrazoles with $NiCl_2(PPh_3)_2$ and $RuCl_2(PPh_3)_3$ respectively. The reactions of the same pyrazoles with $RuBr_2(PPh_3)_3$ and $[RuI_2(PPh_3)_2]_n$, have also been investigated. The preparations have yielded new Ru(II) pyrazole complexes and although the Ni(II) pyrazole products have been previously reported, the synthetic routes used are "clean" and novel. An explanation for the observed preferential coordination of pyrazole over phosphine in Ni(II) complexes is offered in terms of "Pearson's Principle". The reactivity of the resulting Ni(II) and Ru(II) pyrazole complexes towards bases, specifically; triethylamine, potassium hydroxide and 1,8-bis(dimethylamino)napthalene, has also been explored. Whilst deprotonation of a Ni(II) pyrazole complex, trans-$[NiCl_2(pzH)_4]$, has been found to result in the polymeric $[Ni(pz)_2.H_2O]_n$, deprotonation of the analogous 3,5-dimethylpyrazole Ni(II) complex, has not been effected. An explanation is offered for this which involves the pK_a's of the coordinated pyrazoles. Deprotonation of trans-$[RuCl_2(PPh_3)_2(pzH)_2].\frac{1}{2}C_6H_{14}$, using triethylamine or potassium hydroxide has only been achieved in the presence of water and air. The product of this reaction has been proposed to contain both μ^2-pyrazolyl and μ^2-oxo ligands. In the absence of air, reaction of $[RuCl_2(PPh_3)_2(pzH)_2].\frac{1}{2}C_6H_{14}$ with triethylamine in methanol, has been shown to yield trans-$[RuH(CO)(PPh_3)_2(pzH)(MeOH)]$.

In order to ascertain the ability of the Ru(II) pyrazole complexes to undergo reactions associated with the steps involved in a homogeneous catalytic cycle, the reactions of $[RuCl_2(PPh_3)_2(pzH)_2].\frac{1}{2}C_6H_{14}$ with O_2, H_2, MeI, CO and I_2 have been investigated and the products of those reactions characterized as far as possible.

Attempts to generate heterobimetallic complexes containing palladium and the μ^2-pyrazolyl ligand have been made by reacting the complex $[Pd(pz)_2(dppe)]$ with $NiCl_2(PPh_3)_2$ and $RuCl_2(PPh_3)_3$. Preliminary experiments indicate that the latter reaction may produce a Ru(II)-Pd(II) complex. The catalytic activity of this species towards the homogeneous hydrogenation of alk-1-enes has been investigated, using gas chromatography.

The techniques used to characterize complexes include; elemental analysis, infra-red and ^1H, ^{31}P nmr spectroscopy, uv/vis spectroscopy and measurement of magnetic moments. The account also includes descriptions of experimental techniques invoked during the handling of air sensitive materials.

DECLARATION

This thesis has not been nor is being currently submitted for the award of any other degree or similar qualification.

E. W. Evans

E. W. Evans

ACKNOWLEDGEMENTS

I would like to thank my Director of Studies, Dr. M. T. Atlay for his assistance and time, particularly since most of this work was carried out in the evenings. I would also like to extend my thanks to all the staff in the Department, both technical and academic, for their assistance during my studies.

DEDICATION

To Alan

ABBREVIATIONS AND SYMBOLS

Å	angstrom
acac	acetylacetonate ion
az	azolate
BM	Bohr magneton
bpy	2,2′-bipyridine
br.	broad
Bu^t	tertiary butyl group
1,5-COD	cycloocta-1,5-diene
DMAD	dimethylethyne dicarboxylate
DMF	dimethylformamide
$DMpz^-$	3,5-dimethylpyrazolide ion
DMpzH	3,5-dimethylpyrazole
dpae	1,2-bis(diphenylarsino)ethane
dppe	1,2-bis(diphenylphosphino)ethane
Et	ethyl group
fpz^-	3,5-bis(trifluoromethyl)pyrazolide ion
fpzH	3,5-bis(trifluoromethyl)pyrazole
hv	visible irradiation
I.R.	infra-red active
M	metal
m	medium
Me	methyl group
MPL	methyl propiolate
nmr	nuclear magnetic resonance
O_h	octahedral

Ph	phenyl group
py	pyridine
pz^-	pyrazolide
pzH	pyrazole
R	Raman active
s	strong
sal_2enH	N N′-ethenebis(salicylideneimine)
tbp	trigonal-bipyramid
tfb	tetrafluorobenzobarrelene
THF	tetrahydrofuran
TMS	tetramethylsilane
tos	toluenesulphonic acid ion
uv	ultraviolet irradiation
w	weak
ϵ	molar absorbance ($dm^3\ mol^{-1}\ cm^{-1}$)
Π	Π molecular orbital
Π^*	antibonding Π molecular orbital
σ	σ molecular orbital
μ^2	bridging notation; ligand bridges two metal atoms
η^3	hapticity notation; three ligand atoms bonded to metal atom
*	footnote
[2.1]	cross referencing; figure in brackets denotes section

CONTENTS

NAMES OF COMPLEXES

$RuCl_2(PPh_3)_2(pzH)_2]$
Dichlorodipyrazolebis(triphenylphosphine)ruthenium(II)

$[RuCl_2(PPh_3)_2(DMpzH)]$
Dichloro-(3,5-dimethylpyrazole)bis(triphenylphosphine)ruthenium(II)

$[RuBr_2(PPh_3)_2(pzH)_2]$
Dibromodipyrazolebis(triphenylphosphine)ruthenium(II)

$[RuBr_2(PPh_3)_2(DMpzH)]$
Dibromo-(3,5-dimethylpyrazole)bis(triphenylphosphine)ruthenium(II)

$[RuI_2(PPh_3)_2]_n$
Diiodobis(triphenylphosphine)ruthenium(II) polymer

$[RuI_2(PPh_3)_2(DMpzH)]$
Diiodo-(3,5-dimethylpyrazole)bis(triphenylphosphine)ruthenium(II)

$[RuCl_2(PPh_3)_2(pzH)(CO)]$
Carbonyldichloro(pyrazole)bis(triphenylphosphine)ruthenium(II)

OBJECTIVE

OBJECTIVE

In recent years, attention has been focussed on the use of transition metal complexes as homogeneous catalysts. The advantage of such systems lies in their greater selectivity and the less forcing conditions that they require. These metal complexes can contain a variety of organic ligands and have been used in industry for many organic reactions including: carbonylations, oxygenations, hydrogenations and hydroformylations.

Metal complexes with two metal centres which are held in close proximity by the geometry of the bridging ligand(s), whilst having the advantages of homogeneous catalysts, would closely mimic the situation believed to occur in heterogeneous catalysis on metal surfaces, an industrially more important process. Published work has shown that transition metal complexes containing one or two pyrazole ligands can be used to synthesize homobimetallic, or much more rarely, heterobimetallic compounds containing exobidentate bridging pyrazole ligands. The apparent capacity of the pyrazolyl ligand to bridge a relatively wide range of intermetallic separations and to absorb changes in geometry arising from oxidative-addition and related reactions, indicates these complexes may act as homogeneous catalysts. In particular, the preparation of heterobimetallic complexes with metals coordinated to different ligands, having different coordination numbers and with different redox potentials, would lead to systems with enormous potential for study.

This project was broadly divided into three parts. In the first part, attempts were made to synthesize and fully characterize monometallic novel Ni(II) and Ru(II) pyrazole and 3,5-dimethylpyrazole complexes.

Characterization was effected using analytical, magnetic and spectroscopic techniques. These complexes were then reacted with base in an attempt to generate potential metal-containing ligands with pyrazolide groups. The feasibility of reacting such ligands with other complexes containing labile groups in suitable positions, in order to generate homobimetallic or heterobimetallic species, was explored. A Pd(II)/pyrazolide ligand, which has been previously reported in the literature, was also used for this purpose.

The second part of the research project, was devoted to the study of novel complexes that had been prepared. Their reactivity towards small molecules such as CO, H_2, I_2, O_2 and MeI was investigated in order to assess their ability to undergo oxidative-addition reactions and related processes associated with the typical reactions undergone in a homogeneous catalytic cycle. Again, attempts were made to fully characterize the products of the reactions. As far as possible, the reasons for existence of all novel complexes prepared, were rationalized in terms of known bonding theory.

Finally, preliminary investigations were carried out as to whether selected complexes displayed any catalytic activity; specifically towards the homogeneous hydrogenation of alk-1-enes.

SECTION ONE-INTRODUCTION

1.1 HOMOGENEOUS CATALYSIS

Heterogeneous catalysis has been used by the chemical industry for some time. Typically, the catalyst is present in the solid state, reactants are in the gaseous state and the catalysed reaction takes place at the phase interface. Homogeneous catalysis, in which reactions occur in solution, has been the subject of more recent attention[1]. Here, the catalyst takes part in the reaction by being converted into an intermediate compound, which is subsequently reconverted into the original substance.

Homogeneous catalysts can have several advantages over heterogeneous catalysts, in that, they generally operate under much milder conditions of temperature and pressure, give higher selectivity and can be made with definite stoichiometry and structure which can be reproduced and modified as required. These attributes are especially welcome at a time when the chemical industry and society in general, are seeking ways to conserve energy and make the best use of available resources. The solid state or bulk nature of a heterogeneous catalyst system, however, gives it certain advantages over its homogeneous counterpart; separation from the reaction products is easier (assuming these are either liquids or gases) and regeneration of the catalyst can often be accomplished by burning off reaction by-products from the surface. In homogeneous catalyst systems, side reactions decrease the concentration of the active species, so that at some stage it is necessary to resynthesize this species. Generally, this cannot be done "in situ" and is frequently an expensive process.

In a reaction involving a homogeneous catalyst, the mechanism whereby substrates are converted to products and the catalyst is reformed is

known as a catalytic cycle. Because the reaction occurs in solution and involves discrete metal complexes, it can be studied using appropriate spectroscopic techniques. Study of homogeneous catalysis is easier and can be interpreted with less ambiguity than that for heterogeneous catalysis.

Transition metal complexes are well suited to act as homogeneous catalysts in that they can form stable complexes in which the metal centres can exist in different oxidation states and with different coordination numbers. This property can facilitate the coordination of unsaturated molecules to metal centres. The molecules then combine with each other or with other reagents (also coordinated to a metal centre) in specific ways. The product is then eliminated from the complex.

Ligands on the transition metal catalyst can be "participative" or "non-participative". Participative ligands such as alkenes, alkyl, carbonyl or hydride groups, are able to take an active part in the catalytic cycle in the sense that they end up in the product of the cycle e.g. hydride and alkene in a catalytic hydrogenation sequence. Non-participative ligands remain associated with the metal and do not appear as part of the product(s) of the reaction. However, they may play a vital part in determining the activity and selectivity of the catalyst system. Moreover, bridging ligands which can hold two metal centres in close proximity, whilst having the advantages associated with homogeneous catalysts already mentioned, also closely mimic the situation that is believed to occur in heterogeneous catalysis[2] i.e. adsorption, reaction and desorption. The knowledge that may be gained from such dimeric complexes may be ultimately translated into the context of larger aggregates of metal atoms.

1.2 CATALYTIC CYCLES INVOLVING TRANSITION METAL COMPLEXES

The catalytic cycles that describe transition metal catalysed homogeneous reactions contain a number of definite steps that are summarized below: -

(1) Coordination at a vacant site is a vital component of homogeneous catalytic cycles. Therefore, an important property of a homogeneous catalyst is its ability to provide vacant sites. The maximum number of ligands that may be accommodated at a metal centre, can be calculated using the empirical eighteen electron rule which indicates that the presence of eighteen electrons in the valence shells of a transition metal complex confers stability upon that complex. Thus, if an unidentate ligand acts as a two electron donor, the maximum coordination number of a d^n ion = (18-n)/2.

(n = number of electrons present in the d orbitals of the metal ion)

The maximum coordination numbers of some Group VIII metal ions are shown below.

d^n	MAXIMUM COORDINATION NO.	EXAMPLES OF d^n IONS
d^6	6	Ru(II), Os(II), Rh(III),Ir(III) Pt(IV), Pd(IV)
d^8	5	Rh(I), Ir(I), Pd(II),Pt(II)
d^{10}	4	Pd(0), Pt(0)

Table 1 Maximum Coordination Numbers of Group VIII metal Ions

(2) The dissociation or association of a ligand may occur e.g. in the catalysed hydrogenation of alkenes, the following equation represents part of the catalytic cycle:-

$$[RuCl(H)(PPh_3)_3] + \text{alkene} = [RuClH(\text{alkene})(PPh_3)_2] + PPh_3$$

(3) Oxidative-addition and reductive-elimination reactions are often important steps in the catalytic cycle. For oxidative-addition at a single metal centre, the reaction may be written as in fig. 1.

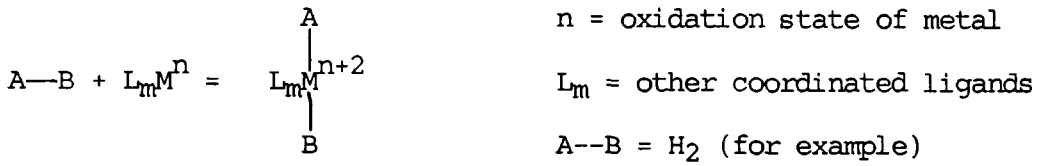

fig. 1

In order to be able to undergo oxidative-addition, the metal must have two stable oxidation states separated by two units. The lower oxidation state should normally exhibit a lower coordination number than the higher oxidation state and should preferably be coordinatively unsaturated. The reverse of oxidative-addition is reductive-elimination, as shown by the equation in fig. 2.

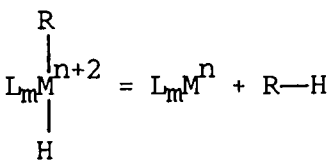

fig. 2

From table 1, octahedral d^6 species are likely candidates for reductive-elimination to form species with lower coordination numbers and lower oxidation states, whilst the best choices for oxidative-addition are four and five coordinate d^8 species. In a situation where the catalyst contains two metal centres held together by a bridging ligand, the metals each need to have two stable oxidation states separated by one unit and need to be able to increase their coordination number by one (fig. 3).

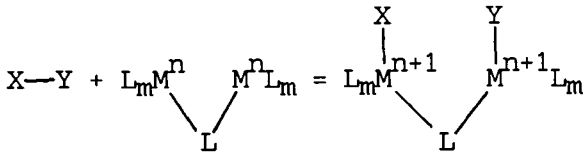

fig. 3 Oxidative-addition of X--Y to a bridged bimetallic complex

Oxidative-addition and reductive-elimination very closely parallel the adsorption of molecules on to solid surfaces and their subsequent desorption.

Other steps in the catalytic cycle may include one or more of the following: -

(4) Ligand combination reactions (insertion reactions), which occur when two groups coordinated to the same metal atom combine (fig. 4).

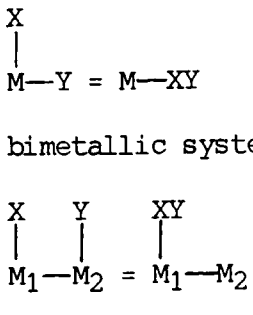

fig. 4

(5) Attack on a coordinated ligand by a reagent that is not coordinated to the metal.

(6) β-hydrogen abstraction from a metal alkyl (fig. 5).

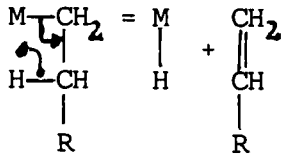

fig. 5

1.3 PYRAZOLE AND THE PYRAZOLIDE ION

Pyrazole is a nitrogen heterocycle in which the nitrogen atom in the 2 position does not have its lone pair of electrons involved in the Π aromatic electron system of the ring (fig. 6). These electrons are therefore available for donation to a suitable metal centre and the resulting complex contains a η^1-pyrazole ligand. A number of such transition metal compounds have been prepared[3,4,5] and two reviews exist on the subject, compiled by Trofimenko[6,7]. The complexes are prepared in neutral or slightly acidic conditions by the reactions of transition metal salts with pyrazole or substituted pyrazoles.

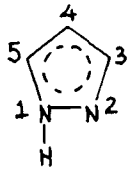

fig. 6

The pyrazolide ion possesses an unshared pair of electrons on each nitrogen atom (fig. 7). These electrons are in the plane of the ring and pointing away from each other and are available for σ coordinate bond formation by overlap with empty d orbitals on metal centres. Because of the orientation of the electrons available for coordination on both nitrogen atoms, the ion is more inclined to act as a ligand bridging two metal centres than a chelating ligand to one metal centre. Thus it generally functions as an exobidentate 1,2-μ^2-bridging ligand.

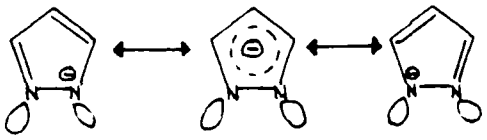

fig. 7

The pyrazole ligand can stabilize metals in low formal oxidation states and in such complexes it is believed that there is occupation of the ligand Π^* orbitals by overlap with full metal d orbitals of the appropriate energy and symmetry i.e. the bonding mechanism is synergic. The μ^2-pyrazolyl ligand behaves similarly when it is coordinated to Group VIII metals in low oxidation states i.e. metals whose d orbitals are fairly well populated with electron density, although in certain circumstances it can behave as a Π donating ligand. For example, the anionic form can enter into considerable Π donation towards a low-spin d^5 centre [such as Ru(III)][8].

The μ^2-pyrazolyl ligand (or its derivatives) is therefore of interest regarding the synthesis and study of potential homogeneous catalysts, in

that it can hold adjacent metal centres in an unusually wide range of intermetallic separations (2.638 Å - 3.690 Å)[9]; this allows the study of a range of intermetallic distances over which molecules coordinated to different metal centres can combine. The ligand also has the necessary property of accepting electron density from the metal centre and allowing it to remain in a low oxidation state. As previously mentioned, oxidation of metal centres and then their subsequent reduction can be important steps in the homogeneous catalytic cycle.

1.4 HOMOBIMETALLIC COMPLEXES WITH μ^2-PYRAZOLYL BRIDGING LIGANDS

Without "end capping" groups on the metal, μ^2-pyrazolyl complexes of transition metals can form a polymeric chain, the metal sometimes coordinated to additional ligands such as water or ammonia[3,9]. Therefore, to synthesize a complex of structure as shown in fig. 8 it is necessary to utilize a complex containing blocking ligands at L. Typical blocking ligands include CO, PPh_3, and 1,5-COD i.e. ligands where the bonding mechanism to the metal is synergic. These ligands tend to form relatively strong bonds with transition metals in low oxidation states and increase the lability of ligands trans to themselves.

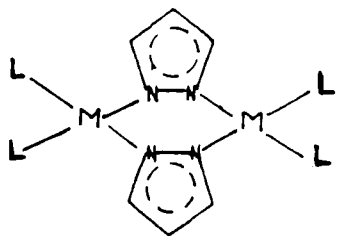

fig. 8

In many preparations of homobimetallic complexes containing μ^2-pyrazolyl ligands, the complex is synthesized from a precursor of the complex shown in fig. 8, containing two μ^2-chloro-bridging ligands which are subsequently replaced by pyrazolide ions or their derivatives. The pyrazolide ion is generated by the addition of a strong base (such as Et_3N) to pyrazole, or by adding a pyrazolide salt to the reaction mixture. Most reactions are carried out in a dry, inert atmosphere. Many μ^2-pyrazolyl complexes are reasonably stable in the solid state, but such stability may not extend to long periods in solution and/or at reflux temperatures, when air is present. Once prepared, complexes appear to remain unaffected by polar solvents and do not easily dissociate into monomeric fragments.

(i)Palladium and Platinum Complexes

Although a platinum(II) complex with a single μ^2-pyrazolyl bridging ligand has been synthesized[10, 11], most of the prepared complexes of palladium and platinum contain two such ligands.

Palladium metallocycles of the general formula shown in fig. 9 have been prepared from μ^2-chloro-bridged dimers containing Π-allyl or substituted Π-allyl derivatives[12]. DMF is used as the solvent.

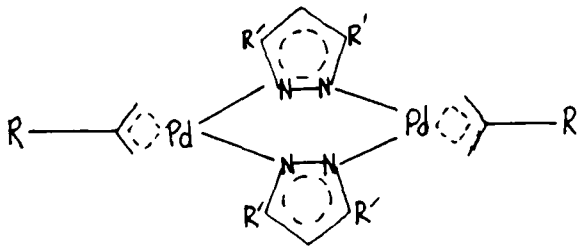

R = C_6H_5, H, CH_3

R′ = H, CH_3

fig. 9 white solids

The reaction of the 2(di-ethylaminomethyl)phenyl palladium(II) chloride dimer with deprotonated 3,5-dimethylpyrazole gives the analogous complex in fig. 10.

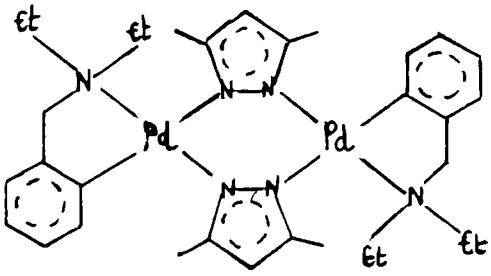

fig. 10

The halogen bridges of the dimeric cyclometallated trimesitylarsine and phosphine complexes of palladium(II) and platinum(II) have also been replaced with pyrazolide ions[13] to give the corresponding μ^2-pyrazolyl bridged complexes in fig. 11.

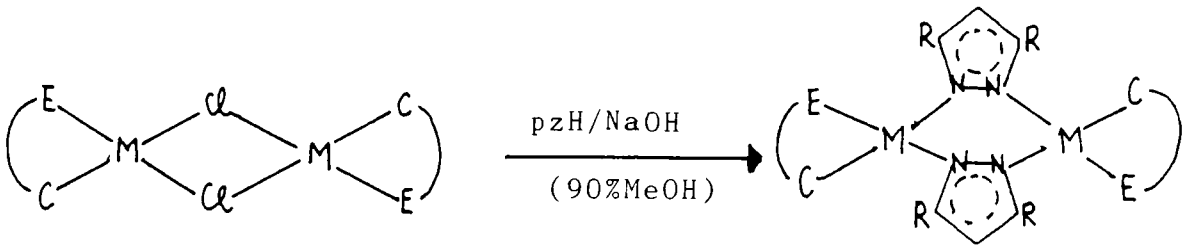

E⌒C = $AsMesityl_2C_6H_2(Me)_2CH_2$

or $PMesityl_2C_6H_2(Me)_2CH_2$

M = Pd or Pt

R = H, CH_3

cream solid

fig. 11

A platinum complex of formula shown in fig. 12 is obtained by reacting the chloro-bridged analogue with a mixture of sodium hydroxide and pyrazole or 3,5-dimethylpyrazole in methanol as solvent[14].

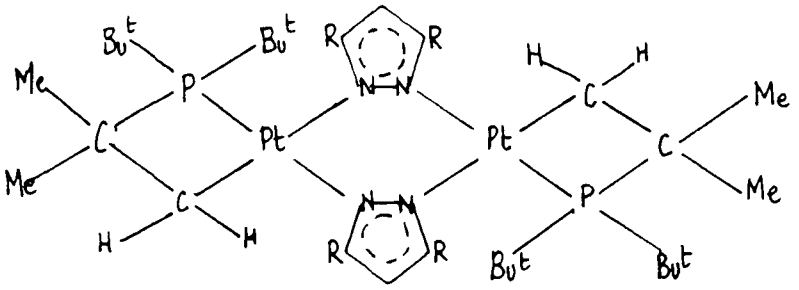

R = H, CH_3 white crystals

fig. 12

After treatment of $(COD)MCl_2$ (M = Pd, Pt) with pyrazole, two reactions[15] occur: formation of the $M(pz)_2M$ ring, and addition of either pz or OMe (from the solvent) to one of the COD double bonds, giving the products shown in fig. 13.

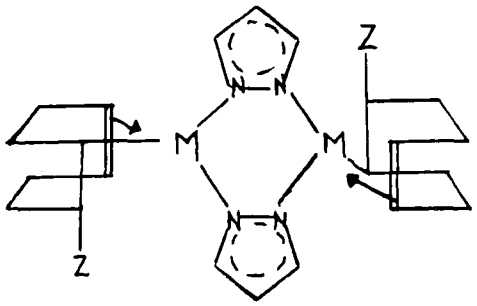

a) Z = pz

b) Z = OMe

fig. 13

(ii) Rhodium and Iridium Complexes

The reaction of the 3,5-dimethyl pyrazolide ion with $[(CO)_2RhCl]_2$ gives a yellow solid assigned the structure shown in fig. 14.

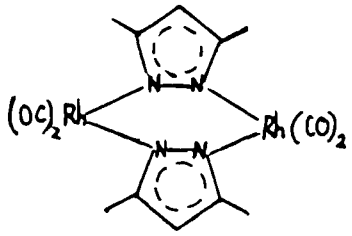

fig. 14

The 1,5-cyclooctadiene complex $[(COD)RhCl]_2$ reacts in a similar fashion[12] Starting with $[Rh(C_5Me_5)(Me_2CO)_3][BF_4]$ and $[\{Rh(C_5Me_5)\}_2(OH)_3][ClO_4]$ a number of pyrazolyl bridged complexes have been synthesized[16] (see fig. 15).

Stobart et al. have prepared and extensively studied[17-22], a series of μ^2-pyrazolyl bridged iridium dimers, prepared from $[(COD)IrCl]_2$ or trans-$[Ir(CO)Cl(PPh_3)_2]$ (Vaska's Complex). A reaction scheme is shown in fig. 16.

The preparation of the methoxo- and hydroxo-bridged pentamethylcyclopentadienyliridium(III) species, which also contain μ^2-pyrazolyl bridges has been reported[23]. These complexes are analogous with the rhodium species described in fig. 15. Complexes of the type $[Rh(pz)(CO)(PCBr)]_2$ are obtained by reacting $[Rh(pz)(CO)_2]_2$ with PCBr or [Rh(acac)(CO)(PCBr)] with pyrazole[24]. The structure of the product(s) is shown in fig. 17.

fig. 15

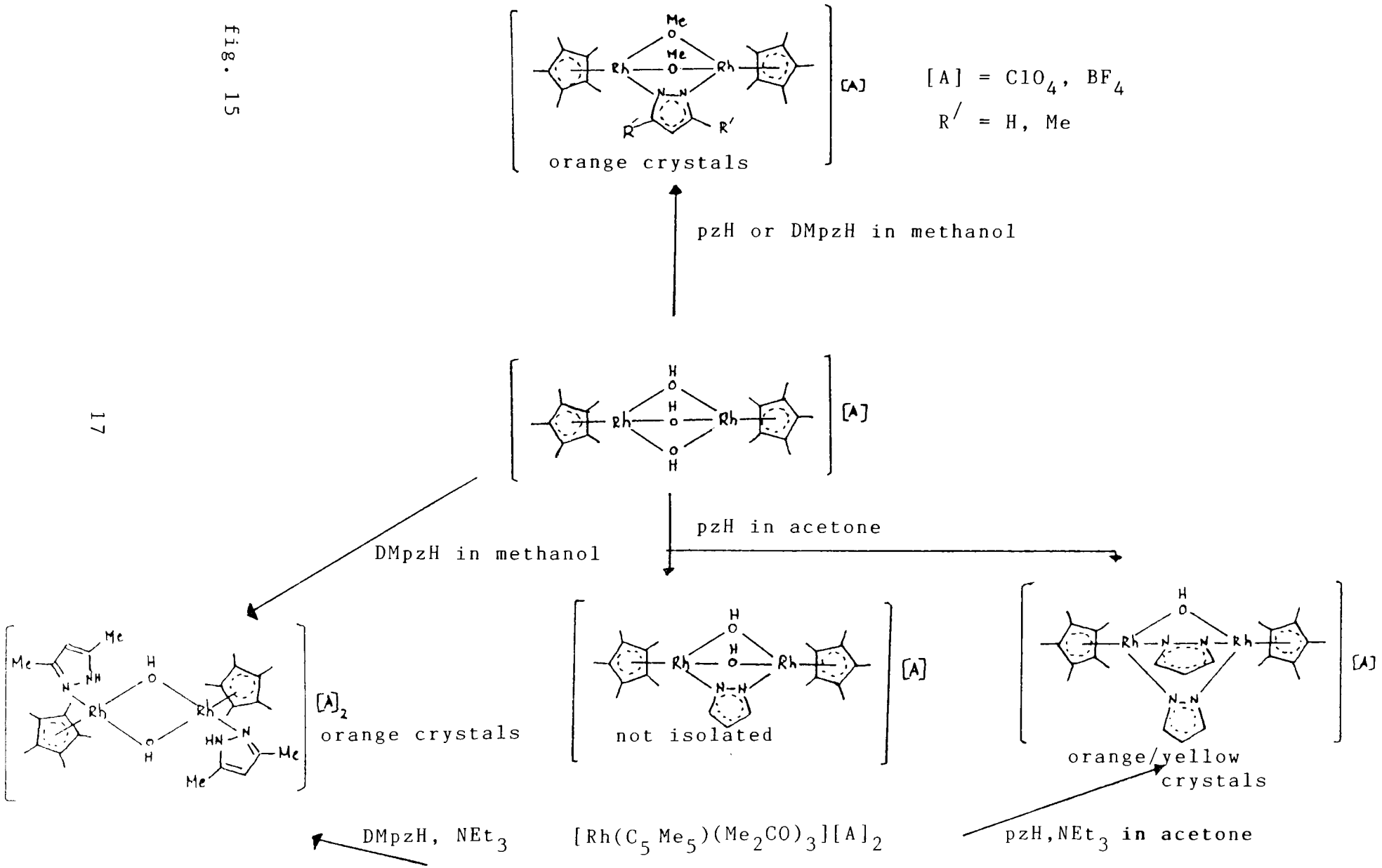
orange crystals
[A] = ClO4, BF4
R/ = H, Me
pzH or DMpzH in methanol
DMpzH in methanol
pzH in acetone
not isolated
orange/yellow crystals
orange crystals
DMpzH, NEt3
[Rh(C5Me5)(Me2CO)3][A]2
pzH,NEt3 in acetone

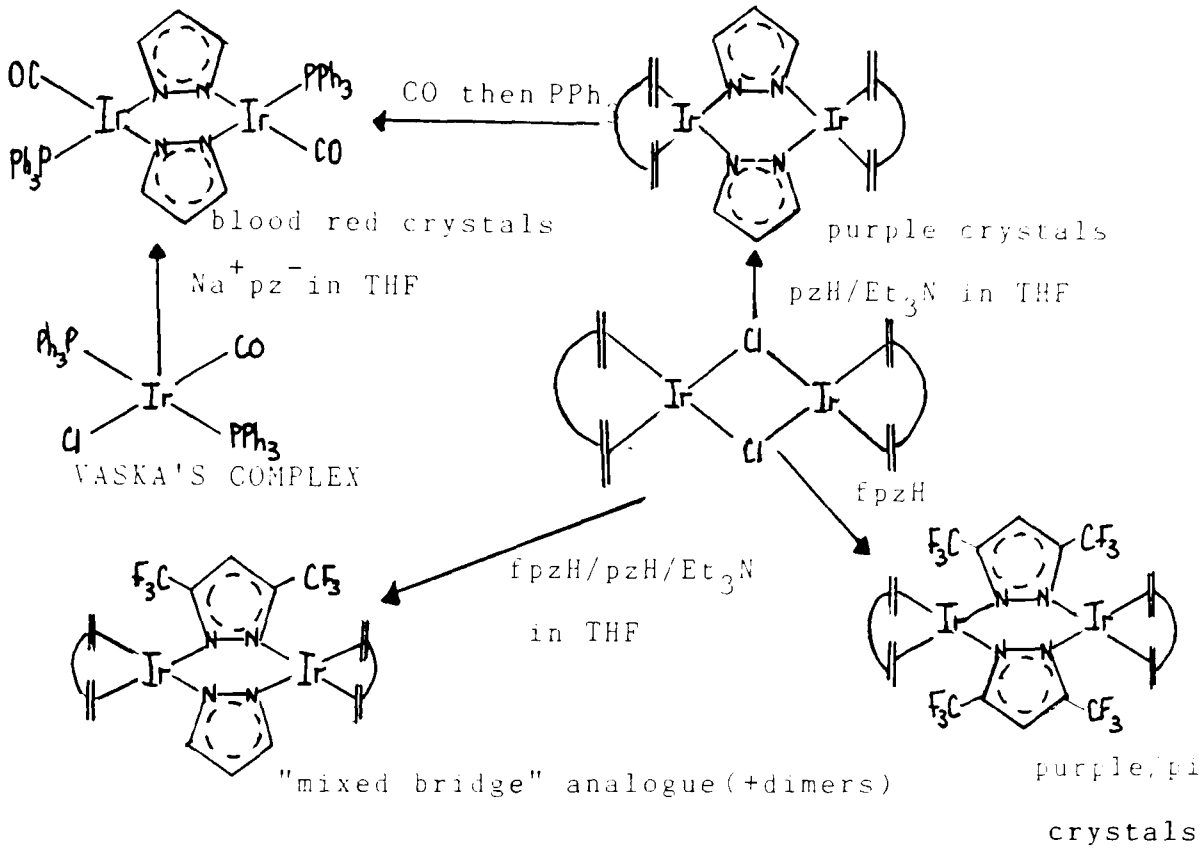

fig. 16

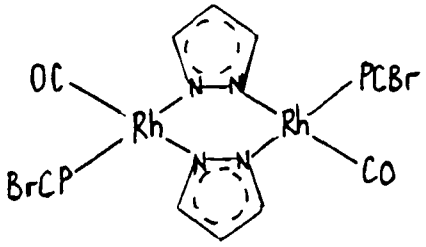

PCBr = $P(o\text{-}BrC_6F_4)Ph_2$ pz = pz, 3-Mpz, 4-Mpz.

fig. 17

Mixed-valence complexes containing pyrazole and/or chlorine groups bridging rhodium(III)-rhodium(I) species, have been prepared[25]. The homobridged pyrazolyl complexes are prepared by the reaction of $[Rh(C_5Me_5)(acac)Cl]$ with the cationic complexes $[RhL(pzH)_2][ClO_4]$ (L = tfb or COD) in the presence of stoichiometric amounts of KOH. Different behaviour is observed when DMpzH is substituted for pzH, the species $[\{RhL(DMpz)\}_2]$ results.

Various complexes having the formula $Rh(\mu\text{-}az)(\mu\text{-}SBu^t)Rh$ for the core have been prepared[26] and their properties have been investigated. Rhodium μ^2-pyrazolyl bridged dimers which contain triphenylphosphines as "blocking ligands" can be synthesized by reacting the complex shown in fig. 14 with phosphine to yield trans substitution products with one CO per rhodium atom[27].

Trans-$[RhCl(CS)(PPh_3)_2]$ reacts with the pyrazolide ion[28] to form the product $[(PPh_3)(CS)Rh\text{-}(pz)_2\text{-}Rh(CS)(PPh_3)]$. The dinuclear species is cleaved in the presence of PPh_3 and $HClO_4$, to give the perchlorate salt[29].

(iii) Ruthenium and Osmium Complexes

A number of monomeric and dimeric complexes of ruthenium[30] are obtained using the precursor cis-$[(bpy)_2RuCl_2]$. The complexes are illustrated in fig. 18.

A ruthenium complex that contains two μ^2-pyrazolyl bridging ligands and a semi-bridging hydride ligand, has been synthesized[31,32] from $[RuH(COD)(NH_2NMe_2)_3][PF_6]$, as shown in fig. 19.

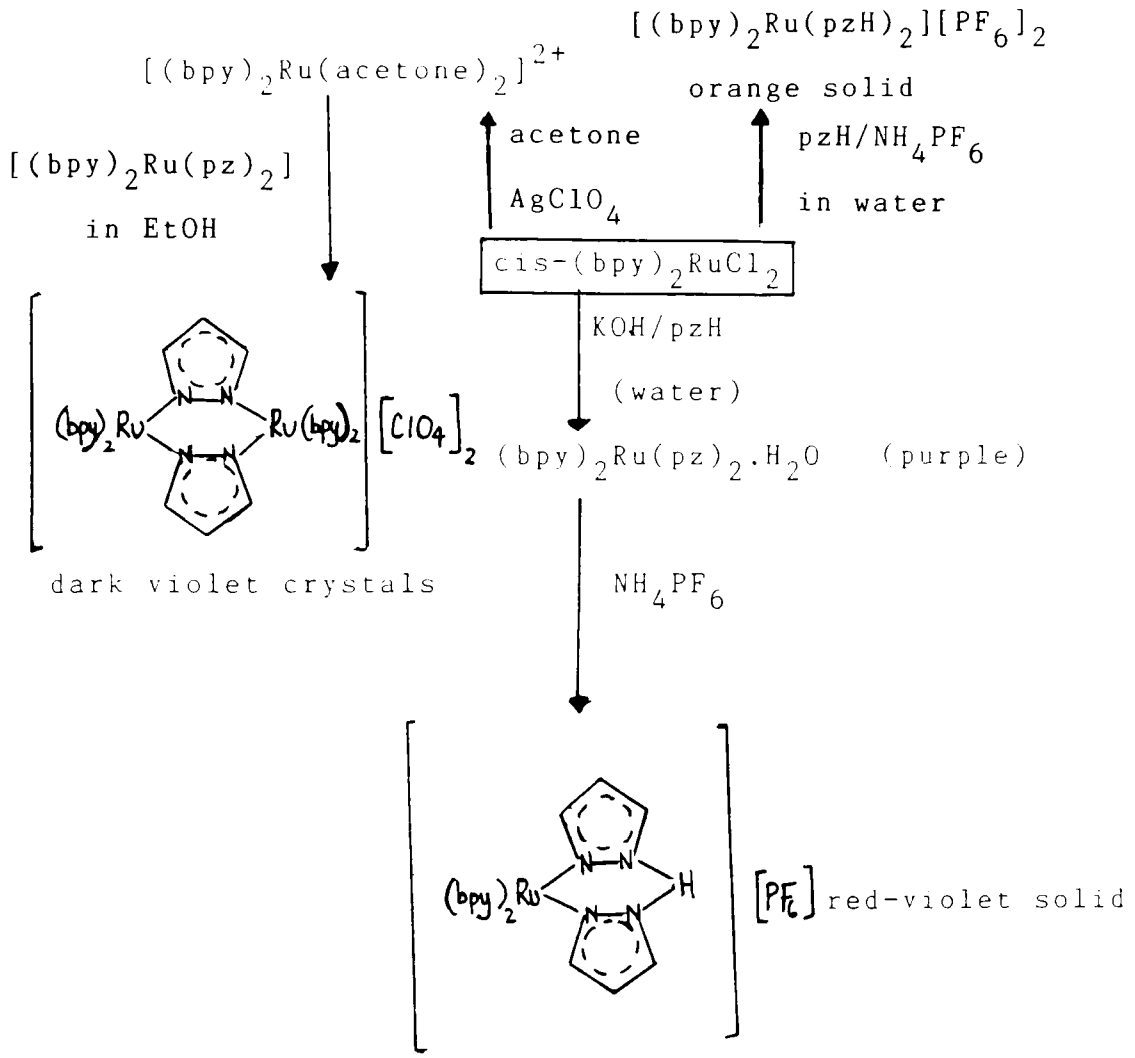
[(bpy)2Ru(acetone)2]2+
[(bpy)2Ru(pzH)2][PF6]2
orange solid
[(bpy)2Ru(pz)2]
in EtOH
acetone
AgClO4
pzH/NH4PF6
in water
cis-(bpy)2RuCl2
KOH/pzH
(water)
(bpy)2Ru(pz)2.H2O (purple)
dark violet crystals
NH4PF6
red-violet solid

fig. 18

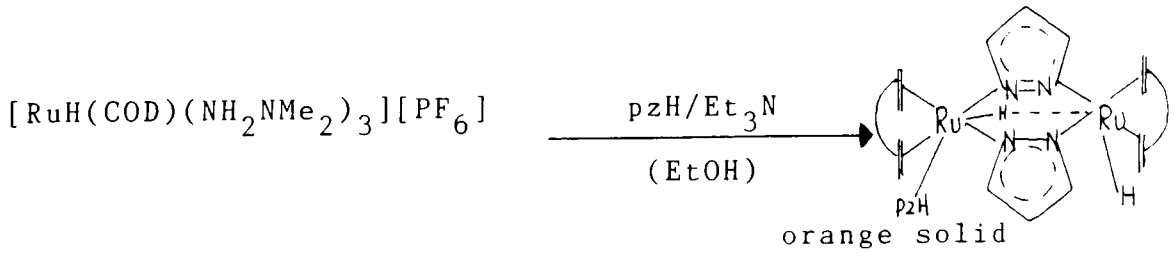
[RuH(COD)(NH2NMe2)3][PF6]
pzH/Et3N
(EtOH)
orange solid

fig. 19

When pyrazole reacts with $[Os_3(CO)_{10}(NCCH_3)_2]$, two products are obtained[33]. These are shown in fig. 20.

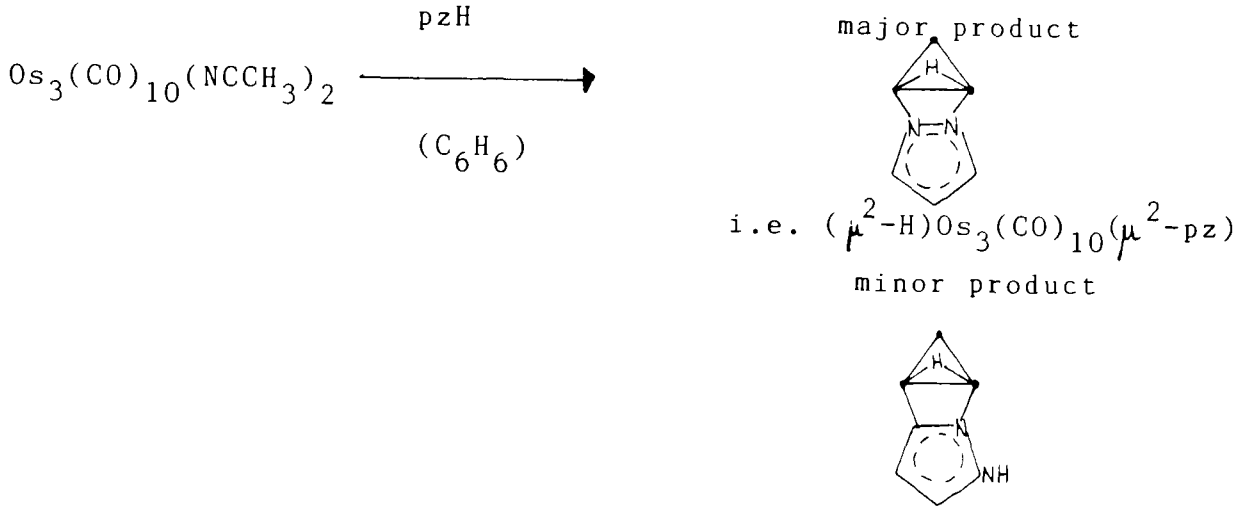

fig. 20

The complexes $[Ru_2(\mu\text{-L})_2(CO)_6]$ where HL = 3,5-dimethylpyrazole, pyrazole, methylpyrazole or indazole, have been obtained by the reaction of $RuCl_3.3H_2O$ with carbon monoxide in refluxing 2-methoxyethanol followed by reduction with zinc in the presence of CO and HL[34]. This synthetic route provides an easy method to prepare ruthenium(I) compounds in high yield.

1.5 HETEROBIMETALLIC COMPLEXES WITH μ^2-PYRAZOLYL BRIDGING LIGANDS

Relatively few heterobimetallic complexes have been isolated. For most of those that have, preparation has been achieved by generating a metal complex that contains one or two η^1-pyrazole ligands, deprotonating such a complex and reacting it with a complex of a different metal that contains labile coordinated groups in suitable positions. One of the

effects of coordination of pyrazole to a metal ion, is that the pyrrole-like nitrogen becomes less basic as compared with the free ligand[8], so that it should be possible to effect deprotonation by the addition of a strong base.

A procedure for the synthesis of heteronuclear bimetallic complexes involving platinum has been described[35]. This reaction involves deprotonation of Zeise's adduct of pyrazole which then reacts with moderately labile substrates to yield binuclear products (fig. 21).

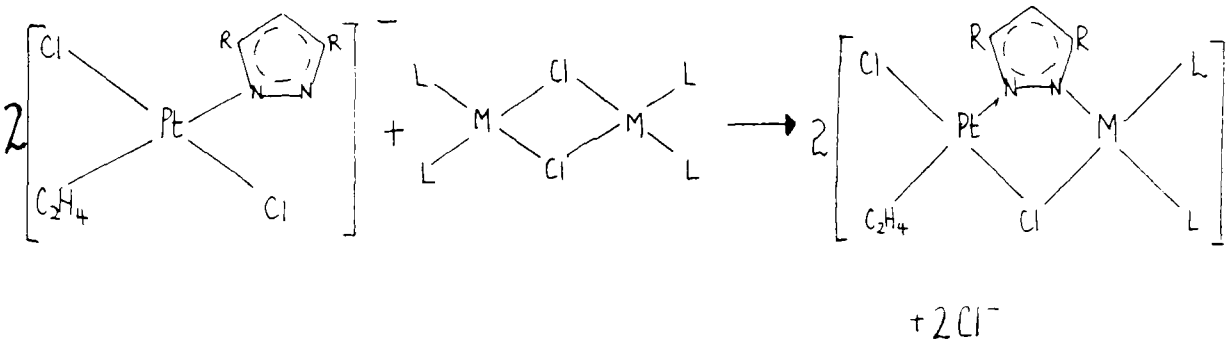

M = Pd(II), Rh(I) L = η^3-allyl, η^3-methallyl or 1,5-COD R = H, CH_3

fig. 21

Deprotonation is effected by stirring trans-[$PtCl_2(C_2H_4)(pzH)$] with excess powdered sodium carbonate in chloroform. Only one μ^2-pyrazolyl bridging ligand is present in the complex.

The bidentate metal-containing ligand in fig. 22 is generated[36] by the reaction of square-planar dichloro metal(II) derivatives with the pyrazolide ion, which can either be generated in situ by the reaction of pyrazole with potassium hydroxide or added directly to the reaction mixture by employing the potassium salt of pyrazole. The pyrazole complex can be prepared in methanol, whilst THF is the preferred solvent

for its 3,5-dimethylpyrazole analogue.

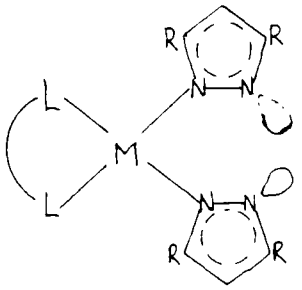

L = dppe, dpae, 1,5-COD or bpy

R = H, $-CH_3$

M = Pd(II), Pt(II)

fig. 22

The above ligand is more inclined to act as a chelating ligand rather than a bridging ligand, because of the orientation of the electron density available for coordination to another metal. Interaction between the pyrazole rings prevents free rotation about the M--N bond. The ligand can be used to generate homobimetallic complexes[36], but has potential as a useful ligand for making mixed-metal complexes and indeed, a heterobimetallic complex has been synthesized by using the analogous ligand in fig. 23 and reacting it with $Cr(CO)_6$[9].

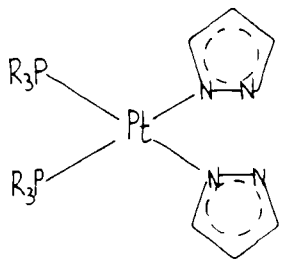

PR_3 = PEt_3, PMe_2Ph

fig. 23

The reaction between the above ligand and $Cr(CO)_6$ is shown in fig. 24.

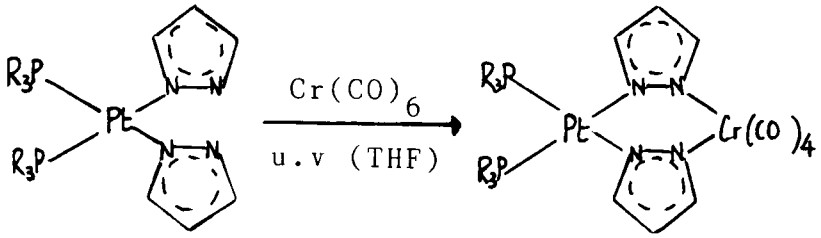

yellow crystals

fig. 24

A complex that contains rhodium(I) and iridium(I) species (fig. 25), is made by the reaction of $[(COD)IrCl]_2$ and $[(COD)RhCl]_2$ with the pyrazolide ion (generated by the reaction of pyrazole with triethylamine) in THF[37].

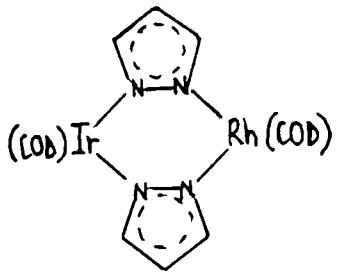

crimson crystals

fig. 25

This preparation can also be effected by reacting the bis-(pyrazole) rhodium cationic complex $[(COD)Rh(pzH)_2][PF_6]$ and $[(COD)IrCl]_2$ with the pyrazolide anion. Both preparations, however, find the product in fig. 25 contaminated with the homobimetallic complexes $[(COD)Ir(pz)]_2$ and $[(COD)Rh(pz)]_2$.

The mixed-metal complex $[(C_5Me_5)Rh(\mu\text{-}pz)(\mu\text{-}Cl)_2Ir(C_5Me_5)][BF_4]$ has been synthesized[23] by the route shown in fig. 26.

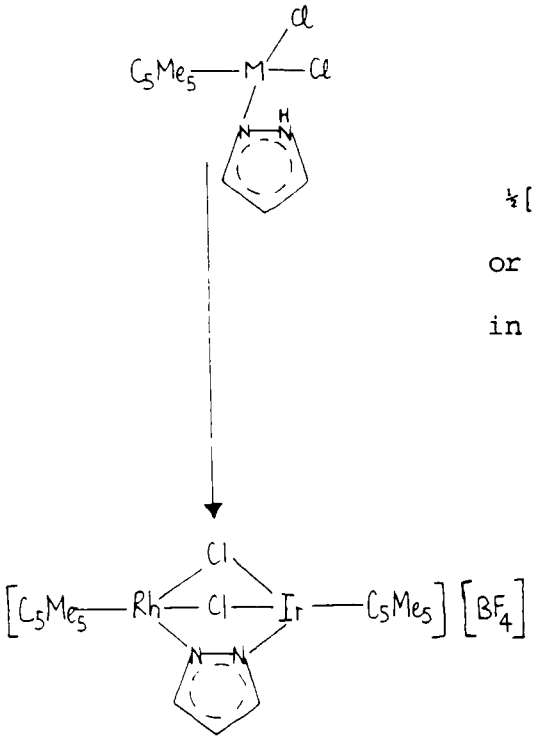
Cl
C5Me5 — M — Cl
H
M = Rh or Ir
½[{(C5Me5)Rh}2(μ-acac)2][BF4]2
or [Ir(C5Me5)(acac)(MeOH)][BF4]
in methanol
Cl
[C5Me5 — Rh — Cl — Ir — C5Me5] [BF4]
orange solid

fig. 26

1.6 STRUCTURE

The majority of binuclear species involving two μ^2-pyrazolyl bridges exhibit a boat conformation for the central six-membered ring, although there are exceptions[9]. Puckering of the central ring helps relieve close contact between the protons of the pyrazolide groups and adjacent non-bridging ligands.

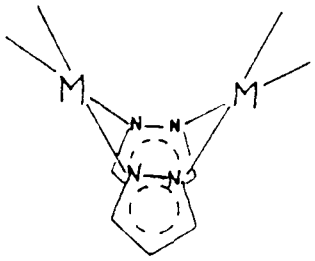

i.e. C_{2v} symmetry rather than planar (D_{2h})

fig. 27

The pyrazolyl ligand remains planar and there are no significant differences in its bond lengths as compared with free pyrazole. The two metal centres are brought closer together than they would be in a planar complex, so that in some cases the metal-metal separation is unusually small[9] and may even be consistent with some degree of metal-metal interaction[20]. Substituents such as $-CF_3$ in the 3,5 bridge positions may force the metal centres even closer together[20].

Different 3,5-substituents on the bridging ligand, resulting in an unsymmetrical bridge, give rise to complexes which exhibit diastereoisomerism (fig. 28).

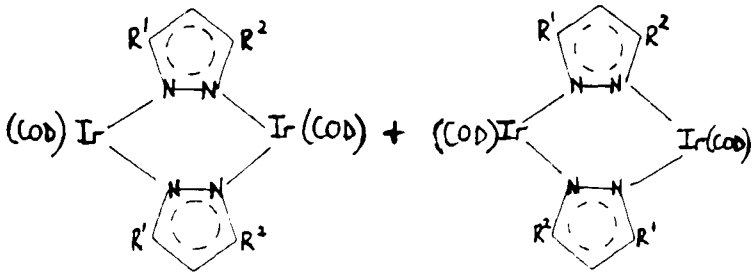

fig. 28

The complex $[(COD)Ir(3\text{-}Ph,5\text{-}Me,pz)]_2$ is prepared as a mixture of diastereoisomers[37], the major constituent of which, is the dissymmetric isomer (fig. 29). This isomer would not be subject to unfavourable interactions between adjacent 3-phenyl substituents.

Two different "end-capping" groups situated mutually trans across the metal-metal axis of a complex containing two μ^2-pyrazolyl bridging ligands, would mean that the complex would, in principle, exist as two non-superimposable mirror image forms. Chiral behaviour of this sort has been postulated[22] for the complex in fig. 30.

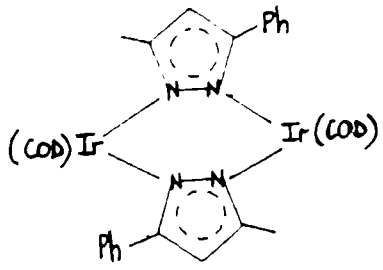

fig. 29

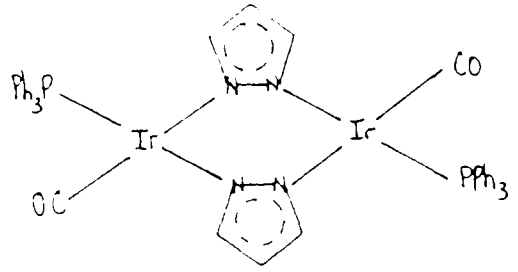

fig. 30

1.7 OXIDATIVE ADDITION/REDUCTIVE ELIMINATION REACTIONS OF μ^2-PYRAZOLYL BRIDGED IRIDIUM DIMERS

Transition metal catalysed homogeneous reactions often depend upon sequential oxidative-addition/reductive-elimination cycles which access two different oxidation states for the metal site. While numerous examples of such behaviour occurring at a single coordinatively unsaturated metal centre exist[6], only quite recently has attention been focussed specifically on polymetallic systems.

The following reactions illustrate how μ^2-pyrazolyl bridged iridium complexes can accommodate oxidative-addition without fragmentation. Two centre oxidative-addition occurs, leading to metal-metal bond formation and showing that the pyrazolyl ligand can absorb drastic contraction of the bridged framework, arising from the formation of the metal-metal bond. The oxidation state of each metal centre increases formally by one. It is also demonstrated that the reverse transformation i.e.

reduction of both metal centres, can be brought about again, without disruption of the dimer.

Oxidative-addition of $[Ir(CO)(PPh_3)(pz)]_2$ results in the formation of d^7—d^7 diamagnetic iridium(II) dimers, incorporating an Ir—Ir bond (fig. 31).

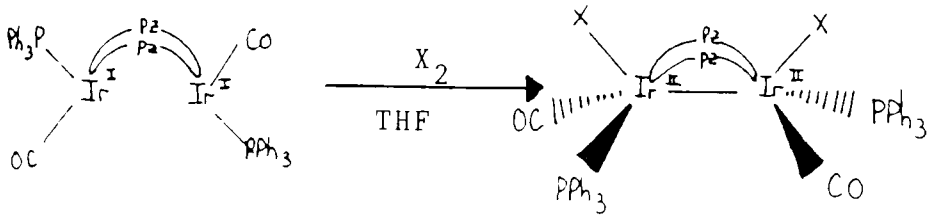

X = H, Br, I pale yellow adducts

fig. 31

A corresponding reaction also occurs with chlorine, in which there is substitution of the 4 position in each pyrazolyl group, emphasizing the chemical stability of the dimeric system[17]. Reaction of the same complex with methyl iodide likewise affords a bright yellow 1 : 1 asymmetric complex formulated as $[(PPh_3)(CO)(Me)Ir\text{-}(pz)_2\text{-}IrI(CO)(PPh_3)]$. The complex $[Ir(CO)(PPh_3)(pz)]_2$ will also form an adduct with DMAD in a mixture of toluene and hexane[38] (fig. 32), but appears unreactive towards MPL. Reaction of the same complex with hexafluorobut-2-yne induces polymerisation of the substrate ethyne, resembling that induced by free triphenylphosphine. This may indicate that free phosphine may be in solution via release from $[Ir(CO)(PPh_3)(pz)]_2$.

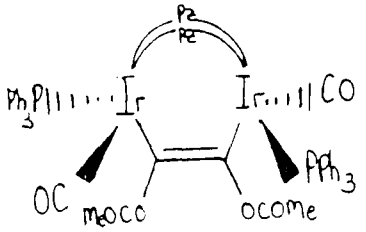

cream crystals

fig. 32

Oxidative addition of $[(COD)Ir(pz)]_2$ occurs by reaction with a number of compounds (fig. 33).

Regeneration of the original complex is obtained by reacting the iodine adduct with Na/Hg, Na/napthalene or $Tl(C_5H_5)$ in THF at ambient temperature. The reaction of the same complex with hexafluorobut-2-yne (fig. 33), gives colourless crystals in which the alkyne has oxidatively added across the two Ir(II) centres to give a 1,2-dimetallato-substituted ethene, the terminal COD groups twisting somewhat to avoid contact with the $-CF_3$ substituents. Here, the Ir--Ir bond is nearly as short as that attributed to a double bond interaction. In contrast, the reaction of the same diiridium(I) complex with methyl iodide (fig. 34), gives an adduct with a very long Ir--Ir bond.

The proposed explanation for this difference between the metal centres in the two adducts is that the electron poor bridge in the first adduct causes contraction of the orbitals involved in bonding between the Ir(II) centres, whilst the complex in fig. 34 has inductive electron donation to the metal.

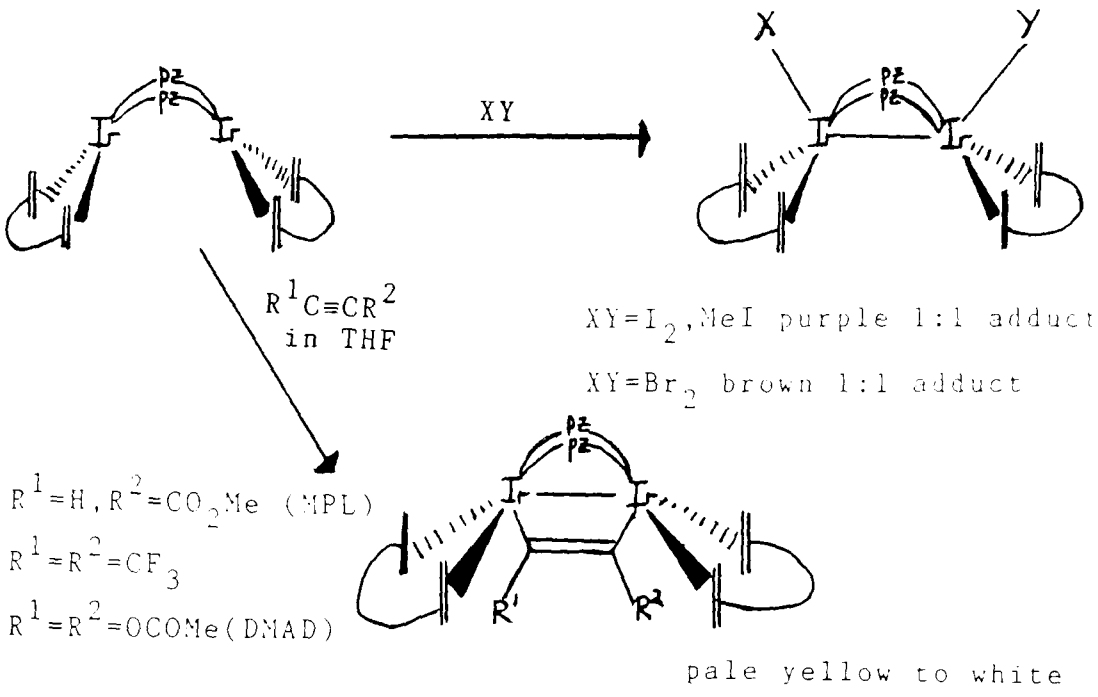
XY
X
Y
Pz
Pz
$R^1C{\equiv}CR^2$
in THF
XY=I_2,MeI purple 1:1 adduct
XY=Br_2 brown 1:1 adduct
R^1=H, R^2=CO_2Me (MPL)
R^1=R^2=CF_3
R^1=R^2=OCOMe(DMAD)
R'
R^2
pale yellow to white
= COD

fig. 33

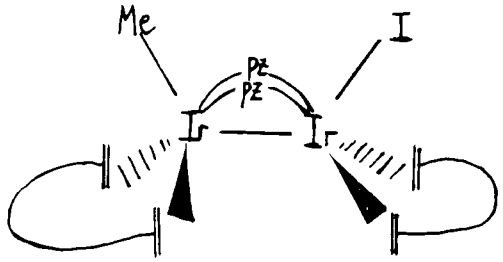

where  = COD

fig. 34

Adduct formation of $[(COD)Ir(pz)]_2$ with hexafluorobut-2-yne, DMAD or MPL, generates a highly distorted environment at each Ir centre with the adjacent metal atom taking up the sixth coordination site.

Photoinduced oxidative addition of $[(COD)Ir(pz)]_2$ is obtained by visible irradiation of the complex[39] in 1,2-dichloroethane or dichloromethane (fig. 35).

Dramatic changes in the reactivity of the binuclear unit may be induced by modification of the bridging pyrazolyl ligand. The complex $[(COD)Ir(fpz)]_2$ is unaffected by hexafluorobut-2-yne, DMAD, iodine or methyl iodide at ambient temperature[19]. This may be because steric influence by the pyrazolyl $-CF_3$ substituents with the axial Ir sites is sufficent to inhibit the initial step of the oxidative addition reaction. Further support for this interpretation is provided by the relatively sluggish reactivity towards oxidative-addition of another dimer[20] $[(COD)Ir(DMpz)]_2$ as compared with $[(COD)Ir(pz)]_2$.

The pyrazolyl/3,5-bis(trifluoromethyl)pyrazolyl "mixed bridge" iridium complex gives a very slow reaction with hexafluorobut-2-yne (fig. 36).

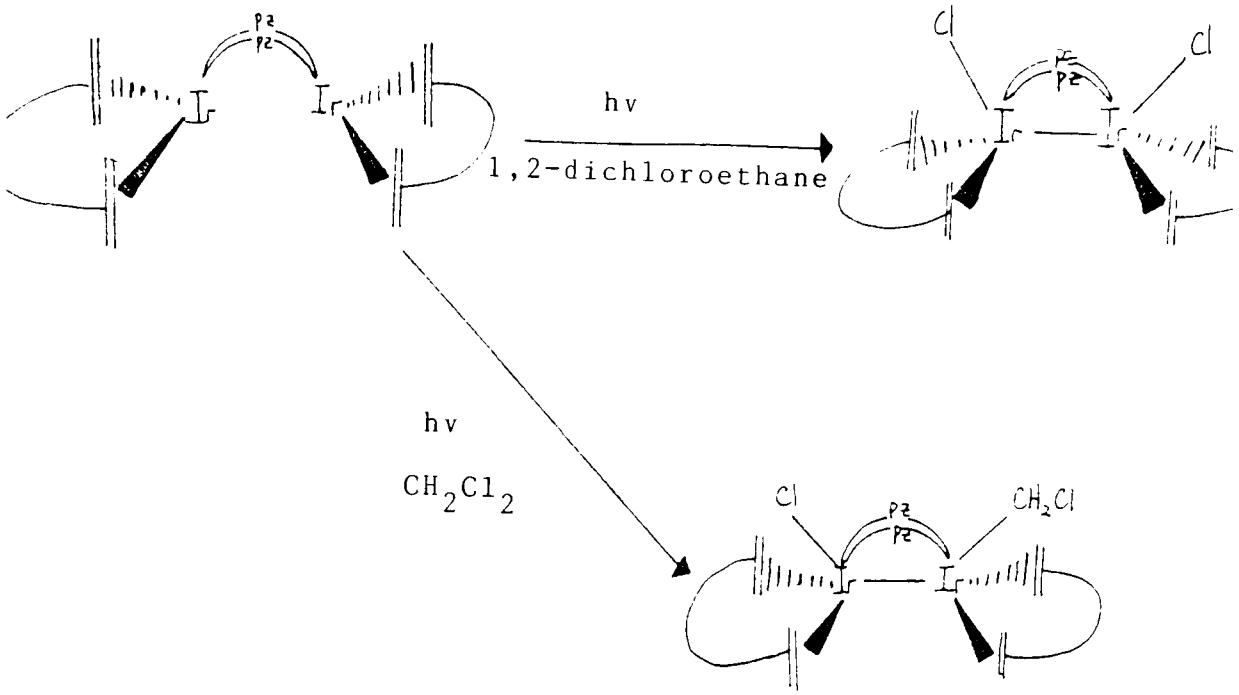

fig. 35

X-ray diffraction shows that the product contains a 1-3,5,6-η C_8H_{11} entity and the fpz bridge has been displaced[19]. The distance between the two iridium centres is more consistent with an Ir(I)-->Ir(III) formalism than Ir(II)--Ir(II). The idea of two iridium centres in different oxidation states is found in a related diiridium complex in which

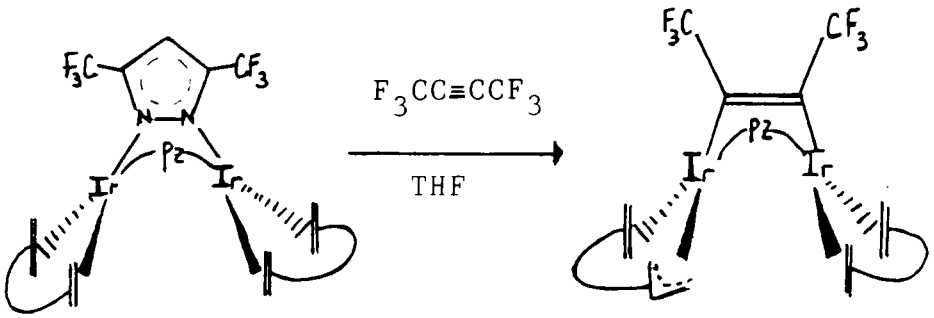

fig.36

pyrazolyl and diphenylphosphido bridging ligands exist together[21]. One

iridium centre has shorter bonds to phosphorus than the other, indicating each has a different oxidation state (fig. 37).

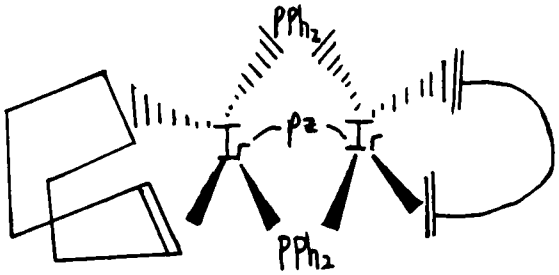

fig. 37

A cationic diiridium complex has been prepared[40], by the action of $[(COD)Ir(pz)]_2$ with $NOBF_4$ (fig. 38). The observed Ir--Ir distance in the cation suggests that the species in fig. 38 should be regarded as a d^8--d^6 system. Interaction between the adjacent centres in the cation may be opposed by the strong trans influence associated with monolinear

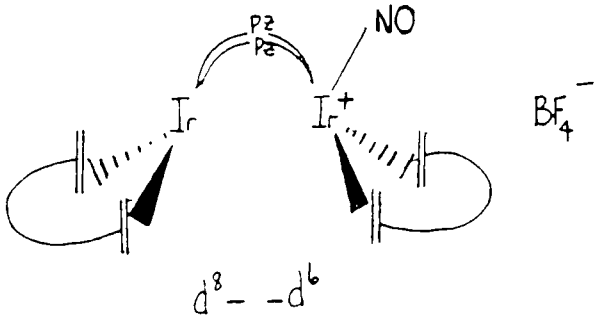

fig. 38

MNO coordination. The same complex reacts with hydrogen chloride gas to give a nitrosyl bridged diiridium(III) cation[41]. Treatment of the

complex with iodine gives the diiodo analogue (fig. 39).

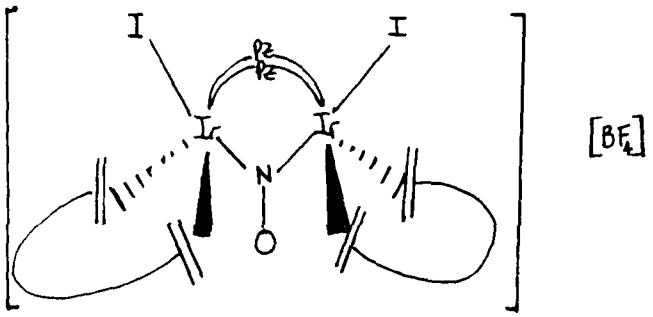

fig. 39

The rhodium analogues of the iridium complexes discussed in this section are not as reactive as their counterparts. Two centre oxidative-addition can be effected for $[Rh(CO)(PPh_3)(pz)]_2$, but its iridium analogue is much more reactive. The complex $[(COD)Rh(pz)]_2$ does not give isolable adducts with, for example, methyl iodide or activated alkynes.

The catalytic activity of the complexes $[Rh_2(\mu\text{-}pz)_2(CO)_2\{P(OMe)_3\}_2]$ and $[Rh_2(\mu\text{-}pz)(\mu\text{-}SBu^t)(CO)_2\{P(OMe)_3\}_2]$ has been investigated[26]. Both complexes display activity as catalysts for the hydroformylation of hex-1-ene and are found to be unchanged after the reaction has taken place.

Preliminary investigation of the catalytic activity of the diplatinum complex shown in fig. 40 has been carried out[10], in which gas chromatography and nmr spectra indicate that hydrogenation of cyclohexene to cyclohexane can be carried out with no detectable decomposition of the complex.

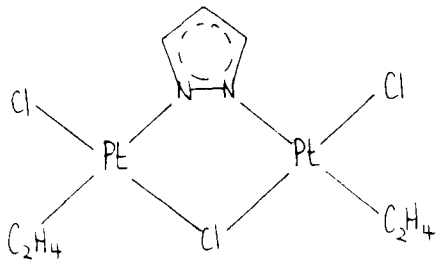

fig. 40

Iodine reacts with the complexes $[Ru_2(\mu\text{-}L)_2(CO)_6]$, where the formula HL = 3,5-dimethylpyrazole or pyrazole, to form $[Ru_2(\mu\text{-}I)(\mu\text{-}L)_2(CO)_6]I_3$ or $[Ru_2I_2(\mu\text{-}L)_2(CO)_6]$, depending on the Ru: I ratio used[34].

1.8 BONDING THEORY THAT MAY BE USED TO EXPLAIN AND PREDICT THE BEHAVIOUR OF TRANSITION METAL COMPLEXES

(i) Pearson's Principle

Pearson[42] has suggested the terms "hard" and "soft" to describe metal ions and ligands. "Hard acids" are small, slightly polarizable metal ions such as light transition metals in high oxidation states, whereas "soft acids" are large, polarizable metal ions. Typical examples of soft acids include heavy transition metals in low oxidation states such as Pd^{2+} or Ru^{2+}. Ni^{2+} is classified as a borderline case between hard and soft. Ligands can similarly be described as being "hard" or "soft" bases. Hard bases are species such as NH_3 or F^-, soft bases are highly polarizable PPh_3 or I^-. The stability of complexes formed between these acids or bases is described as follows: "Hard acids prefer to bind to hard bases and soft acids prefer to bind to soft bases". This rule often usefully predicts the relative stability of acid-base adducts.

There is no complete unanimity amongst chemists concerning the theoretical basis of this effect, however, most of the typical hard acids and bases are those that we might suppose to form ionic bonds. Since the electrostatic energy of an ion pair is inversely proportional to the interatomic distance, the smaller the ions involved, the greater is the attraction between the hard acid and base. Since the electrostatic explanation cannot account for the apparent stability of soft-soft interactions, it is considered that the predominant factor in soft-soft interactions is a covalent one. All really soft acids are transition metals with six or more d electrons, with the d^{10} configuration being extremely soft[43]. The

polarizability of the d electrons is thus high. It may be that Π-bonding contributes to soft-soft interactions[44]. It occurs most readily in those metal ions that have low oxidation states and large numbers of d electrons. Furthermore, the important Π-bonding ligands such as carbon monoxide, phosphines and heavier halogens are all soft bases. The presence of d orbitals on the ligand in each case, except carbon monoxide, enhance Π-bonding. It is also true that London dispersion energies increase with increasing size and polarizability and might thus stabilize a bond between two large, polarizable, (soft) atoms[45].

(ii) Metal-Carbonyl Bonding

At face value, the fact that a generally inert molecule like carbon monoxide is capable of uniting with a metal to form a stable, molecular compound may be surprising. The explanation, however, lies in the multiple nature of the M—CO bond. There is first a dative overlap of the filled carbon σ orbital with an empty metal σ orbital [fig. 41(i)] and second a dative overlap of a filled dΠ or hybrid dpΠ metal orbital with an empty antibonding pΠ orbital of the carbon monoxide [fig. 41(ii)].

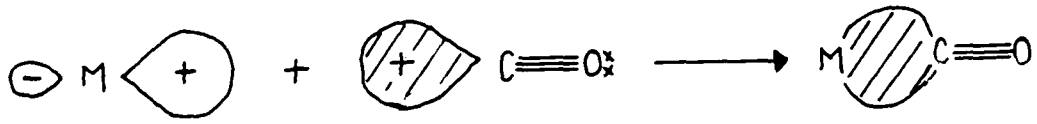

fig. 41(i)

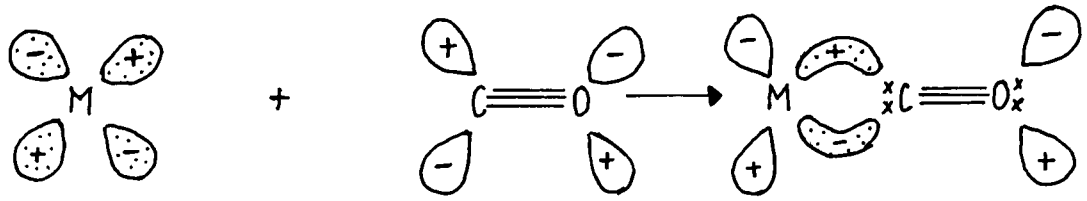

fig. 41(ii)

This results in a synergic mechanism, since the drift of metal electrons into CO orbitals will tend to make the CO as a whole negative and hence increase its basicity via the σ orbital of the carbon; at the same time the drift of electrons to the metal in the σ bond tends to make the CO positive, thus enhancing the acceptor strength of the Π orbitals. So, up to a point, the effects of σ bond formation strengthen the Π-bonding and vice-versa. The dipole moment of the M—C bond is very low, suggesting a close approach to electroneutrality.

In general, trans-dicarbonyl complexes are much less stable than the corresponding cis-dicarbonyl isomers, because of the strong Π-acceptor property of coordinated CO[46]. Thus cis-$[RuCl_2(PPh_3)_2(CO)_2]$ is formed from the trans-isomer on recrystallization with heating[47]. A CO ligand trans to another CO is extremely labile[46] (because of competition for Π electron density), so that for CO, a position trans to a chlorine is more acceptable, since the latter is a much better σ-donor than it is a Π-acceptor.

SECTION TWO-METHODS AND MATERIALS

2.1 VACUUM LINE APPARATUS

Some of the complexes prepared, proved sensitive to oxidation whilst in solution. The vacuum line apparatus shown in fig. 42, provided a means whereby oxygen could be excluded from the reaction mixture during a preparation.

Nitrogen gas was dried by passing through tubes containing P_2O_5 and KOH pellets before entering the main body of the nitrogen line. The nitrogen line was vented at Y, making it possible to use other gases such as carbon monoxide instead of nitrogen and also to vent fumes from volatile solvents. Oil bubblers at Z and X gave a check on the passage of nitrogen through the line. The vacuum system was operated at a pressure of 0.1 mm Hg or less. A trap cooled by liquid nitrogen collected evaporated solvent. Both systems of nitrogen and vacuum could be operated independently, or connected through a series of taps 1 to 4 and A to D. The following techniques were operated:

(i) To De-gas Solvents

This could be effected by simply bubbling nitrogen through the solvent for about five minutes, or, more rigorously by connecting a Schlenk tube containing the solvent to C from E. The connection was made by using thick-walled rubber tubing and the top of the Schlenk tube was closed using a rubber Suba-seal. Tap 3 was opened to the pump and E opened and closed carefully until bubbles appeared in the solvent. Both taps were then closed and tap C opened to nitrogen. When bubbles of nitrogen appeared at X, tap E was opened until the nitrogen line was pressurized. This was again gauged by the presence of nitrogen bubbles at X. This

procedure was repeated twice after which the solvent was judged to be de-gassed.

(ii) Freeze-Thaw De-gassing

For the preparation of complexes that were especially air-sensitive, freeze-thaw de-gassing was employed. This was essentially the same procedure as described above, except that the solvent was solidified by immersing its container in liquid nitrogen. The atmosphere above the solvent was evacuated as before and the solvent was allowed to reach room temperature whilst the pump was connected to the Schlenk tube. This procedure was repeated twice, then the tube was pressurized with nitrogen.

(iii) To Remove Solvent From The Reaction Mixture

The Schlenk tube containing the reaction mixture was connected to the vacuum line via taps E and C, as before. Tap C was kept closed and tap 3 opened. In order to ensure that evaporation was not too vigorous, E was half-opened. The trap was kept full of liquid nitrogen. Warming of the Schlenk tube was effected by surrounding the tube with a warm water bath, this speeded up evaporation and ensured the reaction mixture did not freeze. At the end of the operation, tap 3 was closed and the apparatus pressurized with nitrogen, as before.

(iv) Reflux

A Schlenk tube containing solvent and air-stable reactants was connected to the line via a condenser at B, as shown in fig. 42. The apparatus could be flushed out with nitrogen for five minutes (2 closed, B and E open), then any solid that was air sensitive in solution was added by momentarily dismantling the apparatus at F and adding the reactant through the neck of the Schlenk tube. This operation was carried out in a positive stream of nitrogen by connecting E to C (E open, C open, B and 3 closed). Thereafter, the apparatus was reassembled and flushed out with nitrogen as before, for a further five minutes. During reflux, E was closed but B kept open. Stirring was effected by means of a magnetic stirrer, placed within the tube and the tube was generally heated using an oil bath. All glass joints were greased using Hard Grade High Vacuum Grease.

The technique was modified for more air-sensitive systems. The apparatus was first evacuated (E, B closed, 2 open) and then filled with nitrogen (2 closed, B open). This procedure was repeated a number of times. In this case, the Schlenk tube contained solid reactants and de-gassed solvent was added after thoroughly flushing out the apparatus with nitrogen. The solvent was added from a glass syringe, so that it was necessary to use a two-necked tube, one neck sealed with a rubber Suba-seal. After these precautions, reflux proceeded as before.

(v) Filtration of Air Sensitive Systems

A Schlenk-type filtration apparatus which contained sintered glass (as shown in fig. 43) was used.

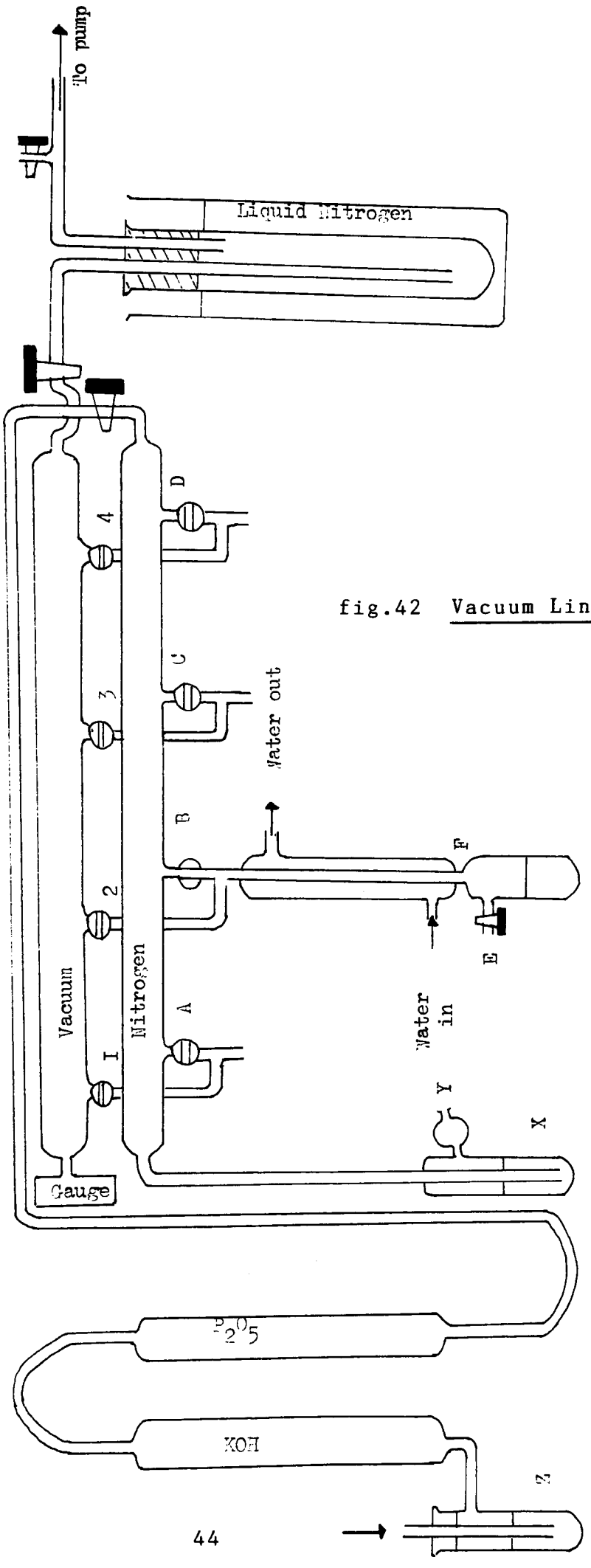

fig.42 Vacuum Line Apparatus

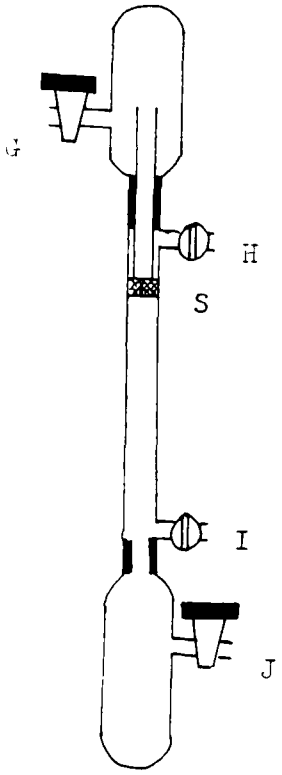

fig. 43 Filtration of Air Sensitive Systems

Schlenk tube J, which contained the reaction mixture, was connected to the apparatus whilst blowing an upward stream of nitrogen over the reaction mixture through the tap at J. The filtration apparatus, which had an empty Schlenk tube attached to its upper end, was connected to the vacuum system (G open and to vacuum, H, I, closed). In this way, as the tube was connected to J, nitrogen was pumped over the reaction mixture and upwards, minimising exposure of the reaction mixture to air. When the apparatus was considered free of air, tap G was closed. The tap

at J was closed when the apparatus was pressurized with nitrogen. The whole was inverted, then nitrogen pumped in at J and vacuum connected at G so that the reaction mixture was pumped through the sinter at S. Solid product that collected on the sinter, could be dried by continuing to pump at G, after closing the tap at J.

(vi) Nmr Spectra

Nitrogen gas was bubbled through the de-gassed solvent contained in the nmr tube, prior to introduction of the solid to be examined. The tube was then sealed with a Suba-seal. Oxidation of the sample was difficult to prevent when nmr spectra were run over a period of some hours (for example ^{31}P nmr spectra). In these cases, it was sometimes useful to run several different spectra at different times (with integration), in order to ascertain which signals might be due to oxidation products. All ^{13}C and ^{31}P nmr spectra included in this work are proton-decoupled. Chemical shifts are expressed in ppm relative to TMS (^{1}H nmr), $CDCl_3$ (^{13}C nmr) and 85% H_3PO_4 (^{31}P nmr) respectively.

2.2 CATALYTIC HYDROGENATION APPARATUS

The apparatus used to measure uptake of hydrogen is shown in fig. 44.

(i) Hydrogenation

The solvent was placed in the flask at A, then connected to the vacuum pump by opening taps B and F, whilst keeping taps C, D, H and E closed. Agitation of the solvent was achieved by operating the magnetic stirrer

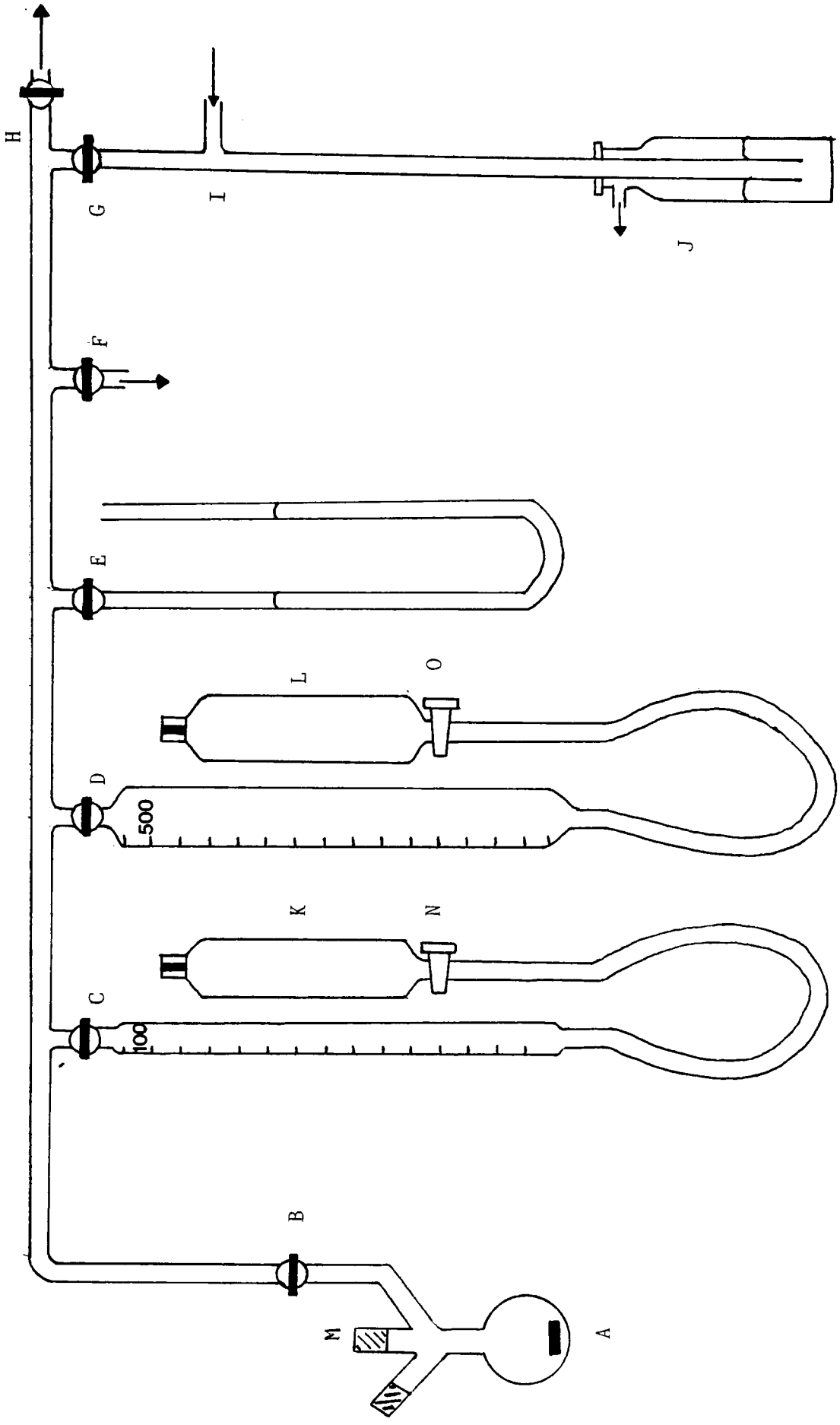

fig.44 Hydrogenation Apparatus

in the flask at A. When bubbles appeared in the solvent, tap F was closed and hydrogen introduced by opening tap G until the apparatus was pressurized i.e. bubbles of hydrogen appeared at J. Tap G was then closed and the operation repeated three times until the apparatus was flushed out with hydrogen. Tap E was used to check the efficiency of the vacuum system. The sample was introduced through the glass stopper at M into the flask at A under a positive stream of hydrogen i.e. taps G and B open, the rest closed. The stopper at M was then greased and replaced. The graduated glass tubes and reservoirs at K and L had been previously filled with water. The reservoirs could be clamped at various heights and initially were kept at a higher level than the graduated glass tubes, so that the tubes were full of water to taps C and D. The stoppers in reservoirs K and L had ridges cut in them so that the contents of K and L were open to atmospheric pressure.

After introduction of the previously weighed sample, the line was again flushed out with hydrogen as previously described, then with taps G, C, B and N open, a volume of hydrogen (ca. 70 cm^3) was introduced into the graduated glass tube associated with reservoir K (reservoir L could be used if larger volumes of hydrogen were needed). The tap at C was closed and when bubbles of hydrogen appeared at J, tap G was closed. Tap C was opened and an initial reading of the volume of water in the graduated tube taken, whilst simultaneously adjusting the height of the reservoir at K. This was done by keeping the level of liquid in K the same as that in the graduated tube associated with it. After the initial reading had been taken, the timer was started and the agitated mixture of sample and solvent left under hydrogen. The volume of water in the graduated tube was read (as previously described), at ten minute intervals until it reached a minimum value, thereafter the system was left for twenty-

four hours and a final reading taken.

In this way, the volume of hydrogen that had reacted with the sample could be determined and by correcting the reading to standard temperature and pressure, the number of mol of hydrogen that could react with one mol of sample could be ascertained. Atmospheric pressure was read using a mercury barometer.

The mixture at A was taken and concentrated, then a precipitate obtained by addition of petroleum ether (60/80). Infra-red spectra of both precipitate and solution were examined for the presence of metal-hydride bands.

(ii) Catalytic Hydrogenation

The procedure was essentially as described for hydrogenation, except that a weighed mass of catalyst (ca. 0.03 g) was introduced into a known volume of solvent (20 cm^3), containing a known amount of oct-1-ene (ca. 0.10 g) at A. The solvent and alkene were de-gassed and flushed out with hydrogen as previously described, before introduction of the catalyst. After a period of time under hydrogen, the mixture was analysed using gas chromatography.

2.3 INSTRUMENTATION

Analyses were carried out by Butterworth Laboratories Ltd., Middlesex and MEDAC Ltd., Brunel University. Electronic spectra were measured on a Perkin Elmer Lambda 3 uv/vis spectrophotometer, infra-red spectra (4000-600 cm^{-1}) on a Perkin Elmer 681 spectrophotometer in conjunction with a Perkin Elmer 3600 data station and far infra-red spectra

(600-250 cm^{-1}) on a Perkin Elmer 580 spectrophotometer (high resolution) or a Perkin Elmer 457 specrophotometer (low resolution). ^{1}H, ^{13}C, and ^{31}P nmr spectra were obtained using a JEOL FX90Q 90MHz Fourier Transform spectrophotometer. Gas chromatographs were obtained using a Perkin Elmer F17 gas chromatography apparatus. Mass spectrometry was provided by the SERC Mass Spectrometry Centre, University of Swansea. Magnetic moments were obtained by using the Gouy Method at room temperature, using $Hg[Co(NCS)_4]$ as calibrant.

2.4 MATERIALS

(i) Solvents were purified as follows:

Toluene This was purchased free from sulphur, distilled prior to use (b.pt. 110-112 °C), then stored over sodium wire.

Diethyl Ether If exposed to air for some time, this could contain peroxides. Therefore, samples were regularly tested by shaking with an equal volume of 2% potassium iodide solution and a few drops of hydrochloric acid. The liberation of iodine indicated the presence of peroxides, which could be removed by shaking with 10 to 20 cm^3 of a concentrated solution of iron(II) sulphate with 1 dm^3 of ether. The concentrated solution of iron(II) sulphate was prepared from the iron(II) salt (15 g), concentrated sulphuric acid (1.5 cm^3) and 28 cm^3 of water.

Petroleum Ether (60/80) This was distilled (b.pt. 60-80 °C) and then stored over sodium wire.

THF This was distilled prior to use (b.pt. 66-68 °C), then stored over sodium wire.

Methanol This was distilled through an efficent fractionating column prior to use (b. pt. 65-67 °C) and stored over molecular sieves (3A).

(ii) Chemicals Pyrazoles were of commercial origin and used without further purification, as was $NiCl_2.6H_2O$. "Ruthenium chloride trihydrate" and potassium hexachloropalladate(II) were obtained on loan from Johnson Matthey Chemical Co.. The commercial ruthenium salt, although containing Ru(II) species such as $RuCl_3.3H_2O$, appears also to contain some polynuclear Ru(IV) complexes[48], but for the purposes of calculation its formula was taken as that on the container.

SECTION THREE NICKEL-PYRAZOLE COMPLEXES

3.1 NICKEL COMPLEXES-INTRODUCTION

(a) The following sections describe the preparation of nickel pyrazole complexes and their reactions with strong bases. The objective was to establish a general method for the preparation of μ^2-pyrazolyl dimers and experiments were conducted using nickel(II) complexes for the following reasons:-

(i) Pd(II) and Pt(II) pyrazole complexes have been utilized to generate mixed-metal dimers[36], by using methods described in [1.5]. Comparisons between first and second or third row transition metals are not always of value. However, since these two ions also have the d^8 electronic configuration, analogous Ni(II) systems may exist.

(ii) Nickel(II) complexes are inexpensive to prepare and are generally air-stable.

(iii) Many nickel complexes have characteristic properties such as colour, absorption spectra and magnetic behaviour which are indicative of oxidation state, coordination number and stereochemistry. This often makes identification of structure relatively straightforward.

(b) Characteristic properties of Ni(II) complexes may be summarized[48] as follows:-

(i) Colour and Absorption Spectra The maximum coordination number of Ni(II) is six. The hexaquonickel(II) ion is bright green and displacement of water molecules by neutral ligands, especially amines

results in complexes which are characteristically blue or purple. Four-coordinate, paramagnetic "tetrahedral" Ni(II) complexes also tend to be blue or green unless the ligands have absorption bands in the visible region. Distinction between the two types of complexes may be made however, in that octahedral complexes have three spin allowed d--d transitions and the molar absorbances are low, namely between 1 and 10. These transitions are Laporte forbidden, but molecular vibrations destroy the symmetry of the complex during oscillation, allowing hybridization of d and p orbitals to occur and so making different orbitals no longer equivalent. Weak bands are therefore observed. Hybridization occurs directly in complexes that do not possess a centre of symmetry and as a result, stronger molar absorbances are demonstrated. This allows a basis for differentiation between tetrahedral ($\epsilon \approx 10^2$) and centrosymmetric octahedral or pseudo-octahedral Ni(II) species. The spin-allowed transitions for Ni(II) complexes of O_h symmetry may be assigned[49]:

$$^3A_{2g} \rightarrow {}^3T_{2g}(F) \quad \nu_1$$
$$^3A_{2g} \rightarrow {}^3T_{1g}(F) \quad \nu_2$$
$$^3A_{2g} \rightarrow {}^3T_{1g}(P) \quad \nu_3$$

Four coordinate, diamagnetic, planar complexes of Ni(II) are frequently red, yellow or brown owing to the presence of an absorption band of medium intensity ($\epsilon \approx 60$) in the range 450-600 nm.

(ii) Magnetic Moment The electronic configurations of the d^8 Ni(II) ion in fields of different symmetries are shown in fig. 45. Although, in principle, a square planar d^8 complex could be high spin with unpaired

electrons in the $d_{x}2-y2$ and $d_{z}2$ orbitals, in practice, this is highly unusual and diamagnetism tends to be indicative of square planar symmetry.

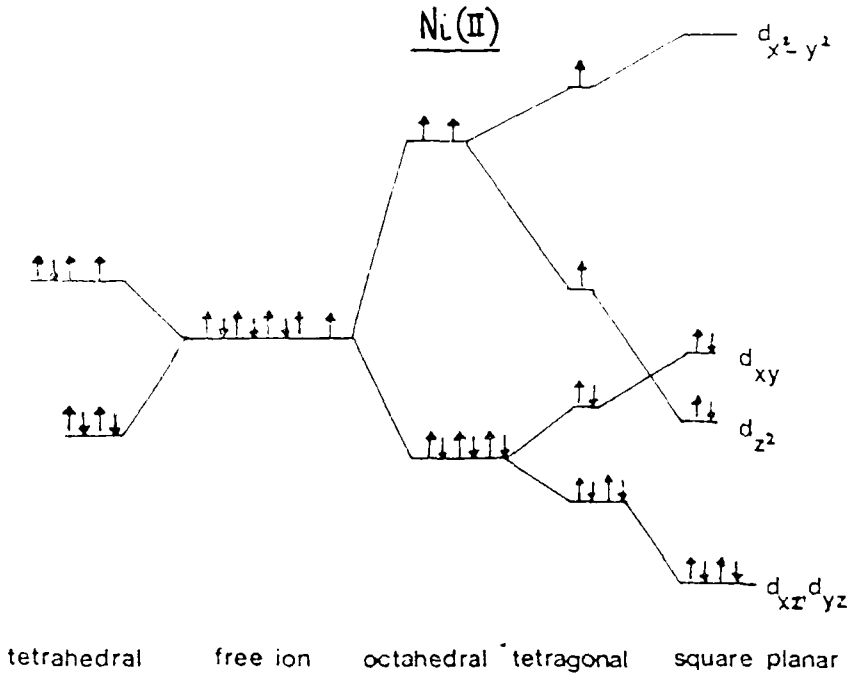

fig. 45 Electronic Configurations of Ni(II)

Both tetrahedral and octahedral/tetragonal symmetries result in unpaired electrons and as a consequence, such complexes exhibit paramagnetism. The "spin only" magnetic moment is calculated as 2.83 BM, but both complexes generally have moments higher than this; tetrahedral complexes have a temperature-dependent orbital contribution built into the

magnetic moment, so that the magnetic moments of these compounds are found to lie in the range 3.2 - 4.1 BM[50], whereas in octahedral/tetragonal complexes there is a small, temperature independent orbital contribution because of spin-orbit coupling between the first excited state $^3T_{2g}(F)$ and the ground state $^3A_{2g}(F)$ (fig. 49). This gives an expression for the magnetic moment:

$\mu = \mu_{spin\ only}\ (1 - 4\lambda/10\ Dq)$

λ = spin orbit coupling constant

10 Dq = the energy separation between the interacting levels

In fact, the values usually fall between 2.9 and 3.3 BM and are almost independent of temperature.

3.2 EXPERIMENTAL

(i) Preparation of $NiCl_2(PPh_3)_2$[51] A solution of hydrated nickel(II) chloride (1.20 g, 5.04 mmol) in ethanol (15 cm^3) was boiled for five minutes and then added to a mixture of refluxing triphenylphosphine (2.80 g, 10.68 mmol) in propan-2-ol (30 cm^3). The dark green crystals obtained were washed with hot ethanol (15 cm^3) and dry diethyl ether (15 cm^3). Yield = 0.90 g (28%).

(ii) Preparation of $NiCl_2(pzH)_4$ Pyrazole (0.80 g, 11.8 mmol) was added to a solution of $NiCl_2(PPh_3)_2$ (1.80 g, 2.75 mmol) in THF (50 cm^3) and the mixture stirred for 30 minutes at room temperature, then cooled to 2 - 3 °C for a further 30 minutes. The pale blue solid that precipitated was filtered and washed with a small amount of petroleum

ether (60/80) (15 cm^3), then dried in vacuo. Yield = 1.00 g (91%).

Analysis

Calculated for $C_{12}H_{16}Cl_2N_8Ni$: C 35.8% H 4.0% N 27.9%

Found* : C 34.7% H 3.9% N 26.7%

A Lassaigne fusion test indicated the presence of chlorine.

(iii) Preparation of $NiCl_2(DMpzH)_2$ The complex was prepared according to a general method described by Guichelaar et al.[52]. Hydrated nickel chloride (0.20 g, 0.84 mmol), was dissolved in boiling ethanol (25 cm^3) and DMpzH (0.20 g, 2.08 mmol) added. After stirring for 30 minutes, the resultant green solution was concentrated to ca. 5 cm^3 and diethyl ether added slowly until a yellow precipitate was obtained. The solid was filtered, washed with with ethanol (10 cm^3) and diethyl ether (10 cm^3), then dried in vacuo. Yield = 0.14 g (54%).

(iv) Preparation of $[Ni(pz)_2.H_2O]_n$ The complex $NiCl_2(pzH)_4$ (0.40 g, 1.00 mmol) was dissolved in methanol (50 cm^3) and excess triethylamine (0.60 g, 5.94 mmol) added. The mixture was stirred at ambient temperature for 30 minutes, whereupon a yellow precipitate formed which was filtered off and washed with methanol (10 cm^3) followed by diethyl ether (10 cm^3). The product was dried in vacuo at 95 °C for five hours. Yield = 0.20 g, (95%).

---

* Initial experiments consisted of reacting pyrazole with $NiCl_2.6H_2O$ in a molar ratio of less than 4 : 1. In this case, the product may well have been contaminated with $NiCl_2(pzH)_2$ which is formed[53] when the molar ratio of pyrazole to Ni(II) salt is slightly less than 2 : 1.

Analysis

Calculated for $C_6H_8N_4ONi$: C 34.1% H 3.7% N 26.5%

Found : C 34.7% H 3.1% N 26.6%

A Lassaigne fusion test indicated the absence of chlorine.

3.3 REACTION OF $NiCl_2(PPh_3)_2$ WITH PYRAZOLE

Reaction of the dark green tetrahedral complex $NiCl_2(PPh_3)_2$ with pyrazole [3.2(i), 3.2(ii)], yielded a pale blue product, characterized by analysis and spectroscopic measurements as trans-$[NiCl_2(pzH)_4]$. The complex had previously been prepared[54] by the reaction of $NiCl_2.6H_2O$ with pyrazole.

(i) Infra-Red Spectra (4000-600 cm^{-1})

The infra-red spectra of the precursor $NiCl_2(PPh_3)_2$ and the product trans-$[NiCl_2(pzH)_4]$ are shown in figs. 46 and 47. Evidence for the coordination of pyrazole is shown by the strong bands at 3300 cm^{-1} and 1140 cm^{-1} in fig. 47, assigned to the N—H stretch and N—H bend in pyrazole[55]. Both bands are absent in the spectrum in fig. 46. Conversely, the P—aryl stretch[56], strongly evident in the spectrum of $NiCl_2(PPh_3)_2$ at 1430 cm^{-1}, is absent in the spectrum of the product.

(ii) Electronic Spectrum

The complex trans-$[NiCl_2(pzH)_4]$ was sufficently soluble in methanol to permit the study of its electronic spectrum in solution. Previous studies[54] have found the compound to be insoluble in most common organic

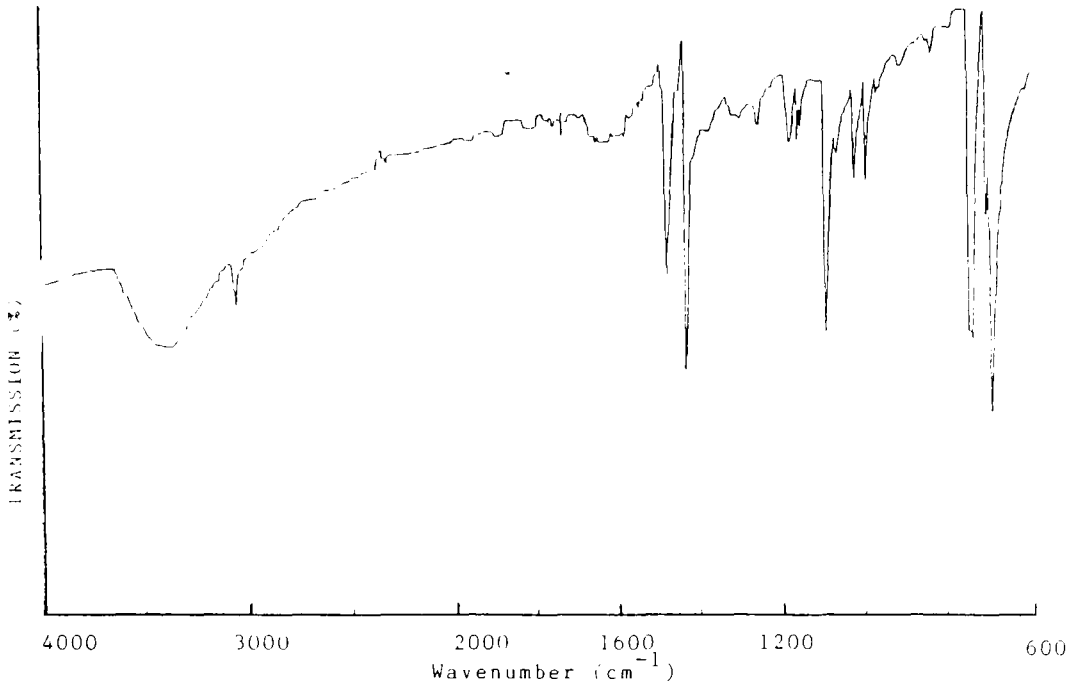

fig.46 Infra-red Spectrum of $NiCl_2(PPh_3)_2$ (KBr disc)

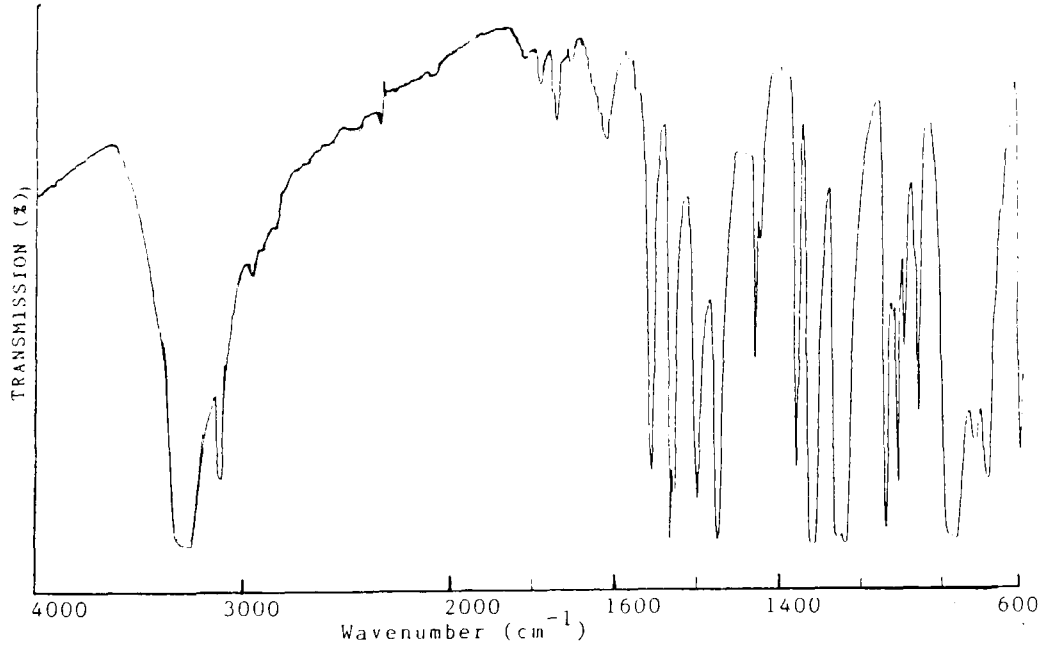

fig.47 Infra-red Spectrum of trans-$[NiCl_2(pzH)_4]$ (KBr disc)

solvents and consequently available data are confined to its reflectance spectrum. The absorption spectra obtained are characteristic of a pseudo-octahedral Ni(II) complex (fig. 48).

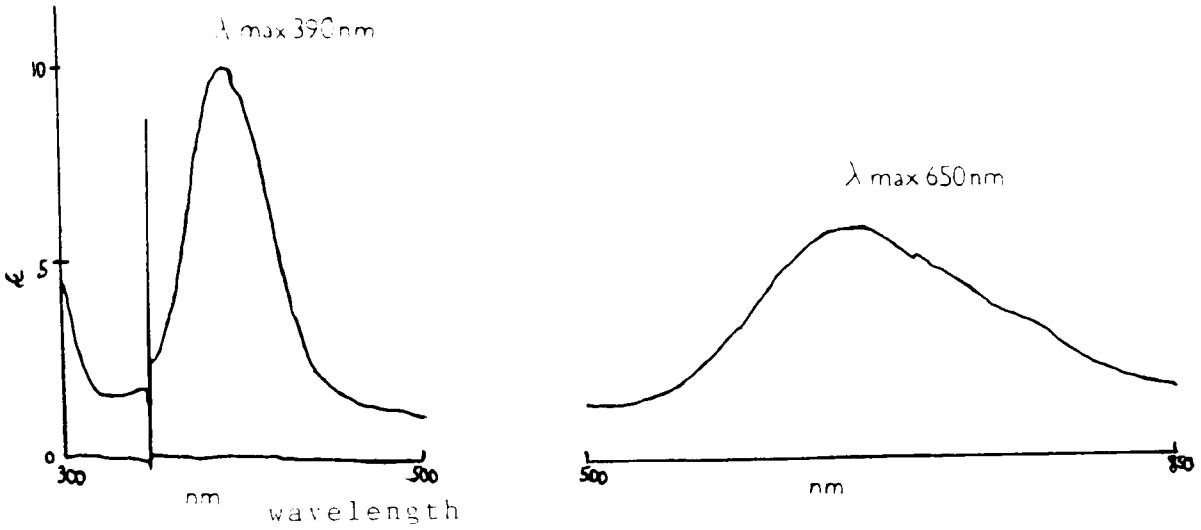

fig. 48 Electronic Absorption Spectrum of trans-$[NiCl_2(pzH)_4]$ in MeOH [0.045 mol dm^{-3}]

Available instrumentation allowed the study of the ν_2 (650 nm, 15,400 cm^{-1}) and ν_3 (390 nm, 25,600 cm^{-1}) transitions [3.1(b)]. Both bands have a Gaussian-like shape, the ν_2 band having a slight shoulder at approximately 760 nm (13,200 cm^{-1}), which may be explained by considering the true symmetry of the complex. Geometric distortions and/or non-identical donor atoms will cause departures from O_h symmetry; subsequent investigation of the far infra-red spectrum of the complex indicated tetragonal (D_{4h}) symmetry, in which case the orbital triplets $^3T_{1g}$ and $^3T_{2g}$ undergo further splitting[57] (see fig. 49).

The resolution obtained from reflectance spectra[54,57], results in five observed bands, three of which occur in the wavelength range studied in solution. The solution spectrum obtained in fig. 48 is broadened as

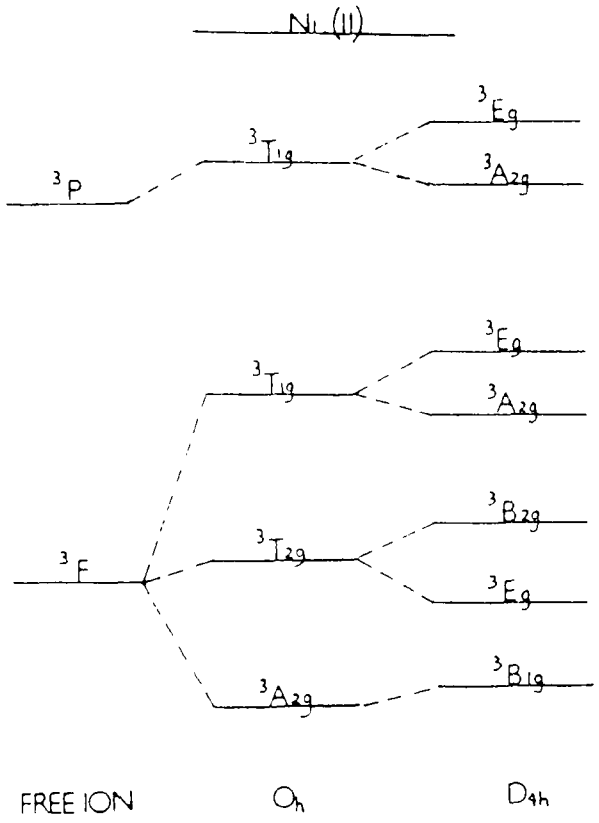

fig. 49 Energy Levels for Different Field Symmetries

compared with the reflectance spectrum, but on the basis of previous interpretation of the electronic absorption spectrum of this complex, the v_2 and v_3 bands are identified with the following spin allowed transitions:

v_2 $\left[\begin{array}{l} {}^3B_{1g} \rightarrow {}^3A_{2g}(F) \\ {}^3B_{1g} \rightarrow {}^3E_g(F) \end{array}\right.$

v_3 ${}^3B_{1g} \rightarrow {}^3E_g,\ {}^3A_{2g}(P)$

(iii) Far Infra-Red Spectrum (610-200 cm^{-1})

The spectrum was shown by scanning a nujol mull of the sample pressed between polythene plates and is shown in fig. 50.

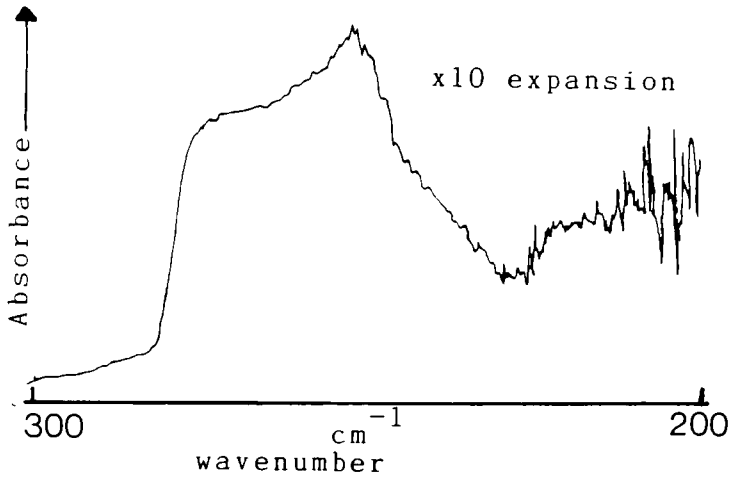

fig. 50 Far Infra-red Spectrum of trans-$[NiCl_2(pzH)_4]$

It shows a strong band at 250 cm^{-1} with a shoulder at approximately 270 cm^{-1} and is in good agreement with previous work[58].

If the pyrazole groups are regarded as point masses, then an isolated molecule of trans-$[NiCl_2(pzH)_4]$ would have D_{4h} symmetry. Group theory generates the following representations for the bonds within the complex:

$$\Gamma_{\nu}(M—X) = a_{1g}(R) + a_{2u}(I.R.)$$

$$\Gamma_{\nu}(M—N) = a_{1g}(R) + b_{1g}(R) + e_{u}(I.R.)$$

Therefore, two bands would be expected in the far infra-red spectrum of this complex, ν(Ni—Cl) and ν(Ni—N). The crystal structure of trans-$[NiCl_2(pzH)_4]$, however, is given in fig. 51 and shows that there

are two non-equivalent pairs of pyrazole rings around each metal atom, lowering the symmetry of the isolated molecules to C_i. It also shows that there is an unusually long Ni—Cl bond distance of 2.507 Å, which is attributed to the fact that attractive forces exist between the pyrazole and chloride groups. The N—H groups in pyrazole point towards the coordinated halide ions resulting in two hydrogen bond interactions per halide ion. These interactions reduce the effective field of the halide ions and this reduction manifests itself directly in the longer Ni—Cl bond lengths.

The foregoing discussion generates two points which must be considered when interpreting the spectrum in fig. 50. Firstly, from the site symmetry (also C_i), one $\nu(M—X)_{au}$ mode and two $\nu(M—N)_{au}$ modes would be expected in the infra-red spectrum. The bands observed are attributed to $\nu(M—N)_{au}$ modes, from comparison with $NiCl_2(py)_4$. Secondly, the long Ni—Cl bond length, makes ν(Ni—Cl) fall below 200 cm^{-1}, out of the

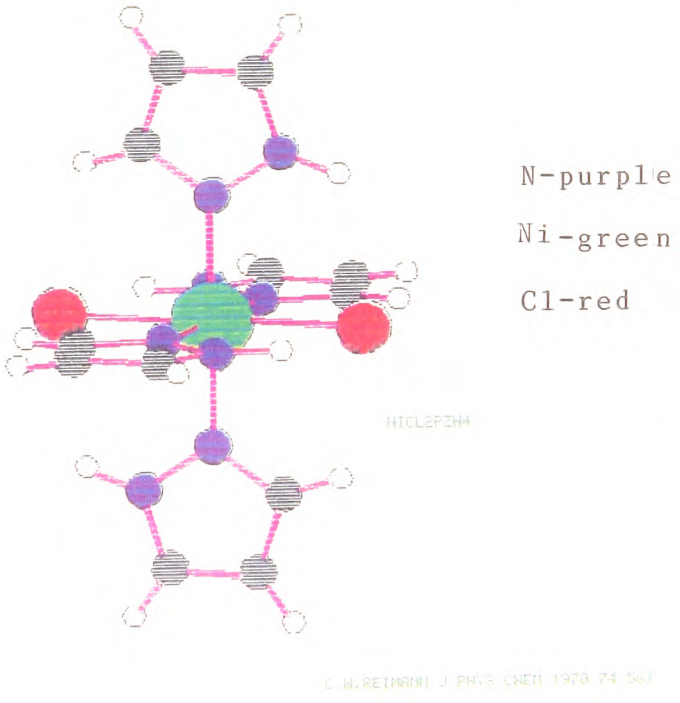

fig. 51 Structure of trans-$[NiCl_2(pzH)_4]$

range of the instrument used. Goldstein and Unsworth[58] observed the band at 185 cm^{-1}.

(iv) Magnetic Moment

The magnetic moment of trans-$[NiCl_2(pzH)_4]$ was measured at 19 °C and found to be 3.29 BM, so satisfying the magnetic criterion for a pseudo-octahedral Ni(II) complex and in reasonable agreement with a previous determination[54] (3.19 BM).

3.4 PREPARATION OF $NiCl_2(DMpzH)_2$

The reaction of hydrated nickel(II) chloride with 3,5-dimethylpyrazole [3.2(iii)], gave $NiCl_2(DMpzH)_2$. The same product was obtained from the reaction of $NiCl_2(PPh_3)_2$ with 3,5-dimethylpyrazole, as identified by its infra-red spectrum.

The infra-red spectrum of the complex is shown in fig. 52. It appears to be easily hydrated; the yellow precipitate from [3.2(iii)] contains green solid until thoroughly dried. The infra-red spectrum of this mixture shows the presence of water from broad bands at 3400 cm^{-1} (O—H str.) and 1640 cm^{-1} (O—H bend). Here, it is assumed that Ni(II) adopts the six-coordinate, pseudo-octahedral structure that is common in many of its complexes, by the addition of water molecules as ligands. Solutions of $NiCl_2(DMpzH)_2$ in acetone are deep purple; this is a reversible process, in that, concentration of the solution (by removing acetone at reduced pressure) changes its colour to dark green. Addition of acetone again restores the purple colour to the mixture. Attempts at isolating the purple solid, however, proved unsuccessful. Slow

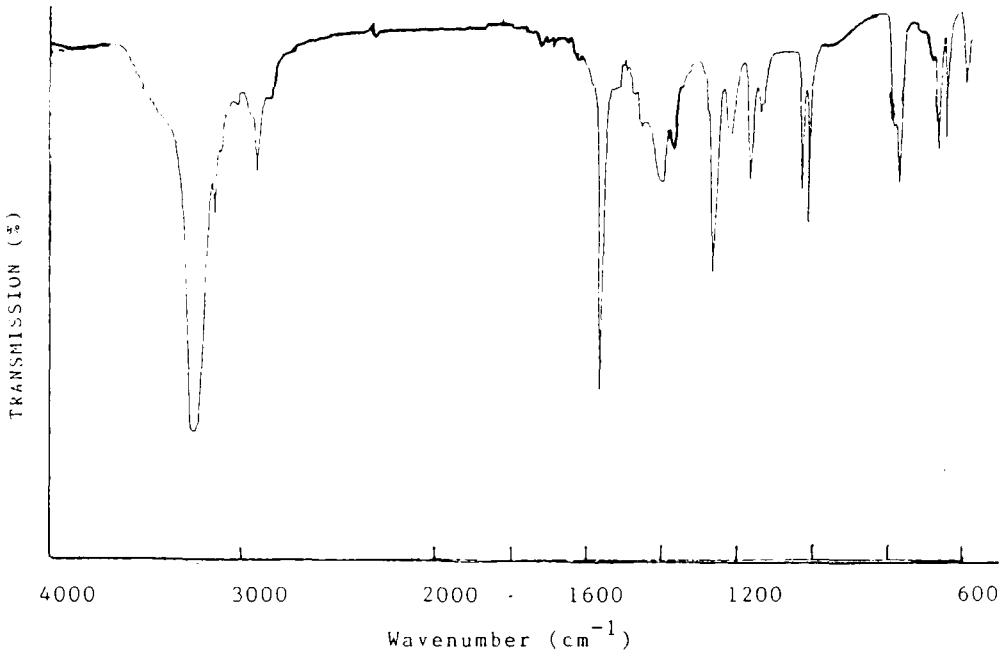

fig. 52 Infra-red Spectrum of $NiCl_2(DMpzH)_2$ (KBr disc)

evaporation of the solvent or precipitation of solid by concentrating the solvent and adding diethyl ether, gave the yellow $NiCl_2(DMpzH)_2$, as characterized by its infra-red spectrum.

3.5 REACTION OF NICKEL - PYRAZOLE COMPLEXES WITH BASE

(i) The Reaction of trans-$[NiCl_2(pzH)_4]$ with Triethylamine in Methanol

This reaction [3.2(iv)] gave a yellow product, characterized by analysis, spectroscopy and magnetic measurements as the polymeric $[Ni(pz)_2.H_2O]_n$.

Magnetic measurements showed the product to be diamagnetic, indicating square planar geometry [3.1(b)]. The compound proved to be insoluble in all common organic solvents and failed to vaporize when subjected to

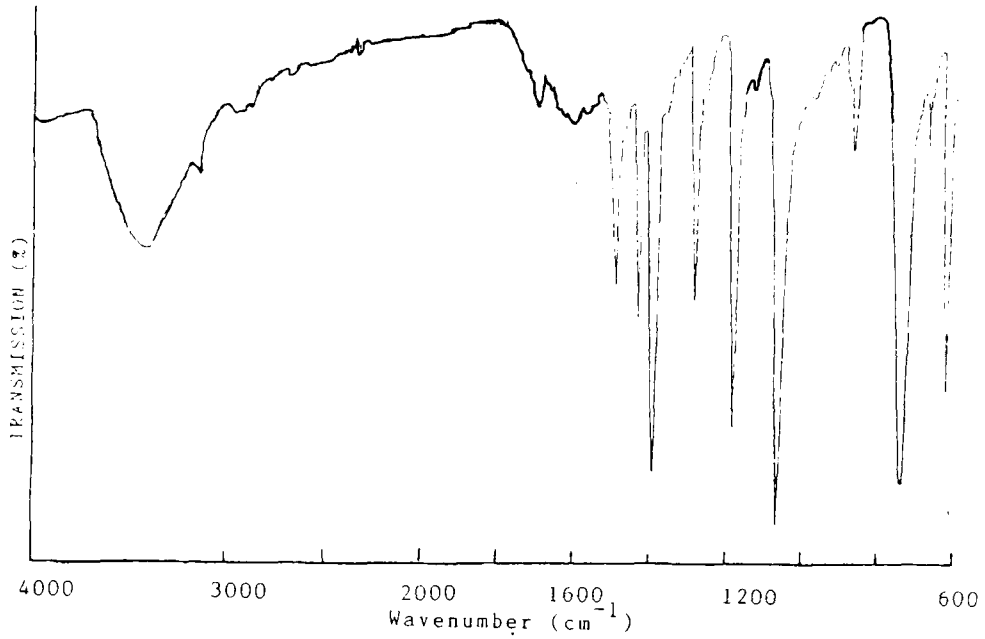

fig. 53 Infra-red Spectrum of $[Ni(pz)_2.H_2O]_n$ (KBr disc)

BAND	INTENSITY	ASSIGNMENT
3420	br., m	O—H str., water,
3120	w	C—H str., pyrazole
1700	w	
1600	w	O—H bend, water
1490	m	ring stretch, pyrazole
1430	m	ring stretch, pyrazole
1395	s	ring stretch, pyrazole
1290	m	C—H bend, pyrazole (in plane)
1185	s	C—H bend, pyrazole (in plane)
1170	s	C—H bend, pyrazole (in plane)
875	w	C—H bend, pyrazole (out of plane)
745	s	C—H bend, pyrazole (out of plane)
680	w	ring deformation, pyrazole
630	m	ring deformation, pyrazole

Electron Ionisation and Chemical Ionisation techniques, in attempts to obtain a mass spectrum. The insolubility and non-volatility of the compound, indicate a polymeric nature.

The infra-red spectrum of the product is shown in fig. 53, together with assignment of the bands[59]. Broad absorbances at 3420 cm^{-1} and 1600 cm^{-1} indicate the presence of water. The band at 3420 cm^{-1} obscures the absence of a N—H stretch, but the absence of a N—H bend at ca. 1140 cm^{-1}, provides evidence for deprotonation.

The yellow polymeric species $[Ni(pz)_2]_n$ has been previously reported from the reaction of a pyrazole solvated metal complex of nickel and a solution of sodium hydroxide, or by dissolving nickel salts and pyrazole in aqueous ammonia[60]. The structure of $[Ni(pz)_2]_n$ is suggested to be as shown in fig. 54. No water is reported present, although it has been found in similar complexes of copper[61] and other complexes of Ni(II) that contain substituted pyrazolyl ligands[62].

It is probable that the prepared complex $[Ni(pz)_2.H_2O]_n$ has a similar structure to that shown in fig. 54 i.e. bidentate pz^- ligand with C_{2v} symmetry, bridging two metal atoms. This results in a chain structure and square planar arrangement of ligands around each Ni(II) ion. The structure is "well fitting" and highly symmetric.

Coordination of one water molecule to each Ni(II) ion, seems unlikely in that most square pyramidal complexes are high spin and therefore paramagnetic. Analogous Cu(II) complexes have one water molecule bridging between two metal ions , but again, this seems unlikely in the case of the Ni(II) complex; a distorted octahedral structure should result, which would be expected to exhibit paramagnetism. It is suggested, therefore, that water does not enter the first coordination sphere of the nickel. Vos et al.[61] refer to "the presence of cavities in

pyrazolato salts where the metal ions are square planar (D_{4h}) coordinated by the nitrogen atoms of the anions". Such cavities may well occlude water molecules.

The solvent for the reaction was reagent grade methanol and this was presumed to be the source of any water found in the complex $[Ni(pz)_2 \cdot H_2O]_n$. Methanol was used, however, because of its ability to dissolve both the precursor complex trans-$[NiCl_2(pzH)_4]$ and the product obtained on deprotonation of the coordinated pyrazole groups, $Et_3NH^+Cl^-$. The same reaction, when carried out in toluene or chloroform, gave impure products with infra-red spectra which gave absorbances around 2500 cm^{-1}. This indicates the $N—H^+$ stretch of an amine hydrohalide (c.f. the infra-red spectrum of $Et_3NH^+Cl^-$, fig. 55). The presence of these absorbances was taken as additional indication that deprotonation had taken place.

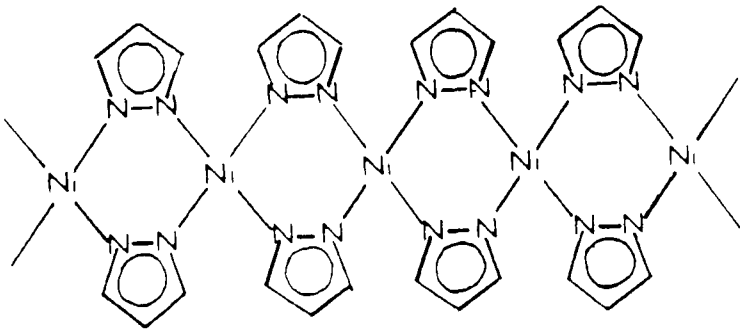

fig. 54 Structure of $[Ni(pz)_2]_n$

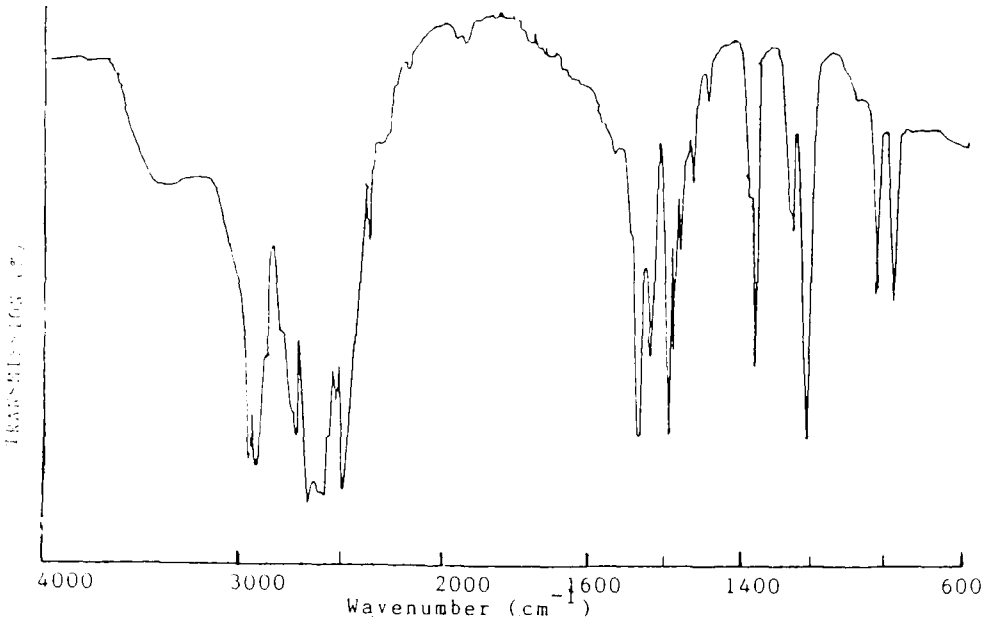

fig. 55 Infra-red Spectrum of $Et_3NH^+Cl^-$ (KBr disc). The absorbance at 2500 cm^{-1} is taken as $\nu(N—H^+)$. The compound was prepared by reacting conc. HCl with triethylamine in THF, it was formed as a white precipitate.

The same reaction was also carried out using a "proton sponge" [1,8-bis(dimethylamino)napthalene] instead of triethylamine. The molecule is a strong base but weak nucleophile, because of steric effects[63] (fig. 56) and is therefore unlikely to coordinate with the nickel ion. The product of the reaction, gave an infra-red spectrum identical to that of $[Ni(pz)_2.H_2O]_n$.

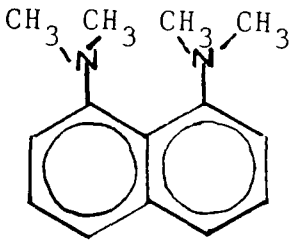

fig. 56 1,8-bis(dimethylamino)napthalene

(ii) Reaction of $NiCl_2(DMpzH)_2$ with Triethylamine

The complex was reacted with triethylamine in acetone. The purple mixture was stirred for about an hour, then concentrated by evaporation under reduced pressure. Precipitation was effected by adding diethyl ether slowly. This yielded a yellow precipitate whose infra-red spectrum was identical with that of the starting material.

Reactions between nickel salts and 3,5-dimethylpyrazole in the presence of sodium hydroxide[61] also failed to yield a product analogous to $[Ni(pz)_2.H_2O]_n$. Vos et al. suggested that methyl groups substituted in the 3 and 5 positions on pyrazole, prevent the expected square planar coordinations of the metal ions by steric hindrance. This work suggests that a more satisfactory explanation as to why Ni(II) complexes with 3,5-dimethylpyrazole do not appear to react with strong bases, is obtained by considering electronic, rather than steric effects. Singh et al.[62] have reported the preparation of the octahedral, polymeric species $[Ni(DMpz)_2.2H_2O]_n$ (fig. 57) by a method that does not involve deprotonation i.e. the condensation reaction of a bis-acetylacetonato Ni(II) complex with hydrazine hydrate. This indicates that inability to remove a proton from coordinated 3,5-dimethylpyrazole and not the geometry of the product is the reason for the failure of the aforementioned experiments. On coordination of pyrazole to a metal centre, the positive charge of the metal ion draws electron density from the ligand by σ induction, depleting the electron density on the pyrrole nitrogen and lowering the pK_a, hence coordinated pyrazole loses a proton more easily than the free ligand[8]. Methyl substituted pyrazoles, contain electron releasing methyl groups, so the pK_a of both the free and coordinated ligand should be higher than that observed for unsubstituted

pyrazole, making removal of the proton attached to the pyrrole-type nitrogen, more difficult.

Complexes of methyl substituted imidazoles show similar electronic effects in that the pK_a of the ligand increases with increased substitution[64] and with proximity of substituents to the pyrrole hydrogen[8].

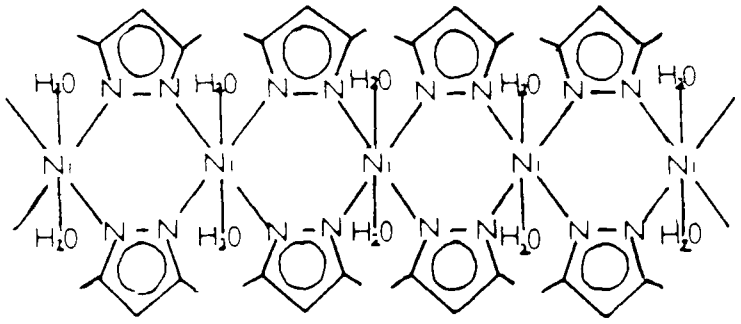

fig.57 Structure of $[Ni(DMpz)_2.2H_2O]_n$

3.6 DISCUSSION-NICKEL PYRAZOLE COMPLEXES

Retention of "end-capping" ligands prevents polymerisation of the product obtained by deprotonation of coordinated pyrazole, as described in section 1.4. Accordingly, in an attempt to prepare novel μ^2-pyrazolyl bridging nickel species, a number of experiments were conducted with the objective of synthesizing a nickel pyrazole complex that also retained phosphine ligands. As has been shown, the reaction of $NiCl_2(PPh_3)_2$ with pyrazole in THF yields trans-$[NiCl_2(pzH)_4]$ and it is apparent that

triphenylphosphine does not complex with nickel halides in ethanol[65], instead butanol is a preferred solvent[66]. The preparation was therefore repeated in butan-1-ol and tertiary butanol respectively, but in both cases the product was trans-$[NiCl_2(pzH)_4]$.

The complex $[NiCl_2(dppe)]$) was prepared by the reaction of the nickel halide with 1,2-bis(diphenylphosphino)ethane in ethanol, as described by Booth et al.[67]. The diamagnetic, yellow-brown complex (fig. 58) derives a certain stability from its chelating ligand. This so-called "chelate effect"[48] refers to the enhanced stability of a complex system containing chelate rings, as compared with the stability of a system that is as similar as possible, but contains none or fewer rings. The five-membered ring that is created by coordination of this particular ligand to a metal, is especially stable[68].

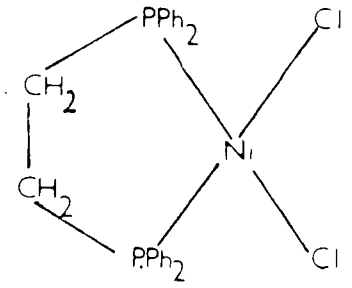

fig. 58 Structure of $[NiCl_2(dppe)]$

Addition of excess pyrazole (greater than 6: 1 molar ratio) to a solution of $[NiCl_2(dppe)]$ in THF produced a yellow solution from which precipitated trans-$[NiCl_2(pzH)_4]$. If the molar ratio of pyrazole to nickel complex was lower than this, concentration of the yellow

solution, followed by addition of diethyl ether, gave a green precipitate which was found to be a mixture of trans-$[NiCl_2(pzH)_4]$ and $[NiCl_2(dppe)]$. The separation of these was effected by dissolving the green precipitate in acetone, in which the pyrazole complex is insoluble. The reaction between trans-$[NiCl_2(pzH)_4]$ and dppe in methanol (a tenfold molar excess of phosphine was used) also failed to produce a nickel complex that contained both pyrazole and phosphine ligands. Concentration of this solution, followed by precipitation using diethyl ether, yielded the brown $[NiCl_2(dppe)]$. Additon of less phosphine, gave a mixture as before.

No reason for the preferential coordination of pyrazole(s) to Ni(II) as compared with phosphines, has been found in the literature. However, "Pearson's Principle" [1.8] offers an explanation. No information exists as to the classification of pyrazole in this scheme, but although nitrogen is usually hard because of its small size, the presence of polarizable substituents can affect its behaviour. Pyridine is therefore sufficently soft to be considered borderline, If pyrazole can be expected to behave similarly, then Ni^{2+} (which is classified as borderline between a hard and soft acid) would be expected to preferentially coordinate with pyrazole rather than the soft, polarizable phosphines.

However, the synthesis of a nickel complex that contains phenylphosphines and pyrazole ligands deserves further consideration. Recent literature shows that similar diphosphine complexes may demonstrate usefulness in the synthesis of heterobimetallic systems[69]. This is discussed in more detail in the conclusion.

SECTION FOUR RUTHENIUM-PYRAZOLE COMPLEXES

4.1 RUTHENIUM COMPLEXES-INTRODUCTION

(i) Dichlorotris(triphenylphosphine)ruthenium(II)

This complex detectably dissociates in toluene, possibly according to the following equation[70]:

$$2RuCl_2(PPh_3)_3 = [RuCl_2(PPh_3)_2]_2 + 2PPh_3 \quad \ldots\ldots\ldots\ldots (1)$$

The red brown $RuCl_2(PPh_3)_3$ has a distorted square-pyramidal structure; trans-chlorines and trans-phosphines in the basal plane, apical phosphine, with one of the ortho-hydrogens blocking the sixth coordinating position[48] (fig. 59). Dissociation of triphenylphosphine, allows "unblocking" of the sixth position and reaction with other ligands may allow Ru(II) to adopt the octahedral coordination that is usual for this metal in oxidation state +2.

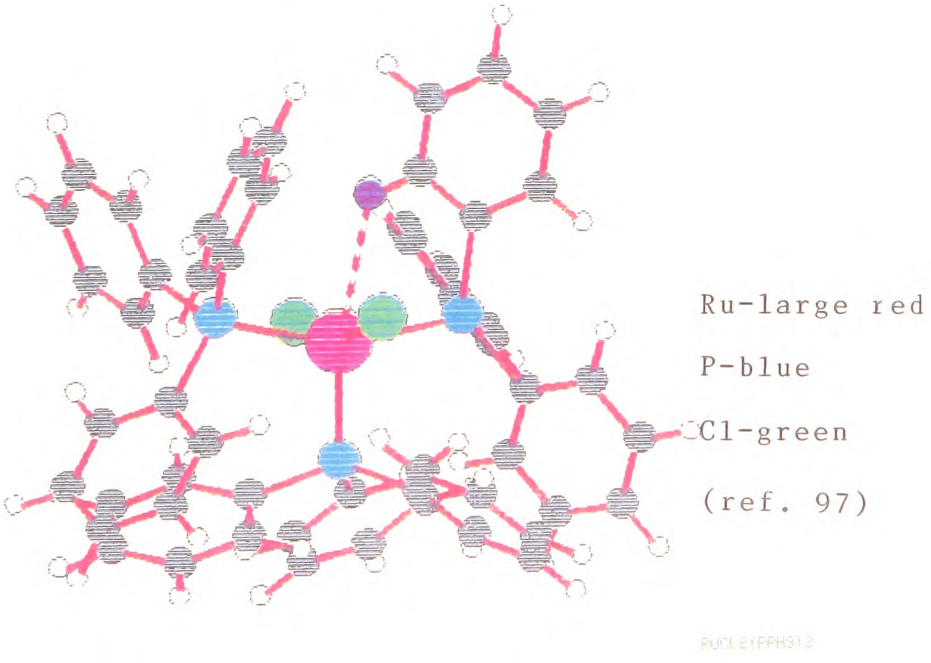

fig. 59 Structure of $RuCl_2(PPh_3)_3$

(ii) Reaction with Oxygen

$RuCl_2(PPh_3)_3$ is air-stable only in the solid state, whilst its red-brown solutions rapidly become green in the presence of air, due to their fast reaction with oxygen[71,72]. The mechanism of this oxidation is still unclear. However, spectrophotometric ^1H and ^{31}P nmr measurements[70,73] indicate that the complex initially dissociates in solution, probably due to the equilibrium shown in equation (1). It seeems likely from kinetic measurements that the next slow step of the reaction involves the uptake of oxygen, perhaps to form a peroxo-bridged complex[74], although to date, this complex has not been identified. The next step(s) in the cycle are unclear, but the final oxidation product has been analysed (although not well characterized) as having empirical formula $[RuCl_2(OPPh_3)_2]$ and it is a diamagnetic entity[71]. In solutions of $RuCl_2(PPh_3)_3$ exposed to oxygen, the ^{31}P nmr spectrum shows peaks due to free PPh_3, (+5.5δ), free $O{=}PPh_3$ (-29δ) and a number of resonances between -45 and -47δ which have not been identified. Possibilities could be; a ruthenium $-O{=}PPh_3$ complex, peroxo-dimers with equivalent phosphines or cationic species[74,75]. Kinetic measurements indicate that a complex in which triphenylphosphine oxide is complexed to Ru(II) may be an intermediate in the catalytic oxidation of triphenylphosphine by a related ruthenium-oxygen-phosphine complex[76].

(iii) Reaction with Hydrogen

The same complex $RuCl_2(PPh_3)_3$ reacts with molecular hydrogen at ambient temperature and pressure, in the presence of a base such as triethylamine (or in a basic solvent), to form the hydrido complex

$RuClH(PPh_3)_3$. The complex is isolated as its solvate[77]. The base is important since it removes the hydrogen chloride produced in the reaction[47,78].

$$RuCl_2(PPh_3)_3 + H_2 + Et_3N \xrightarrow[109\ ^\circ C]{C_7H_8} RuClH(PPh_3)_3 + [Et_3NH]Cl \quad \ldots\ldots\ldots (2)$$

The hydrido complex exhibits ν(Ru—H) in its infra-red spectrum[79] at 2020 cm^{-1}. The complex has a tbp structure and is one of the most active catalysts known for homogeneous hydrogenation of alkenes, with remarkable specificity towards 1-alkenes[77].

(iv) Reactions with Carbon Monoxide

Carbonyl derivatives of $RuCl_2(PPh_3)_3$, are well established[80]. Direct reaction with carbon monoxide gives dicarbonyl complexes and the isomer obtained depends upon the reaction conditions. In THF or DMF, white cis-$[RuCl_2(PPh_3)_2(CO)_2]$ is obtained, whilst warm acetone yields the yellow trans product[81]. The cis form is more stable at high temperatures. In N,N-dimethylformamide the trans isomer can be obtained at 35 °C, but at 75 °C the cis isomer is the product[47].

When the reaction between $RuCl_2(PPh_3)_3$ and carbon monoxide is carried out in N,N-dimethylacetamide, intermediate monocarbonyl compounds can be obtained. A six-coordinate O-(N,N-dimethylacetamide) complex is first isolated, but this easily loses N,N-dimethylacetamide to give the pentacoordinate monocarbonyl complex $RuCl_2(PPh_3)_2(CO)$. The latter complex can react with more carbon monoxide to form the two dicarbonyl complexes[47].

$$RuCl_2(PPh_3)_2(CO) + CO = \begin{cases} \xrightarrow{CO/35\ ^\circ C} trans\text{-}[RuCl_2(PPh_3)_2(CO)_2] \\ \xrightarrow{CO/75\ ^\circ C} cis\text{-}[RuCl_2(PPh_3)_2(CO)_2] \end{cases} \quad \ldots\ldots\ldots (3)$$

(v) Catalysis with Ruthenium Complexes and Methyl Iodide

Methyl iodide has been used as a promoter for the selective homologation of aliphatic carboxylic acids via ruthenium homogeneous catalysis. C_{3+} carboxylic acids are prepared[82,83] from synthesis gas plus acetic acid solutions of ruthenium precursors such as RuO_2, $Ru_3(CO)_{12}$ and $H_4Ru_4(CO)_{12}$.

$$CH_3COOH \xrightarrow{CO/H_2} C_nH_{2n+1}COOH \quad \ldots\ldots\ldots\ldots (4)$$

It has been shown that whilst a broad range of ruthenium oxide, carbonyl and hydrocarbonyl species are effective catalyst precursors for acid homologation, complexes which contain ruthenium bonded to bulky stabilising ligands such as $RuCl_2(PPh_3)_3$ are generally much less effective. It has also been demonstrated that no homologation occurs in the absence of the halogen promoter. The mechanism of the process is not clearly understood, however ruthenium iodocarbonyl species have been identified in the reaction solution.

Ruthenium carbonyl or iodocarbonyl complexes, together with methyl iodide[84] have also been shown to be effective for the homologation of methanol to ethanol and ethyl ethers. Selectivities higher than 60%

cannot be reached, however, owing to the side formation of dimethyl ether and acetic esters. These can be further carbonylated to ethyl acetate using diiodotetracarbonylruthenium(II) in the presence of methyl iodide[85].

(vi) Oxo-Compounds of Ruthenium

Ruthenium (VI, VII and VIII) oxidation states are found in the tetroxides and oxo anions. These compounds are formed by treating ruthenium solutions with powerful oxidising agents: for example, RuO_4 is formed in acid solution by oxidation with HIO_4, MnO_4^- or Ce^{4+}; fusion with alkali in the presence of permanganate produces RuO_4^- or RuO_4^{2-}. Oxidation of Ru(III) complexes with H_2O_2 or Ce^{4+} can produce oxoruthenium(VI) species[86,87]. These compounds display a band at around 770 cm^{-1} in their infra-red spectra which is assigned to $\nu(Ru{=}O)$ and they are paramagnetic with magnetic moments around 2.9 BM, as expected for complexes with two unpaired electrons.

A series of oxo-bridged complexes of Ru(III) have been prepared[88], with the general formula $[(AA)_2XRu{-}O{-}RuX(AA)_2]^{n+}$, where AA = 2,2′-bipyridine or 1,10-phenanthroline and X^- = Cl^-, NO_2^-, or H_2O. The related complex[89] $[(bpy)_2(py)Ru{-}O{-}Ru(L)(bpy)_2]^{4+}$ (where L = py or H_2O), has also been characterized. The complexes are prepared by stirring an acetone solution of $[Ru(bpy)_2Cl(Me_2CO)]^+$ under oxygen. The reaction produces the symmetrical bpy/chloride oxo-bridged dimer and reaction of this dimer with the appropriate ligand, X, will allow chlorine to be replaced by that ligand, creating a new oxo-bridged dimer. All these complexes display a characteristic, unique dark blue colour. Also, their electronic spectra show a high intensity

absorbance at about 650 nm which is not observed in related monomeric Ru(III) and Ru(II) complexes. The bands are assigned to Π^{b} -» Π^{*} transitions which involve delocalised Ru—O—Ru levels (fig. 60a).

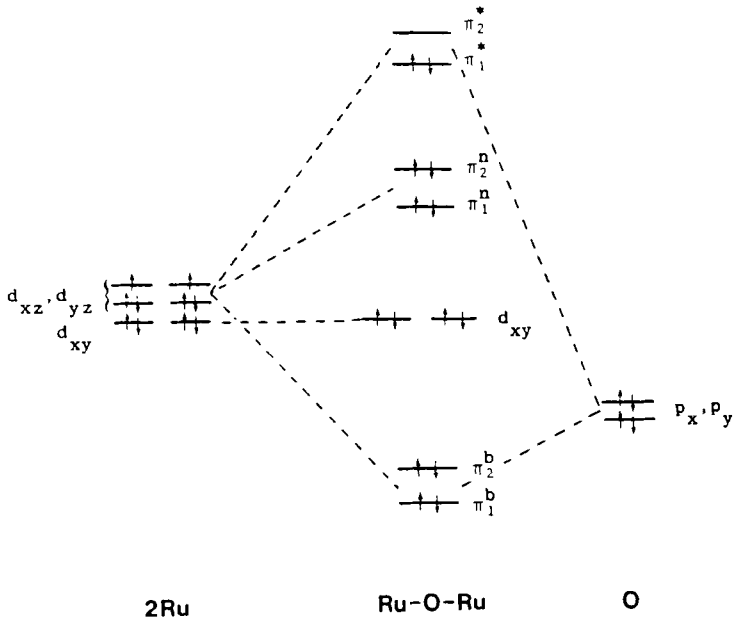

fig. 60a

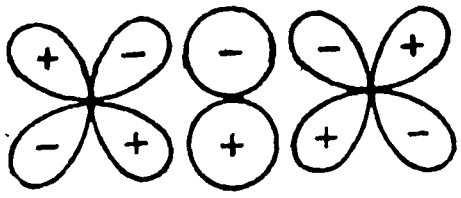

fig. 60b

The transitions would be symmetry allowed and the bands would have high molar extinction coefficents. The Ru(III) ion has electronic configuration t_{2g}^5 with one unpaired electron. However complexes which have linear Ru—O—Ru systems have been found to exhibit diamagnetism[90,91]. In the blue complexes, the Ru—O—Ru linkage is reported as being bent (165.4°)[92]. The application of molecular orbital theory to the Ru—O—Ru system results in 3-centre Π-bonding involving overlap of an oxygen p orbital and two d orbitals of the Ru ions (fig. 60b). This gives rise to a singlet ground state $^1(\Pi_1{}^{*2})$ and a relatively low lying triplet excited state $^3(\Pi_1{}^*, \Pi_2{}^*)$ and is given as the reason why the dimers exhibit temperature-dependent paramagnetism. The magnetic moment of some of these dimers is reported as 1.8 BM at room temperature. No evidence of direct Ru—Ru interaction is given. The infra-red spectra of linear M—O—M species[93] shows an asymmetric stretch in the range 800 - 900 cm^{-1}. Bending of the linkage lowers this frequency and can make the symmetric stretch infra-red active from 200 cm^{-1} to about 500 cm^{-1}. Neither vibrations are identified in the infra-red spectra of the oxo-bridged dimers. The suggested explanation is that they may be "masked" by ligand vibrations[93].

A characteristic of ruthenium ammine chemistry is the formation of highly coloured red or brown species usually referred to as ruthenium reds[90]. Thus if $RuCl_3.3H_2O$ is treated with air and ammonia, a red solution is obtained, from which can be crystallized ruthenium red, $[Ru_3O_2(NH_3)_{14}]Cl_6.4H_2O$. This contains an essentially linear trinuclear ion;

$$[(NH_3)_5Ru^{3+}—O—Ru^{4+}(NH_3)_4—O—Ru^{3+}(NH_3)_5]^{6+}$$

The ethylenediamine derivative is similar. Here, the ammonia ligands on the central ruthenium ion are replaced by two ethylenediamine ligands. Both complexes are diamagnetic because of linear Ru—O—Ru Π-bonding. The red +6 ion is oxidised in acid solution to a brown species with the same constitution but charge +7.

4.2 EXPERIMENTAL

(i) Preparation[80] of $RuCl_2(PPh_3)_3$ Ruthenium trichloride (0.20 g, 0.77 mmol) was dissolved in methanol (50 cm^3) and refluxed for five minutes under nitrogen. The mixture was allowed to cool and triphenylphosphine (1.20 g, 4.58 mmol) added in a positive stream of nitrogen. The whole was refluxed for one hour in a nitrogen atmosphere. Dark brown crystals were obtained which were filtered in air, washed with methanol (5 cm^3) and sodium dried diethyl ether (10 cm^3), then dried in vacuo. Yield = 0.70 g (96%).

(ii) Preparation of $[RuCl_2(PPh_3)_2(pzH)_2].\frac{1}{2}C_6H_{14}$ Pyrazole (0.05 g, 0.74 mmol) was dissolved in de-gassed toluene (25 cm^3) and $RuCl_2(PPh_3)_3$ (0.2 g, 0.21 mmol) added in a positive stream of nitrogen. The mixture was stirred under nitrogen for 20 minutes, at ambient temperature. The resultant yellow solution was concentrated to ca. 5 cm^3 and hexane (25 cm^3) added. The yellow precipitate obtained was filtered, washed with hexane (15 cm^3) and dried in vacuo. Yield = 0.10 g (60%).

Analysis

Calculated for $C_{45}H_{45}Cl_2N_4Ru$: C 61.7% H 5.1% N 6.4%

Found: C 61.7% H 5.1% N 6.3%

iii) Preparation of $[RuCl_2(PPh_3)_2(DMpzH)]$ In acetone (30 cm^3) was dissolved 3,5-dimethylpyrazole (0.06 g, 0.63 mmol) and the mixture de-gassed. The complex $RuCl_2(PPh_3)_3$ (0.40 g, 0.42 mmol) was added in a positive stream of nitrogen and the whole refluxed under nitrogen for three hours. The yellow precipitate obtained was filtered, washed with acetone (10 cm^3), then dried in vacuo. Yield = 0.21 g, (64%).

Analysis

Calculated for $C_{41}H_{38}Cl_2N_2Ru$: C 62.1% H 4.8% N 3.5%

Found: C 62.1% H 5.1% N 3.8%

(iv) Preparation[80] of $RuBr_2(PPh_3)_3$ Ruthenium trichloride (0.20 g, 0.77 mmol) was stirred with anhydrous lithium bromide (0.50 g, 2.99 mmol) for 24 h in methanol (50 cm^3). The resulting mixture was refluxed for 15 minutes under nitrogen, then triphenylphosphine (1.20 g, 4.58 mmol) added under a positive nitrogen pressure. Refluxing for a further 4 h, gave the complex, which was washed with methanol (20 cm^3) and small portions of diethyl ether (20 cm^3 in total). Yield = 0.68 g, (65%).

(v) Preparation of $[RuBr_2(PPh_3)_2(pzH)_2].\frac{1}{2}C_6H_{14}$ Pyrazole (0.03 g, 0.44 mmol) was dissolved in toluene (25 cm^3) and the mixture de-gassed. The complex $RuBr_2(PPh_3)_3$ (0.20 g, 0.21 mmol) was added in a positive stream of nitrogen. The mixture was stirred at room temperature for 30 minutes, whereupon the orange solution was concentrated to 5 cm^3 and hexane (25 cm^3) added. The light brown precipitate obtained was washed with hexane (15 cm^3) and dried in vacuo. Yield = 0.12 g (65%).

Analysis

Calculated for $C_{45}H_{45}Br_2N_4Ru$: C 56.0% H 4.7% N 5.8%

Found: C 56.7% H 4.6% N 6.4%

(vi) Preparation of $[RuBr_2(PPh_3)_2(DMpzH)]$ The complex $RuBr_2(PPh_3)_3$ (0.20 g, 0.21 mmol) was added to a de-gassed solution of 3,5-dimethylpyrazole (0.04 g, 0.59 mmol) in acetone (25 cm^3), under a positive stream of nitrogen. The mixture was refluxed for 2 h. The orange precipitate obtained was filtered, washed with acetone (10 cm^3), then dried in vacuo. Yield = 0.10 g (57%).

Analysis

Calculated for $C_{41}H_{38}Br_2N_2Ru$: C 55.9% H 4.3% N 3.2%

Found: C 56.8% H 4.3% N 3.9%

(vii) Preparation[74] of $[RuI_2(PPh_3)_2]_n$ Ruthenium trichloride trihydrate (0.20 g, 0.77 mmol) was stirred with $AgClO_4$ (0.48 g, 2.30 mmol) in methanol (30 cm^3) for 24 h . The white precipitate was removed by centrifugation and filtration and potassium iodide (0.38 g, 6.02 mmol) added to the filtrate. This mixture was refluxed under nitrogen for 15 minutes and triphenylphosphine (1.20 g, 4.57 mmol) added. The mixture was then refluxed for 4 h and the dark brown precipitate obtained washed with methanol (20 cm^3) and diethyl ether, then dried under suction. Yield = 0.65 g (96%)

(viii) Preparation of $[RuI_2(PPh_3)_2(DmpzH)]$ This was prepared as for $[RuBr_2(PPh_3)_2(DMpzH)]$ using $[RuI_2(PPh_3)_2]_n$ (0.52 g, 0.60 mmol) and 3,5-dimethylpyrazole (0.08 g, 0.83 mmol). The mixture was refluxed under nitrogen for 6 h. The light brown precipitate obtained was

characterized by spectroscopy, alone. Yield = 0.38 g (65%).

(ix) Reaction of Pyrazole with $[RuI_2(PPh_3)_2]_n$ When pyrazole (0.20 g, 2.94 mmol) was added to $[RuI_2(PPh_3)_2]_n$ (0.60 g, 0.68 mmol) in toluene (25 cm^3) under nitrogen and the mixture refluxed for 24 h, a dark brown solution resulted. A brown precipitate was obtained by concentration of the solution and addition of petroleum ether (60/80). The precipitate was subsequently analysed by spectroscopy and concluded to be a mixture of products.

(x) For Identification Purposes, the Salt $MePPh_3^+I^-$ was prepared: Methyl iodide (0.60 g, 4.23 mmol) was stirred with triphenylphosphine (1.00 g, 3.82 mmol) in toluene (25 cm^3) for 30 minutes. The white precipitate obtained was filtered, washed with diethyl ether and dried under suction. Yield = 1.29 g (84%).

4.3 REACTION OF RUTHENIUM-PHOSPHINE COMPLEXES WITH PYRAZOLES

(a) The reaction of $RuCl_2(PPh_3)_3$ with pyrazole in toluene gave a yellow complex, subsequently characterized by analysis and spectroscopy as $[RuCl_2(PPh_3)_2(pzH)_2].\frac{1}{2}C_6H_{14}$ [4.2(ii)]. Despite prolonged periods in a vacuum (3 - 4 hrs.) at temperatures of 50 - 60 °C, the complex retained a fraction of a mole of hexane as shown in its analysis and infra-red spectrum (fig. 61). This is attributed to "trapped hexane" within the crystal structure, since the possibility of coordinated non-polar hexane is highly unlikely. The complex appeared to be reasonably soluble in both polar and non-polar organic solvents and magnetic susceptibility measurements showed it to be diamagnetic, indicating oxidation of Ru(II)

had not taken place i.e. Ru(II) tends to be low spin with no unpaired electrons (t_{2g}^6). A solution of the complex in toluene appeared to remain air-stable for about an hour, eventually turning from brown to green, indicating that a reaction with air had taken place. Prolonged exposure to air of the green solution (one week) resulted in a black mixture with insoluble product that could not be identified, indicating probable decomposition. The solid yellow complex, $[RuCl_2(PPh_3)_2(pzH)_2].\frac{1}{2}C_6H_{14}$ decomposed at 140 °C.

(i) Infra-Red Spectrum

The infra-red spectrum of $[RuCl_2(PPh_3)_2(pzH)_2].\frac{1}{2}C_6H_{14}$ is shown in fig. 61. Coordination of pyrazole is demonstrated by strong bands assigned to the N—H stretch and bend at 3270 cm^{-1} and 1130 cm^{-1} respectively[55]. The presence of triphenylphosphine is shown by the strong P—aryl[56] stretch at 1430 cm^{-1}, medium C—H aromatic stretch at 3050 cm^{-1} and strong bands at 690 cm^{-1} and 740 cm^{-1} are assigned to out of plane aromatic deformations (appendix I). A weak band at 2920 cm^{-1} is attributed to the C—H aliphatic stretch of "trapped hexane".

(ii) Nmr Spectra

The ^1H, ^{13}C and ^{31}P spectra of the product $[RuCl_2(PPh_3)_2(pzH)_2].\frac{1}{2}C_6H_{14}$ are shown in figs. 62 - 64. Solvents and temperature are indicated on each spectrum.

The ^1H nmr spectrum of pyrazole (appendix IV) shows a singlet at 12.1δ

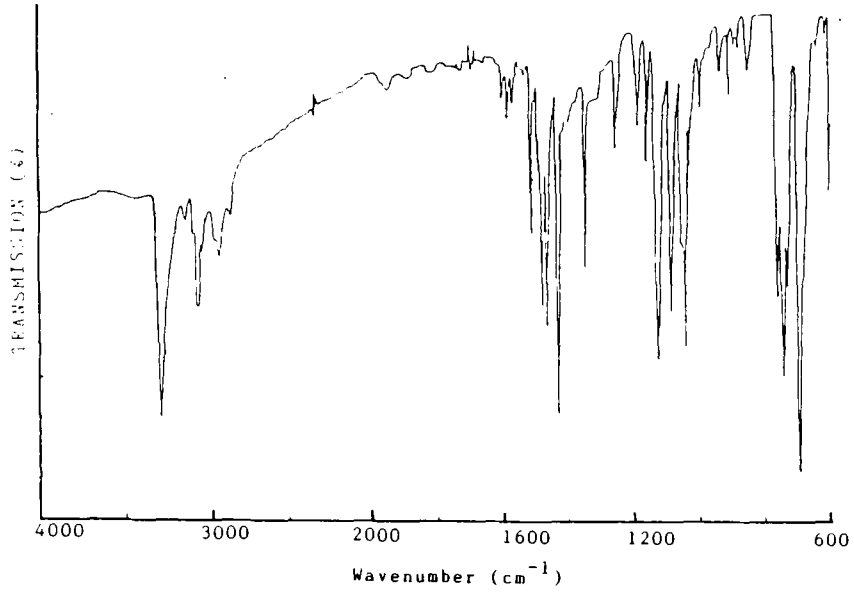

fig. 61 Infra-red Spectrum of $[RuCl_2(PPh_3)_2(pzH)_2].\frac{1}{2}C_6H_{14}$

which represents the proton attached to nitrogen, substantially deshielded because of the high electronegativity of nitrogen. The resonance is broadened due to the large electric quadrupole moment of nitrogen. A similar effect occurs in pyrrole[94]. Also evident in the spectrum, are a doublet at 7.68 (C3 and C5 protons) and a weakly defined triplet at 6.38 (C4 proton). The equivalence of the protons in the C3 and C5 positions demonstrates that in solution pyrazole is tautomeric, the hydrogen atom attached to nitrogen migrates between N1 and N2[95]. The ^1H nmr spectrum of triphenylphosphine (appendix II) shows two close resonances at 7.38, representing the coupled protons of the benzene ring.

^1H nmr of $[RuCl_2(PPh_3)_2(pzH)_2].\frac{1}{2}C_6H_{14}$ (fig. 62) shows a broad singlet at 11.78, attributed to N—H protons and broad resonances at 8.18 and 5.98 which are assigned to the C3 and C4 protons of the coordinated pyrazoles. These are assigned by comparison with data provided by

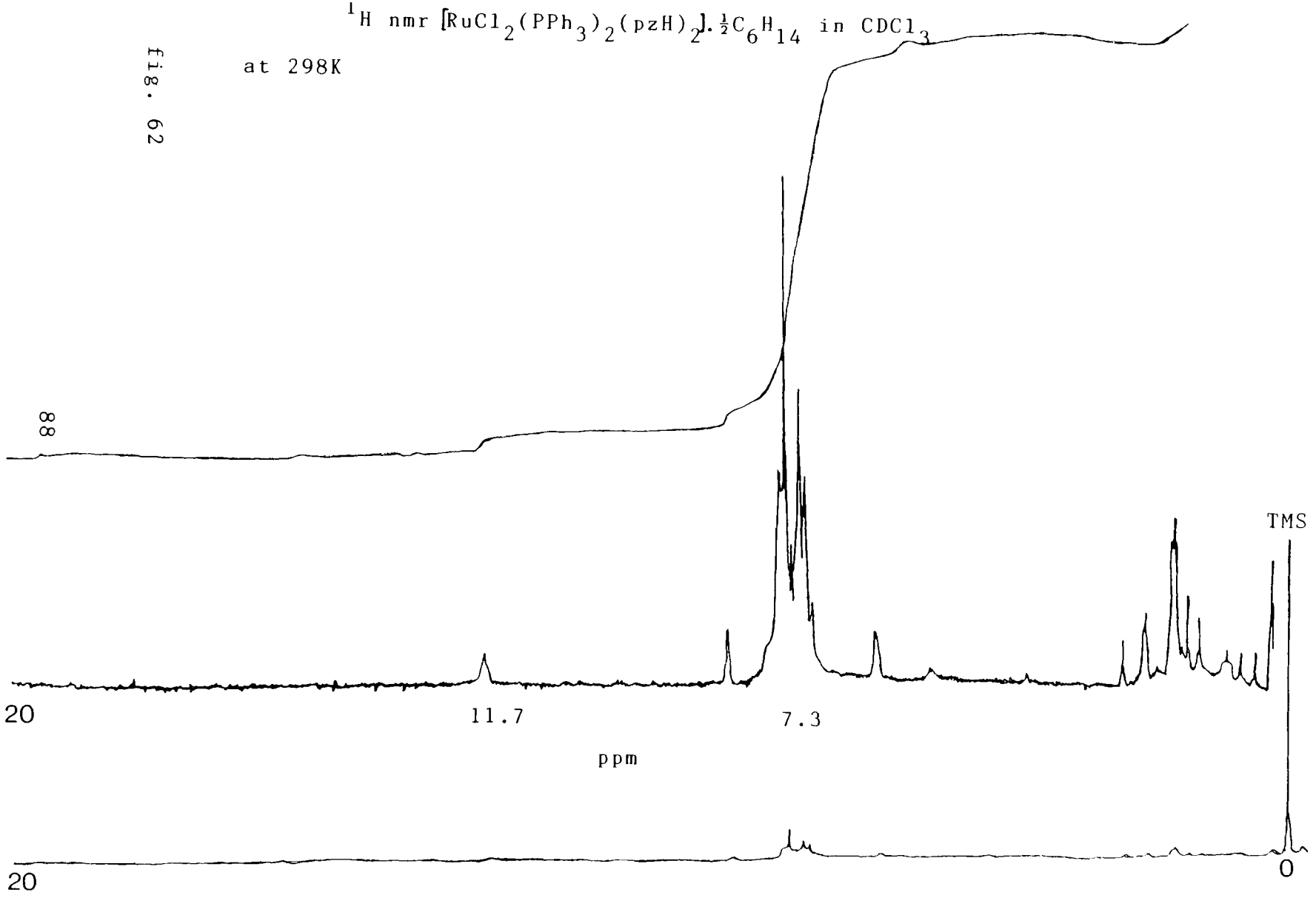
^{1}H nmr [RuCl$_2$(PPh$_3$)$_2$(pzH)$_2$].½C$_6$H$_{14}$ in CDCl$_3$
at 298K
fig. 62
88
TMS
20
11.7
7.3
ppm
20
0

^{13}C nmr $[RuCl_2(PPh_3)_2(pzH)_2] \cdot \frac{1}{2}C_6H_{14}$

in $CDCl_3$, 298K

fig. 63

fig. 64

^{31}P nmr $[RuCl_2(PPh_3)_2(pzH)_2].\frac{1}{2}C_6H_{14}$ in $CDCl_3$, 298K

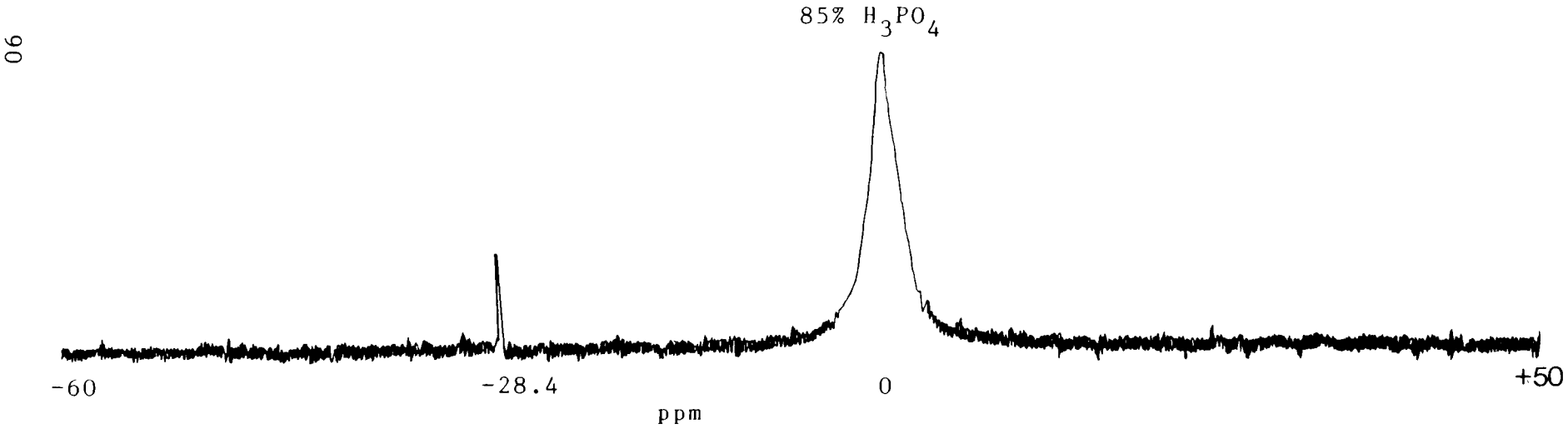

Ashworth et al.[32], who prepared the complex $[\{Ru_2(pz)_2Cl(pzH)(cod)_2\}(\mu\text{-}H)]$, which exhibits both terminal and bridging pyrazole groups. Coordination of pyrazole to ruthenium, (fig. 62), makes the C3 and C5 protons no longer equivalent, so that the doublet expected to represent the C5 protons, is assumed to form part of the complicated splitting pattern observed in the range 7.6 - 6.7δ, together with the aryl protons in triphenylphosphine. For many preparations of the complex, petroleum ether (60/80) was used as an inexpensive alternative to hexane. The multiplet that occurs in the range 0.2 -2.4δ is taken as representing "trapped solvent". Integration of the peaks gives a ratio of 2: 2: 32: 2 for N1: C3: C5+PPh_3: C4 protons, as expected in the formula $[RuCl_2(PPh_3)_2(pzH)_2].\frac{1}{2}C_6H_{14}$.

The proton decoupled ^{13}C nmr spectrum of the complex (fig. 63), shows signals at 140δ and 135δ (C3, C5 of pyrazole) and 106δ (C4 of pyrazole). Again, these are assigned by comparison with published data[32,37]. Resonances between 129 - 127δ are attributed to the carbon atoms in triphenylphosphine.

^{31}P nmr of the same complex (fig. 64) shows a singlet at -28.4δ, indicating equivalent triphenylphosphines with a chemical shift that is appropriate for these groups in a trans arrangement[70].

(iii) Structure of $[RuCl_2(PPh_3)_2(pzH)_2].\frac{1}{2}C_6H_{14}$

Gilbert and Wilkinson[96] prepared a number of complexes by reacting nitrogen donating ligands, such as pyridine, with $RuCl_2(PPh_3)_3$. They found that, in general, preparations in acetone led to cis coordination of the nitrogen ligands, whereas preparations in toluene resulted in the formation of trans isomers. In both isomers, the triphenylphosphine

ligands adopted a mutually trans position. The ^{31}P nmr spectrum has indicated equivalent, trans-triphenylphosphine groups and since the complex under discussion is prepared in toluene, it might be reasonable to expect it to be the trans-pyrazole isomer. The structure of the complex might therefore be proposed to be as shown in fig. 65.

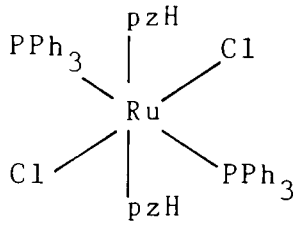

fig. 65 Structure of trans-$[RuCl_2(PPh_3)_2(pzH)_2]$

The far infra-red spectrum (600 - 250 cm^{-1}) of the complex $[RuCl_2(PPh_3)_2(pzH)_2].\frac{1}{2}C_6H_{14}$ is shown in fig. 66. One band at 326 cm^{-1} is shown in the region expected for v(Ru—Cl) and v(Ru—N). The literature[96] gives values of v(Ru—Cl) trans to another chlorine atom between 300 and 323 cm^{-1}. The precursor complex, $RuCl_2(PPh_3)_3$, has v(Ru—Cl) at 315 cm^{-1} and its ruthenium-chlorine bonds are unusually short[97]. Values found for v(Ru—N), trans to another nitrogen donor, however, also may be found in the 250 - 358 cm^{-1} region[96,98]. The band at 326 cm^{-1} was taken to be v(Ru—Cl), since it was found to be absent in the far infra-red spectrum of the analogous bromo-complex [4.2(v)]. The spectrum in fig. 66 also shows a number of absorbances in the region 550 - 400 cm^{-1}, which are attributed to triphenylphosphine.

In the crystalline state it exhibits a complicated spectrum in this area, but shows no absorbance in the region expected for v(Ru—Cl)[99].

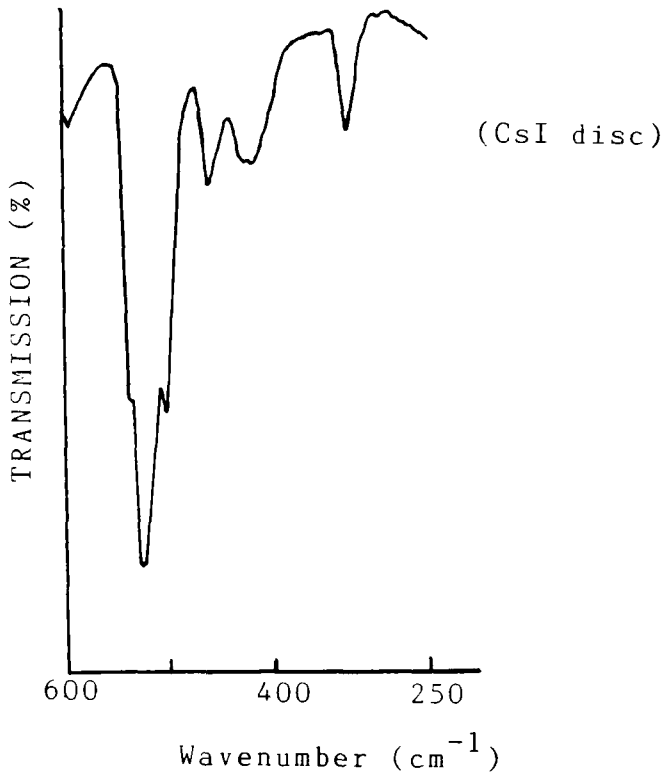

fig. 66 Far Infra-red Spectrum of $[RuCl_2(PPh_3)_2(pzH)_2].\frac{1}{2}C_6H_{14}$

The symmetry of the complex in fig. 65 (D_{2h}) suggests that one band should be expected for v(Ru—Cl) in the far infra-red spectrum. Further clues as to the structure of the complex under discussion may be obtained by considering the structure[57] of trans-$[NiCl_2(pzH)_4]$. Here, hydrogen bonding between the N1 protons and chloride ions, results in unusually long Ni—Cl bonds[58]. If hydrogen bonding interactions exist in the ruthenium complex, then two possibilities exist for the isomer shown in fig. 65. That in which there is one interaction per chloride ion (C_{2h} symmetry) and that in which both pyrazole groups interact with the same chloride ion (C_{2v} symmetry). The former structure is shown in fig. 67 and would give one infra-red active band (B_u) for v(Ru—Cl). The proposed structure of the complex, therefore, is as shown in fig. 67.

P-blue

N-purple

Ru-red

Cl-green

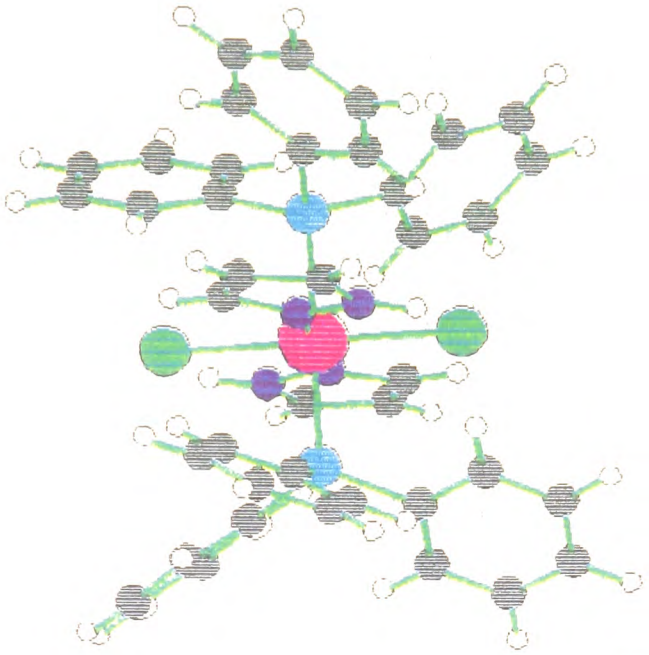

fig. 67 Proposed Structure of trans-$[RuCl_2(PPh_3)_2(pzH)_2]$

(b) The reaction of $RuCl_2(PPh_3)_3$ with 3,5-dimethylpyrazole in acetone [4.2(iii)] gave a yellow solid, subsequently characterized by analysis and spectroscopy as $[RuCl_2(PPh_3)_2(DMpzH)]$. The product was found to be less soluble than its pyrazole counterpart, proving sparingly soluble in a variety of polar and non-polar organic solvents. It was, however, sufficently soluble in choroform to allow nmr study although solutions turned green rapidly, indicating oxidation. Magnetic measurements showed the complex to be diamagnetic i.e. Ru(II).

(i) Infra Red Spectrum

This is shown in fig. 68. Coordination of 3,5-dimethylpyrazole is shown by the strong N—H stretch at 3250 cm^{-1} and N—H bend at 1160 cm^{-1} (appendix V). The C—H (ring) stretch is shown by a weak band at

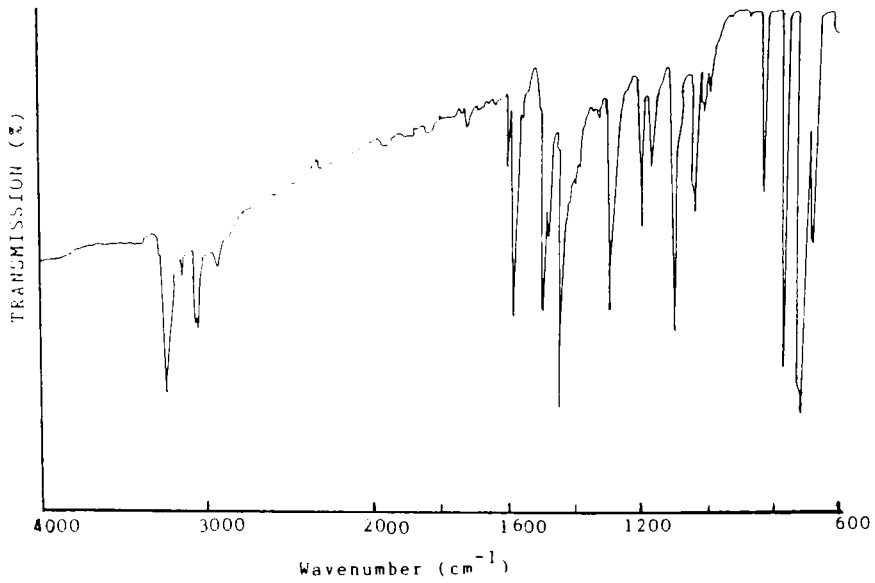

fig.68 Infra-red Spectrum of $[RuCl_2(PPh_3)_2(DMpzH)]$ (KBr disc)

3150 cm^{-1} and the C—H aliphatic stretch occurs at 2925 cm^{-1}. The presence of triphenylphosphine is taken from the strong band at 1440 cm^{-1} (P—aryl str., [4.3(a)]) and the medium band at 3050 cm^{-1} (C—H aromatic stretch).

(ii) Nmr Spectra

The ^1H nmr spectrum of the complex is shown in fig. 69. The broad singlet at 10.8δ is attributed to the N—H proton of 3,5-dimethylpyrazole (appendix VII), that at 5.3δ to the C4 proton. The complicated pattern at 7.1δ is taken to represent the aryl protons of coordinated triphenylphosphines, whilst the resonance at 1.8δ is taken as the singlet representing the methyl protons of the substituted pyrazole. Integration gives a ratio of 1 : 30 : 1 : 6 for N1 : PPh_3 : C4 : Me protons,

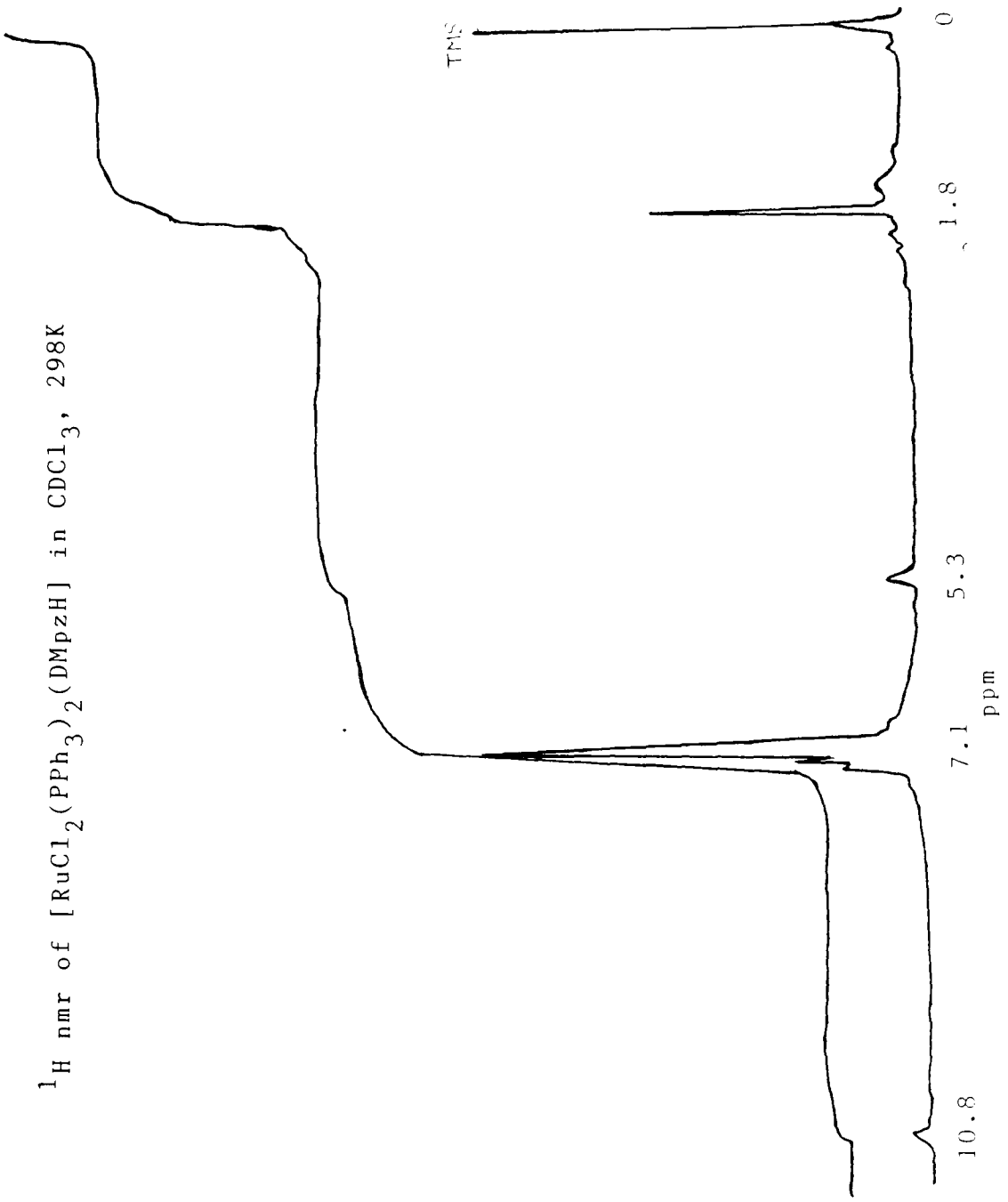

fig. 69

confirming the formula suggested by the analysis.

The nmr solutions began to turn green over the period of time required to obtain a ^{31}P nmr spectrum (some 2 - 3 hrs.), indicating oxidation. The ^{31}P nmr spectrum, together with a subsequent spectrum of the same sample taken some time later, is shown in fig. 70. Spectrum 70(a) shows resonances at -29.1, -26.1, -24.5 and +4.9δ. That at 4.9δ is attributed to free phosphine[100], probably liberated from the complex after reaction with traces of oxygen {c.f. the reaction of oxygen with $RuCl_2(PPh_3)_3$, [4.1(ii)]}. Integration of this singlet in 70(a) and 70(b) shows an increase of the concentration of this species in the sample, with time. As oxidation proceeds, the integration of the resonance at -29.1δ also shows an increase; this is attributed to $O{=}PPh_3$ (appendix VIII). The singlet at -26.1δ shows a decrease in concentration with time, suggesting it is representative of the unoxidised complex and the chemical shift indicates trans-phosphines[70]. The integration of the resonance at -24.1δ does not appear to change appreciably , making it difficult to ascertain whether it arises as a product of oxidation or is perhaps an impurity. An additional resonance is present in 70(b) at -35.5δ. Presumably this is the result of the formation of another oxidation product.

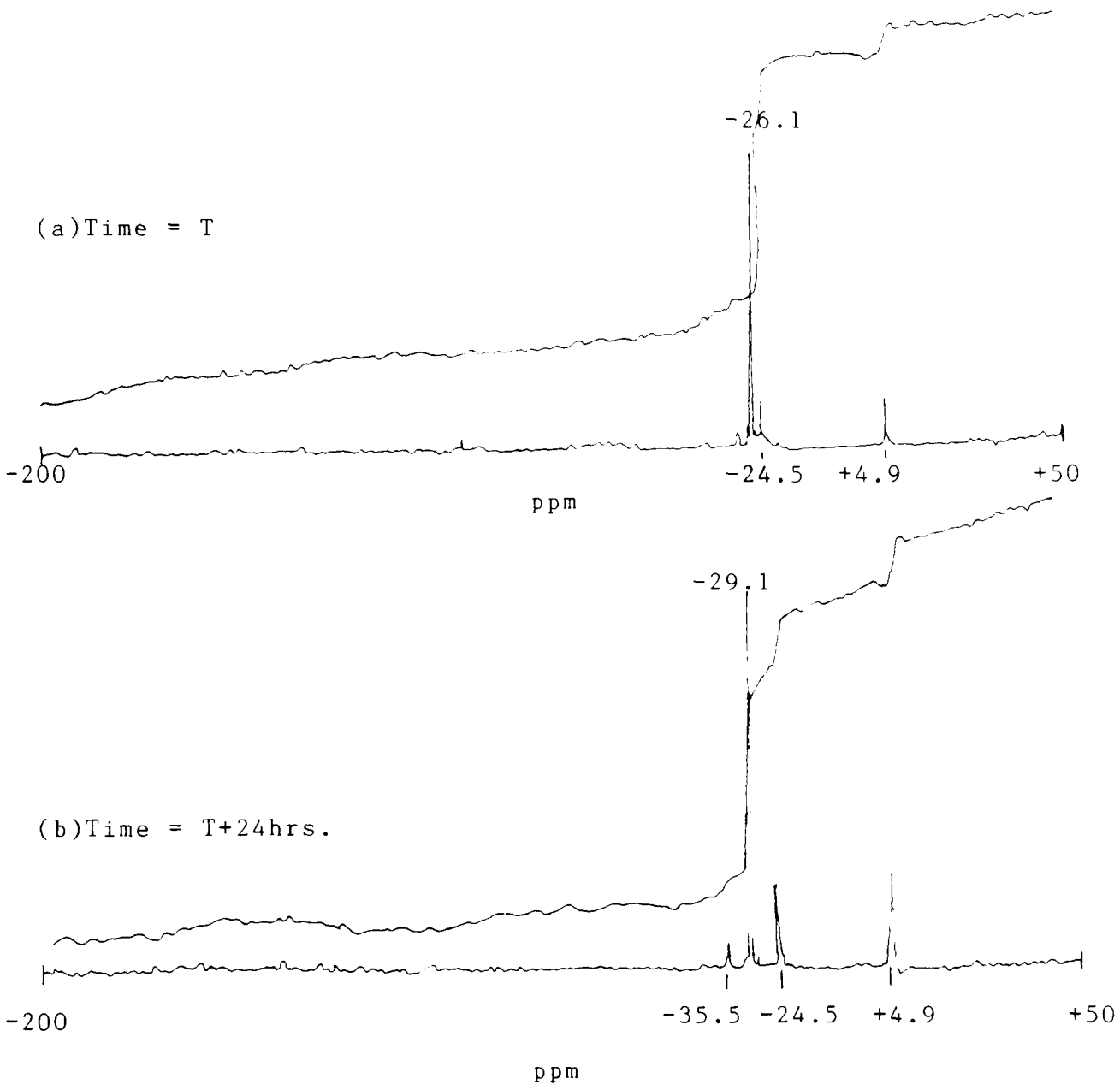

fig. 70 ^{31}P nmr Spectrum of $[RuCl_2(PPh_3)_2(DMpzH)]$ in $CDCl_3$, 298K

(iii) Far Infra-Red Spectrum of $[RuCl_2(PPh_3)_2(DMpzH)]$

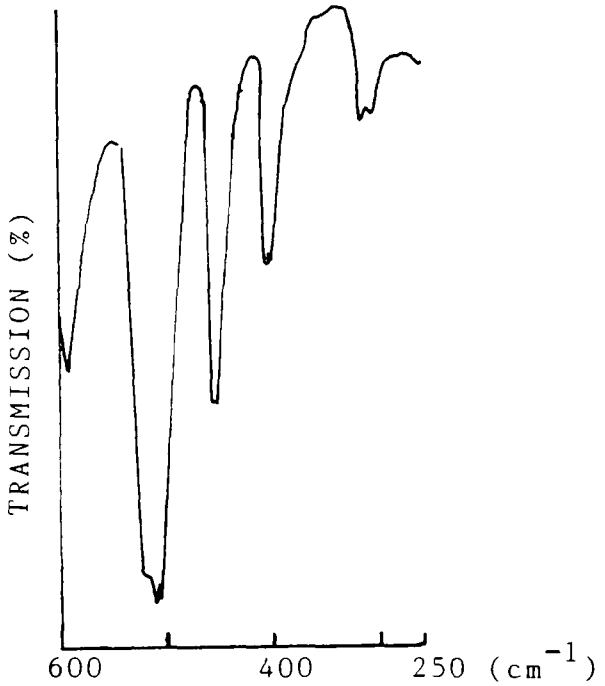

fig. 71 Far infra-red Spectrum of $[RuCl_2(PPh_3)_2(DMpzH)]$ (CsI disc)

Two bands are shown for ν(Ru—Cl) at 300 and 312 cm^{-1}. These suggest that the chlorines are mutually trans[96] (fig. 72).

(iv) Structure of $[RuCl_2(PPh_3)_2(DMpzH)]$

This can only be tentatively assigned by taking into account the crude spectroscopic evidence and considering the structure of the previously prepared $[RuCl_2(PPh_3)_2(pzH)_2].\frac{1}{2}C_6H_{14}$. It is assumed that the complex adopts a distorted square pyramidal shape with the sixth coordination position "blocked" as in the precursor complex $RuCl_2(PPh_3)_3$. The increased bulk of the 3,5-dimethylpyrazole ligand as compared with pyrazole probably accounts for this, resulting in a five coordinate species rather than a six coordinate species. Of the six isomers

possible for such a complex with this shape, one is possible with trans-phosphines and trans-chloride ions. It is therefore proposed that the major product of the reaction between $RuCl_2(PPh_3)_3$ and 3,5-dimethylpyrazole has the structure shown in fig. 72.

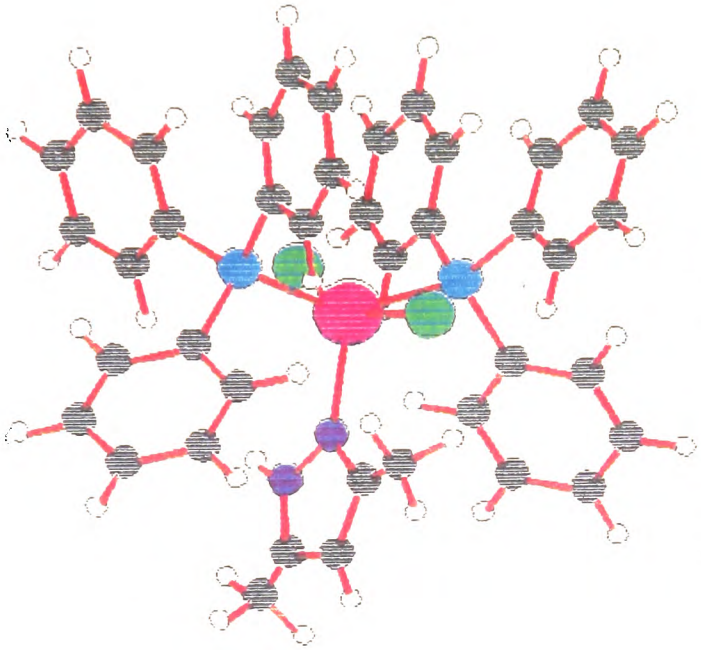

The complex has C_{2v} symmetry which gives two infra-red active bands for v(Ru—Cl) (A_1) and (B_1).

Ru-red

Cl-green

N-purple

P-blue

fig. 72 Proposed Structure of $[RuCl_2(PPh_3)_2(DMpzH)]$

(c) The bromo and iodo analogues of the ruthenium pyrazole complexes were prepared using $RuBr_2(PPh_3)_3$ and $[RuI_2(PPh_3)_2]_n$ as starting materials [4.2(iv) -(ix)]. The infra-red spectra of the bromo and iodo complexes are shown in figs. 73 - 75. The important features of both the infra-red and nmr spectra of the same complexes are summarized in table 2. The far infra-red spectra of the precursor complexes $RuBr_2(PPh_3)_3$ and $[RuI_2(PPh_3)_2]_n$ showed no band in the region expected for v(Ru—Cl). Increasing the bulk of the halogen in the ruthenium compounds

appears to make the complexes less stable to heat and more difficult to prepare in a pure state. Attempts to dry $[RuI_2(PPh)_3)_2]_n$ and $[RuI_2(PPh_3)_2(DMpzH)]$ in a moderately warm vacuum oven (ca. 80 °C) resulted in decomposition of the complexes, even though they appeared to be stable in refluxing toluene. This may explain the fact that iodo derivatives are not well reported in the literature.

COMPOUND	^{1}H nmr(δ)	^{31}P nmr(δ)	I.R. cm^{-1}
$[RuBr_2(PPh_3)_2(pzH)_2].\frac{1}{2}C_6H_{14}$	11.7(br., 1H, NH) 8.1(d, 2H, C3{pzH}) 7.3(m, 32H, {2H, C5[pzH]+ 30H, [PPh_3]}) 5.9(t, 2H, C4{pzH})	-28.4	ν(N—H) 3260
$[RuBr_2(PPh_3)_2(DMpzH)]$	10.9(br., 1H, NH) 7.2(m, 30H, [PPh_3]) 5.4(s, 1H, C4{DMpzH}) 1.8(s, 6H, -CH_3{DMpzH})	-26.0	ν(N—H) 3255
$[RuI_2(PPh_3)_2(DMpzH)]$	10.9(br., 1H, NH) 7.3(m, 30H, [PPh_3] 5.4(s, 1H, C4{DMpzH}) 1.8(s, 6H, -CH_3{DmpzH})	-25.0	ν(N—H) 3245

Table 2 Nmr parameters of Ruthenium-Pyrazole Complexes

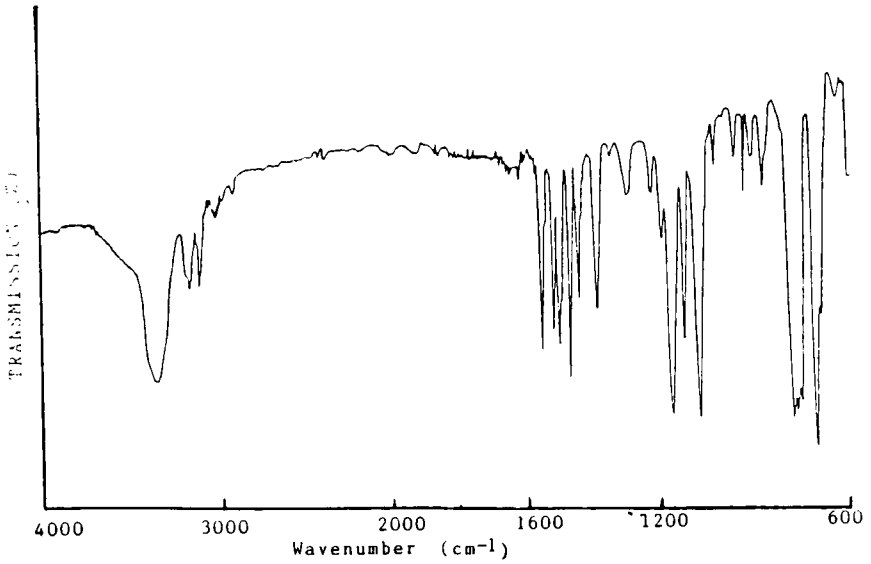

fig. 73 Infra-red Spectrum of $[RuBr_2(PPh_3)_2(pzH)_2].\frac{1}{2}C_6H_{14}$ (KBr disc)

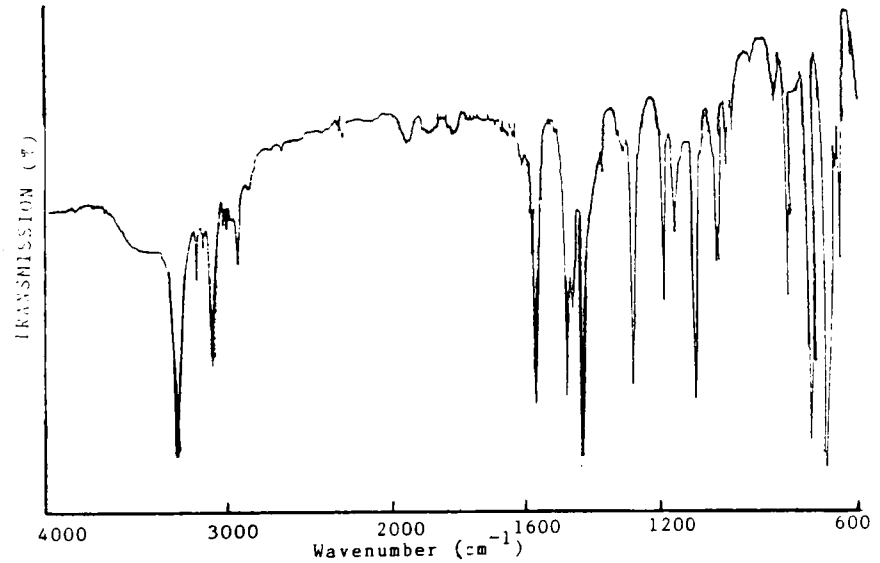

fig. 74 Infra-red Spectrum of $[RuBr_2(PPh_3)_2(DMpzH)]$ (KBr disc)

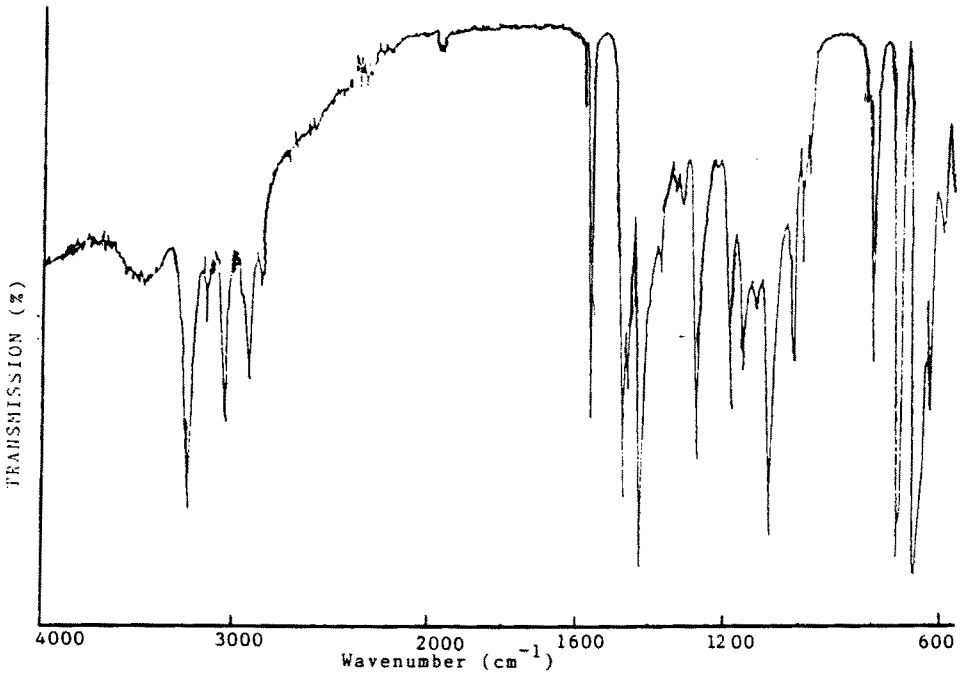

fig. 75 Infra-red Spectrum of $[RuI_2(PPh_3)_2(DMpzH)]$ (KBr disc)

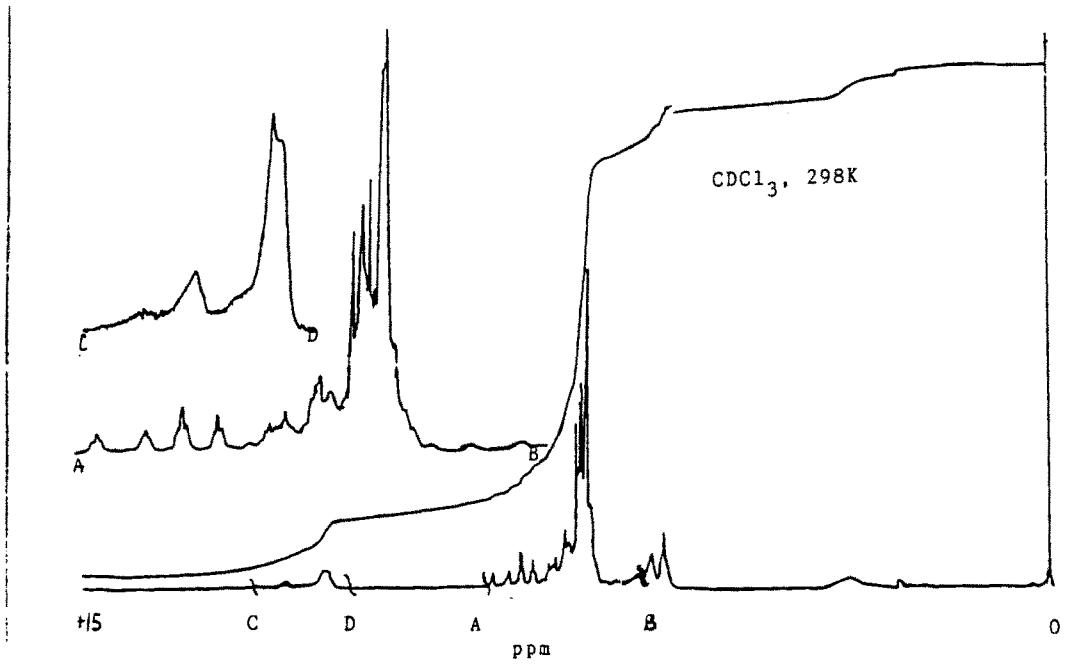

fig. 76 ^1H nmr of the Product of the Reaction between $[RuI_2(PPh_3)_2]_n$ and Pyrazole

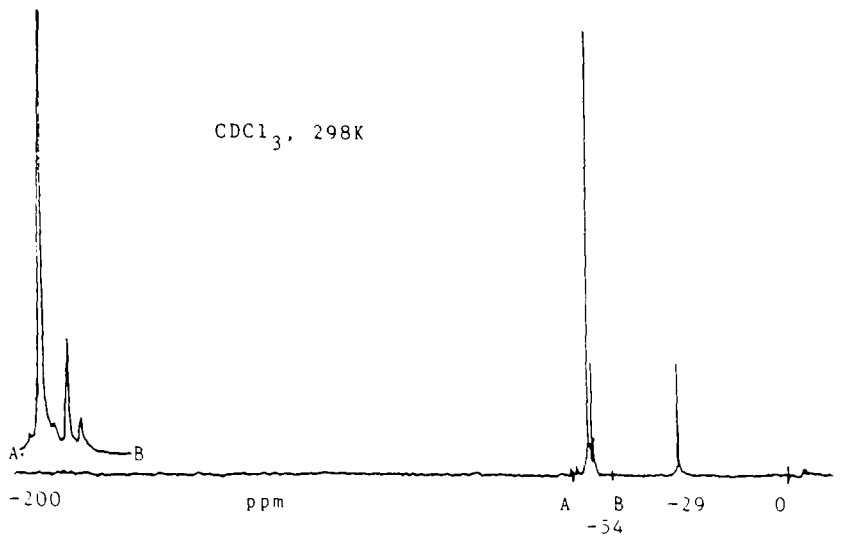

fig. 77 ^{31}P nmr of the Product of the Reaction between $[RuI_2(PPh_3)_2]_n$ and Pyrazole

The ^{1}H and ^{31}P nmr spectra of the product of the reaction between pyrazole and $[RuI_2(PPh_3)_2]_n$ are shown in figs. 76 and 77. The ^{1}H nmr spectrum shows two resonances for the N—H proton in pyrazole at 11.9 and 11.2δ, multiplets at 8.7 and 8.4δ (C3{pzH}), 8.3 and 8.1δ (C5{pzH}) and 6.3 and 6.1δ (C4{pzH}), together with a complicated resonance at 7.2δ, representing the triphenylphosphine protons. The ^{31}P nmr spectrum gives singlets at -29, -53 and -54δ. From comparison with the ^{31}P nmr spectrum of the precursor complex (appendix XIV), it is suggested that unreacted $[RuI_2(PPh_3)_2]_n$ is responsible for the signal at -29δ.

The values of the ^{31}P nmr chemical shifts can depend on a number of factors including:- the electronegativity of the substituents on phosphorus, the substituent-phosphorus-substituent (SPS) angle, the nature of the metal and the change in SPS angle on coordination[101,68]. Angle opening on coordination is consistent with the usually observed downfield shift (negative δ), although the SPS angles of ligands with large substituents generally open less on coordination. This makes prediction of chemical shift shown by a phosphorus atom in a

particular structure very difficult and therefore rationalising a chemical shift with a particular structure is best done by comparison with published data, which is limited. Although substitution of halide ions by larger halide ions has been shown to shift ^{31}P resonances downfield, the effect is not pronounced[70]. The resonances at -53 and -54δ suggest a completely different structure for the complex as compared with the other pyrazole complexes under consideration. Possibilities include Ru(II) cationic and five coordinate species which tend to have chemical shifts in this area (table 3).

^{31}P nmr parameters

COMPLEX	CHEMICAL SHIFT(δ)	TEMP. °C	REF.
$[Ru(sal_2enH)(PPh_3)][BF_4]$	-64.2	25	102
$[Ru(sal_2enH)(PPh_3)][tos]$	-64.2	25	102
$[RuCl(PPh_3)_2(O_2NMe)_3]Cl$	-46.1	25	73
$RuHCl(PPh_3)_3$	-59.0	30	70
$RuClBr(PPh_3)_3$	-42.8	30	70
$RuBr_2(PPh_3)_3$	-43.8	30	70

Table 3 ^{31}P nmr Parameters for Ruthenium Cationic and Five-Coordinate Species

It is therefore suggested that species such as $[RuI(PPh_3)_2(pzH)_2]I$ or

$[RuI_2(PPh_3)_2(pzH)]$ may be responsible for these resonances*, cationic or five coordinate complexes being formed because of the overcrowding resulting from the increased size of the halogen. In contrast, the nmr spectrum of the coordinatively unsaturated $[RuI_2(PPh_3)_2(DMpzH)]$ would seem to indicate that it is formed in a reasonably pure state and the ^{31}P nmr chemical shift of the five coordinate complex (-25δ) suggests that cationic species are probably responsible for the spectrum in fig. 77. Conductivity measurements did not provide meaningful results because of the insolubility of the species in suitable solvents.

(d) In an attempt to prepare cis-pyrazole complexes of Ru(II), a precursor complex with a bidentate chelating phosphorus ligand was used. The reaction of $RuCl_3.3H_2O$ and 1,2-bis(diphenylphosphino)ethane in methanol gave a yellow product which remained inactive when refluxed with pyrazole under nitrogen for several hours. A similar result was obtained when the yellow solid was refluxed with a mixture of pyrazole and triethylamine, with the object of preparing a ruthenium pyrazolide complex. The product of the reaction between $RuCl_3.3H_2O$ and the phosphine was identified in the literature[68] as the coordinatively saturated $[RuCl_2(dppe)_2]$, which is inactive. Its inactivity presumably stems from the fact that the two five-coordinate chelate rings it contains confer stability upon it.

---

* see reaction with methyl iodide [4.4(f)]

4.4 REACTIONS OF $[RuCl_2(PPh_3)_2(pzH)_2].\frac{1}{2}C_6H_{14}$

(a) Reaction with Acetone

Attempts to prepare the cis isomer of the complex $[RuCl_2(PPh_3)_2(pzH)_2].\frac{1}{2}C_6H_{14}$ by reacting $RuCl_2(PPh_3)_3$ with pyrazole in acetone, in accordance with the method described by Gilbert and Wilkinson[96], [4.3(iii)], led to the formation of a product with the infra-red spectrum shown in fig. 78. Reprecipitation of the trans complex from acetone/hexane mixtures, led to the formation of the same dark yellow, solid product.

The N—H stretch and bend of pyrazole[55] are shown at 3260 and 1130 cm^{-1}, P—aryl stretch of triphenylphosphine[56] at 1430 cm^{-1} and the band at 1710 cm^{-1} is assigned to the carbonyl stretch of coordinated acetone[103]. Free acetone, as a solution in CCl_4, gave $\nu(C{=}O)$ at 1720 cm^{-1}. The ^1H nmr spectrum of a solution of the dark yellow solid in $CDCl_3$ is shown in fig. 79. The spectrum is very similar to that shown in fig. 62, with an additional singlet at 1.58. This resonance is taken to provide further evidence of the presence of coordinated acetone within the complex[103]. Free acetone, shows a resonance at 2.18. Integration of N1: C3(pzH): C5(pzH)+PPh_3: C4(pzH): Me_2CO protons gives a ratio of 1: 1: 31: 1: 6, as expected.

Spectroscopic evidence and the fact that five-coordinate Ru(II) species tend to be red in colour[70,104], leads to the conclusion that the solid obtained in acetone is the six-coordinate species $[RuCl_2(PPh_3)_2(pzH)(Me_2CO)]$, rather than the acetone solvate. The reaction of $RuCl_2(PPh_3)_3$ with pyrazole in acetone yielded the original bis-pyrazole complex [4.2(ii)] when a large molar ratio of pyrazole was

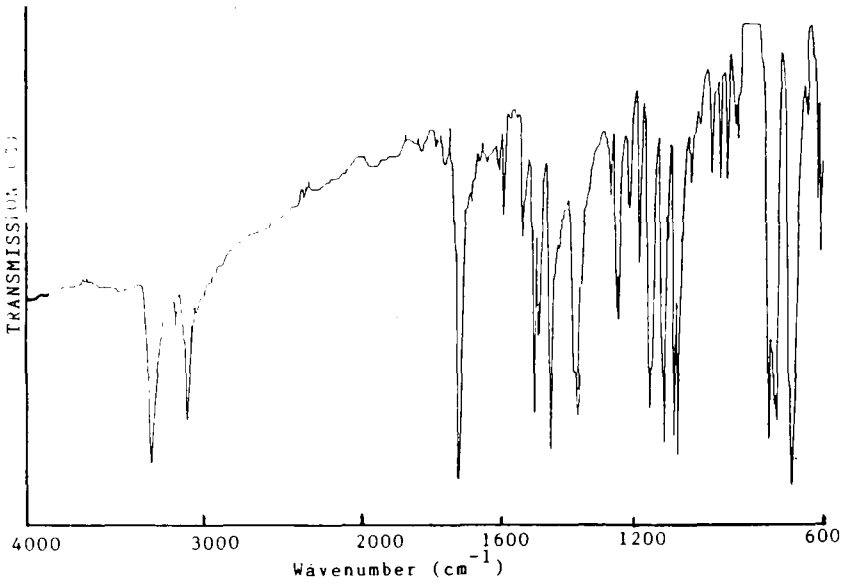

fig.78 Infra-red Spectrum of $[RuCl_2(PPh_3)_2(pzH)(Me_2CO)]$ (KBr disc)

used (greater than 10:1 pzH: $RuCl_2(PPh_3)_3$). This product [4.2(ii)] was identified from its infra-red and far infra-red spectrum and was determined to contain trans-chloride ions, because it contained one band for ν(Ru—Cl) at 330 cm^{-1}.

(b) Reaction of $[RuCl_2(PPh_3)_2(pzH)_2].\frac{1}{2}C_6H_{14}$ with Methanol in the Presence of Base

The complex $[RuCl_2(PPh_3)_2(pzH)_2].\frac{1}{2}C_6H_{14}$ was refuxed with a large excess of triethylamine (1:20 molar ratio) in freshly distilled, dry methanol and under a nitrogen atmosphere for a period of 2 - 3 hours. A brown mixture resulted, which was refrigerated at 2°C for 2 days, whereupon a red solution and brown precipitate were separated by filtration. Over a series of preparations, infra-red spectra of the precipitates obtained

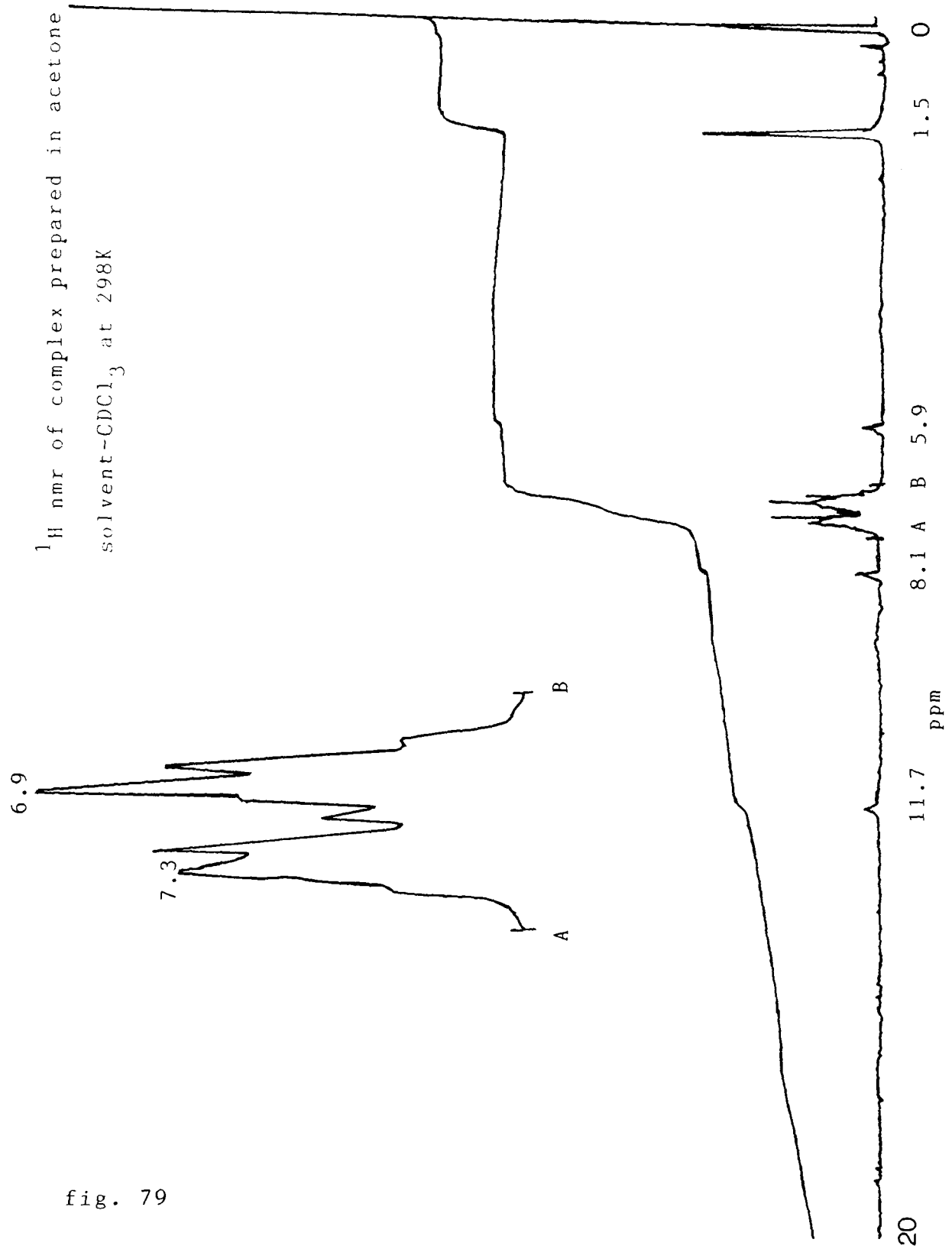
^{1}H nmr of complex prepared in acetone
solvent-$CDCl_3$ at 298K
6.9
7.3
B
A
11.7
8.1 A
B 5.9
1.5
0
20
ppm

fig. 79

gave broad peaks and proved inconsistent with one another. The brown precipitate was therefore concluded to be a mixture of products. Methanol was removed from the red solution and the solid product obtained dissolved in the minimum of toluene. Concentration of this solution and addition of petroleum ether (60/80), gave more brown solid, the infra-red spectrum again indicated a mixture. The red solution obtained on filtration gave a red oil when stripped of its solvent. Precipitation of a dark red solid from the red oil was effected by adding just a few drops of petroleum ether (60/80). The product could then be dried in vacuo. The yields obtained from a series of these preparations were invariably quite low (ca. 30%).

The infra-red spectrum of the dark red product is shown in fig. 80. A single, weak absorption at 2020 cm^{-1} indicates the presence of a Ru—H bond[103]. The strong absorption at 1940 cm^{-1} suggests a terminal CO group trans to a hydride[77]. The broad band at 1045 cm^{-1} is assigned to coordinated methanol[103]. This assumption is reinforced by the band at 2910 cm^{-1} assigned to the C—H aliphatic stretch of methanol.

The proton nmr spectrum of the red complex is shown in fig. 81. Peaks at 7.5 and 7.3δ are associated with coordinated triphenylphosphine and pyrazole, the N—H proton of pyrazole appears at 11.7δ and the singlet at 6.6δ is assigned to the $-CH_3$ protons of methanol[103]. The resonance at 5.5δ may be the C4 proton of pyrazole or possibly the O—H proton in methanol. Protons which exhibit hydrogen bonding tend to show variable chemical shifts over a wide range; hydrogen bonding deshields the proton and is a function of concentration

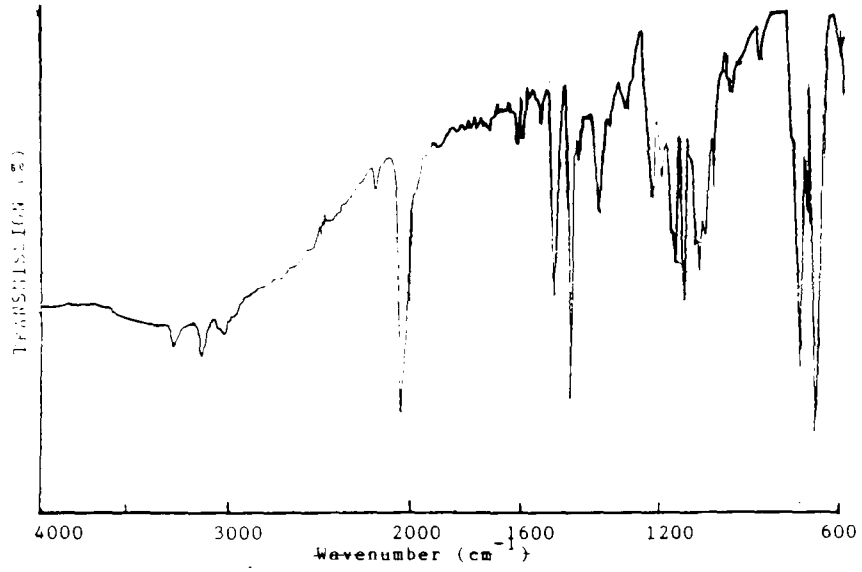

Infra-red Spectrum of the Product of the Reaction Obtained by Reacting $[RuCl_2(PPh_3)_2(pzH)_2].\frac{1}{2}C_6H_{14}$ with Methanol in the Presence of Base

WAVENUMBER	INTENSITY	ASSIGNMENT
3210	w	N—H str., (pyrazole)
3050	w	C—H str., (aromatic)
2910	w	C—H str., aliphatic (MeOH)
2020	w	Ru—H str.
1940	s	C≡O str., terminal carbonyl
1480	m	C—C str., aromatic (PPh_3)
1430	s	P—aryl str.
1120	m (br.)	N—H bend, in plane (pyrazole)
1045	m (br.)	C—O str., coordinated MeOH
740	s	C—H deformation, out of plane
695	s	C—H deformation, out of plane

fig. 80

and temperature. More structural information is available from analysis of the high field region of the ^1H nmr spectrum (fig. 82), where a well resolved hydride resonance is shown. The triplet obtained at -13.18 indicates coupling of hydrogen to two equivalent phosphorus atoms with $J_{P—H}$ = 20Hz. This suggests that the hydride is cis to two equivalent phosphines[46,103]. The magnitude of the coupling constant, $J_{P—H}$, for a trans arrangement to phosphine is of the order of 100Hz[46].

On the basis of infra-red and nmr evidence, therefore, the structure of the red product may be proposed to be as that shown in fig. 83. Integration of the ^1H nmr spectrum in fig. 81 gives a ratio of 1: 32: 3: 1 for the N1: PPh_3+C3, C5(pzH): Me: C4(pzH) protons, in agreement with the structure shown in fig. 83. The deep red colour of the product, however, is indicative of a five-coordinate species[70,104], with

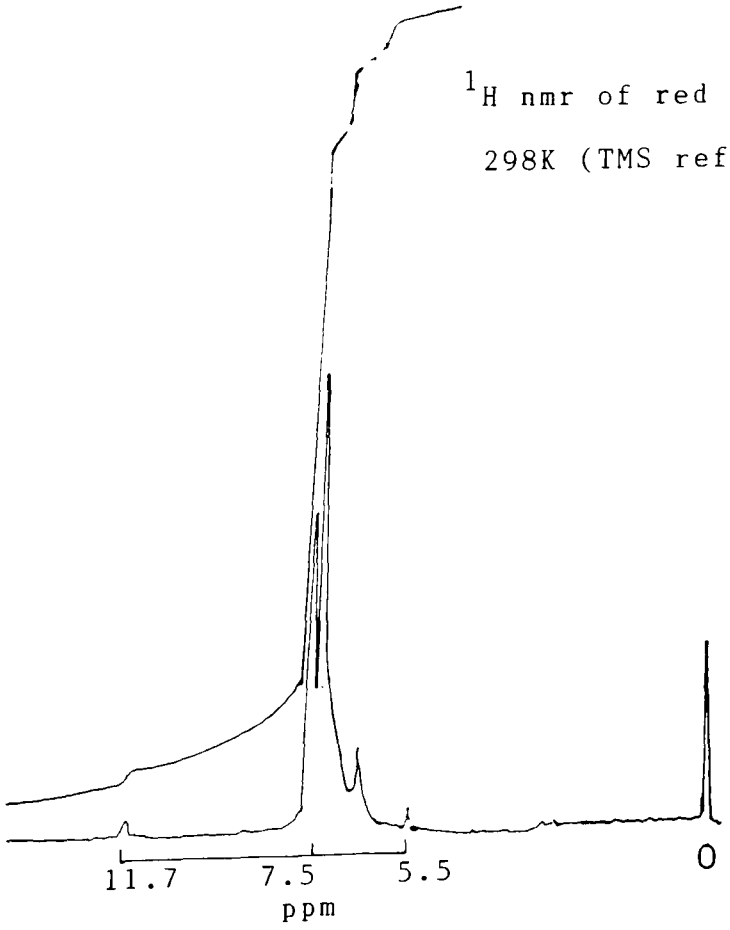

fig. 81

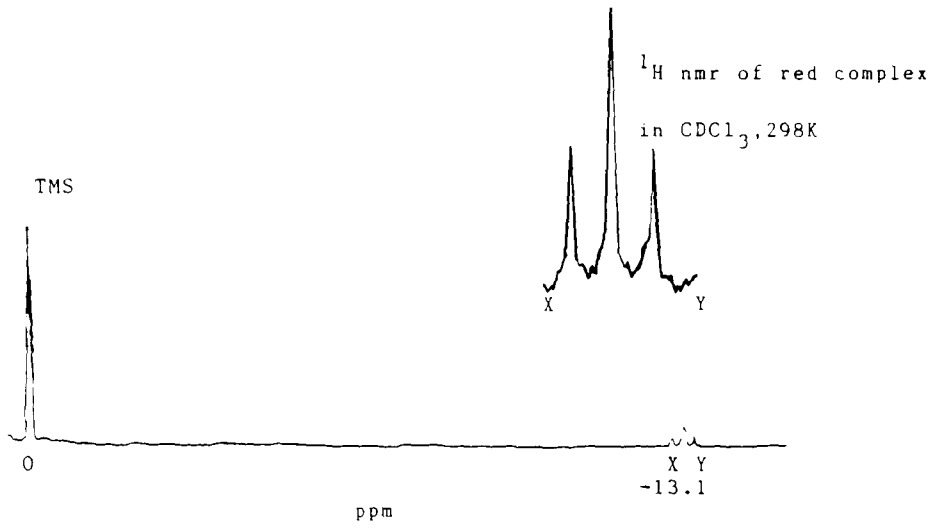

fig. 82

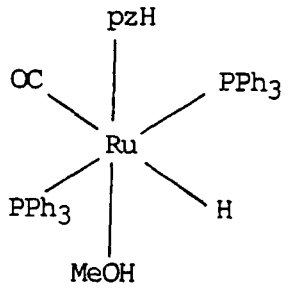

fig. 83 Structure of Dark Red Product

one molecule of alcohol of crystallization. Chaudret et al. describe a similar complex, whose spectra show evidence of coordinated methanol as in this case[103] and suggest that the five-coordinate species is rearranging slowly at room temperature. The product in fig. 83 may well exhibit similar behaviour.

The mechanism of this reaction presents an interesting topic for further study. Ruthenium chloride tertiary phosphine complexes have been shown to react with alcohols, especially in the presence of base to give stable hydridocarbonyl complexes of ruthenium. Triphenylphosphine appears essential for the reaction to take place. Previous reports[46, 103, 105] suggest that the initial steps in the mechanism of the hydridocarbonyl reaction are the formation of an alkoxide complex, followed by β hydrogen transfer (i.e. transfer of the hydrogen from the atom adjacent to coordinated oxygen). The hydride transfer reaction appears to be promoted by the base and leads to carbonylation, in this case via a hydridoformyl derivative. When the preparation was carried out in tertiary butanol instead of methanol, it led to the production of a brown solid. The infra-red spectrum of this product gave no band for ν(Ru—H) or ν(C≡O), but in other respects was similar to that in fig. 80 and showed a broad band at 1045 cm^{-1}, which could be assigned to ν(C—O) of $^{t}BuOH$. This result is in agreement with the above mechanism, in that those alcohols that do not contain β hydrogen on the alkoxide ion, should form complexes incapable of promoting hydrogen transfer and consequently it should be possible to isolate the intermediate alkoxide species.

For the reaction in methanol, dissociation of $[RuCl_2(PPh_3)_2(pzH)_2].\frac{1}{2}C_6H_{14}$ to a coordinatively unsaturated species, probably by loss of triphenylphosphine, would appear to be necessary

before replacement of a chloride ion by methoxide and subsequent hydrogen transfer.

(c) Reaction with Oxygen

The complex $[RuCl_2(PPh_3)_2(pzH)_2].\frac{1}{2}C_6H_{14}$ is stable in the solid state. However, solutions of this compound in toluene, in air, turned from yellow to dark green-brown over a period of one to two hours. Concentration of these solutions and addition of petroleum ether (60/80) gave a dark brown precipitate and a green solution. The dark brown precipitate was found to be diamagnetic, indicating Ru(II), whilst the green solution was assumed to contain traces of Ru(III) species (this colour is very often indicative of that oxidation state). A sample of the species present in solution could not be isolated.

The infra-red spectrum of the dark brown compound does not seem different from that of $[RuCl_2(PPh_3)_2(pzH)_2].\frac{1}{2}C_6H_{14}$. No new bands in the 800 -900 cm^{-1} region are observed; this region shows absorbances due to peroxo groups bound to ruthenium[106]. The v(P==O) stretching frequency in free triphenylphosphine oxide (1190 cm^{-1}) lowers by approximately 50 cm^{-1} on complexation with transition metal cations, phosphine oxides coordinate through oxygen and the lowering of the P==O bond order is explained in terms of a decrease in $p\Pi \rightarrow d\Pi$ back bonding (i.e. $O^- \rightarrow P^+$)[107,108]. No new band can be detected in the 1200 - 1100 cm^{-1} area of the infra-red spectrum of the oxidised complex, providing evidence for coordination of triphenylphosphine oxide to ruthenium. However, this section of the spectrum contains many bands which could have obscured such an absorbance.

The ^{31}P nmr spectrum of the same complex (fig. 84) shows singlets at -29δ (free O=PPh_3), +6δ (free PPh_3) and a ^{1}H nmr spectrum run under the same conditions has proved difficult to interpret because of broadening of the peaks; presumably paramagnetic Ru(III) species present in solution contribute to this effect.

From consideration of what is known of the mechanism of the oxidation of $RuCl_2(PPh_3)_3$, it is suggested that initially $[RuCl_2(PPh_3)_2(pzH)_2].\frac{1}{2}C_6H_{14}$ may lose a bulky phosphine in solution to form a coordinatively unsaturated, sixteen electron species as shown by the following equation:

$$[RuCl_2(PPh_3)_2(pzH)_2] = [RuCl_2(PPh_3)(pzH)_2] + PPh_3 \quad \ldots\ldots\ldots\ldots (5)$$

It is presumed that the equilibrium constant for this reaction would be small, as it is[71] with $RuCl_2(PPh_3)_3$, explaining why no free phosphine is observed in the nmr spectrum of the unoxidised complex [4.3(a)]. If the next stage in the process is oxidation of the sixteen electron complex, the equilibrium in equation (5) would adjust with further dissociation of $[RuCl_2(PPh_3)_2(pzH)_2]$ and free phosphine would eventually be observed in the ^{31}P nmr spectrum.

The next steps in the mechanism can only be speculative, but it seems that oxidation of PPh_3 to O=PPh_3 occurs as in the oxidation of $RuCl_2(PPh_3)_3$, so that a similar species to that found in the ^{31}P nmr spectrum of oxidised $RuCl_2(PPh_3)_3$ gives the singlet at -42δ.

The oxidation of $[RuCl_2(PPh_3)_2(DMpzH)]$ has been discussed in a previous section [4.3(b)]. The ^{31}P nmr spectrum of the oxidised complex again shows resonances indicative of free PPh_3 and O=PPh_3, together with an

unexplained singlet at -36δ, so suggesting a similar mechanism of oxidation as compared with the pyrazole complex.

(d) Reaction of Ruthenium-Pyrazole Complexes with Carbon Monoxide

(i) Reaction of CO with $[RuCl_2(PPh_3)_2(pzH)_2].\frac{1}{2}C_6H_{14}$ When carbon monoxide was bubbled through a yellow toluene solution of $[RuCl_2(PPh_3)_2(pzH)_2].\frac{1}{2}C_6H_{14}$ (ca. 0.2 mmol in 20 cm^3 toluene) for 2 hours at ambient temperature and pressure, the mixture became pale yellow in colour. Concentration of the solution and addition of petroleum ether (60/80) gave a pale yellow product which was subsequently characterized as $[RuCl_2(PPh_3)_2(pzH)(CO)]$.

The infra-red spectrum of the pale yellow product is shown in fig. 85 and its far infra-red spectrum in fig. 86. One band is observed at 1940 cm^{-1} which indicates the presence of one terminal carbonyl group. Evidence for coordinated pyrazole and triphenylphosphine is provided by the bands at 3270 cm^{-1} {ν(N—H)} and 1430 cm^{-1} {ν(P—aryl)} respectively. The far infra-red spectrum gives a broad band for ν(Ru—Cl) at 327 cm^{-1} (trans-chlorines). The ^1H nmr spectrum of the complex is shown in fig. 87. This gives; a broad singlet at 11.3δ (N1 proton, pyrazole), a multiplet at 7.3δ (C3, pyrazole and phosphine protons), a broad resonance at 6.8δ (C5 proton, pyrazole) and a multiplet at 5.8δ (C5 proton, pyrazole). Integration of these signals gives the expected ratio for the suggested formulation of this complex i.e. 1:31:1:1.

fig. 84

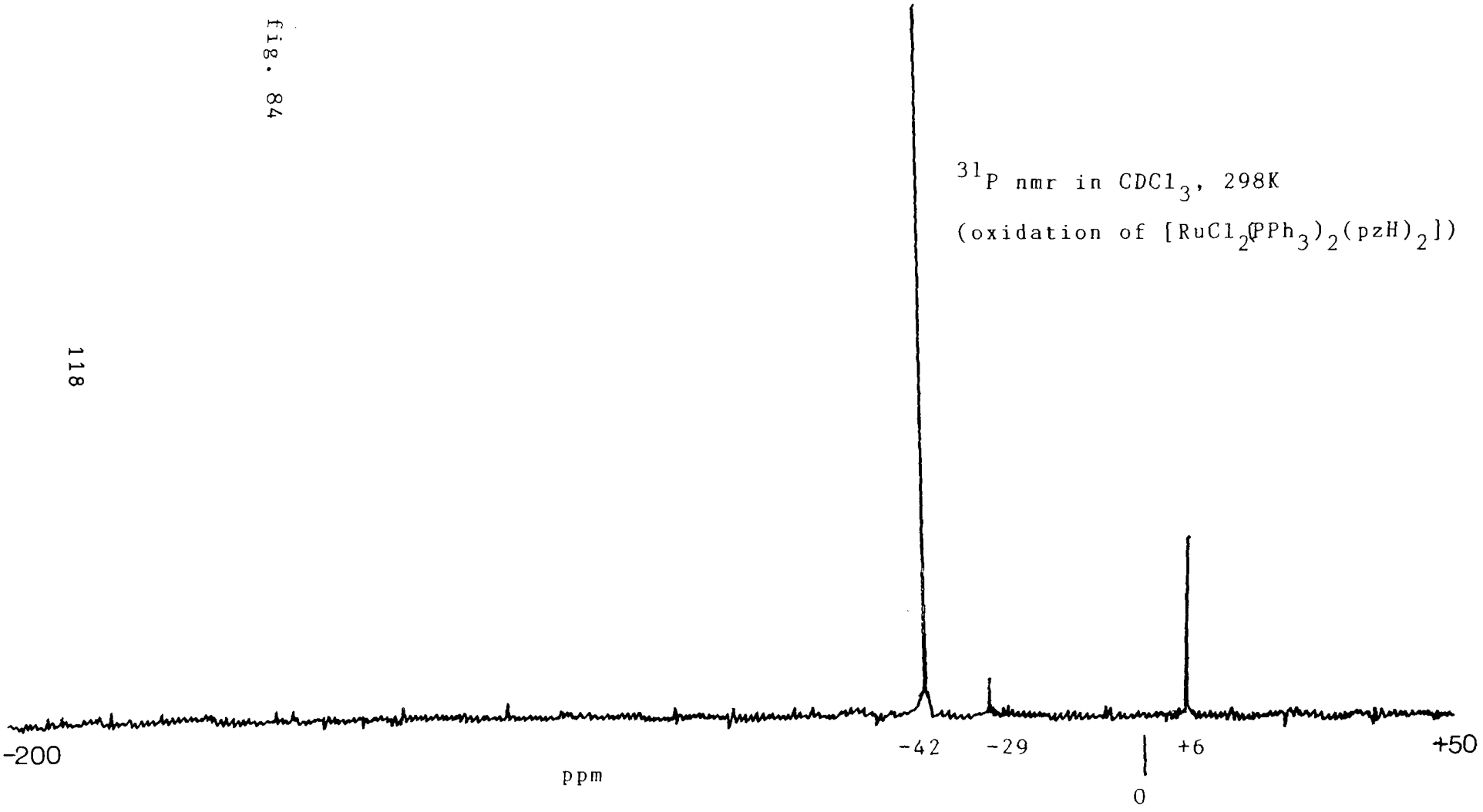
^{31}P nmr in $CDCl_3$, 298K
(oxidation of $[RuCl_2(PPh_3)_2(pzH)_2]$)
-200
ppm
-42
-29
0
+6
+50

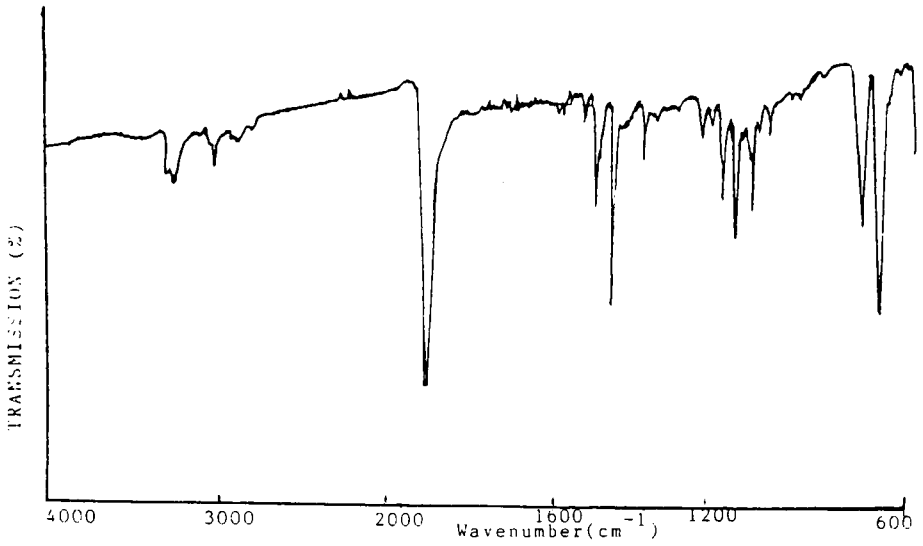

fig. 85 Infra-red Spectrum of $[RuCl_2(PPh_3)_2(pzH)(CO)]$

(KBr disc)

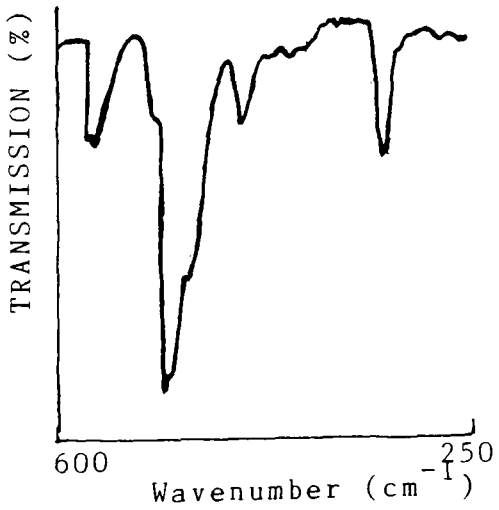

fig. 86 Far Infra-red Spectrum of the above Complex

(CsI disc)

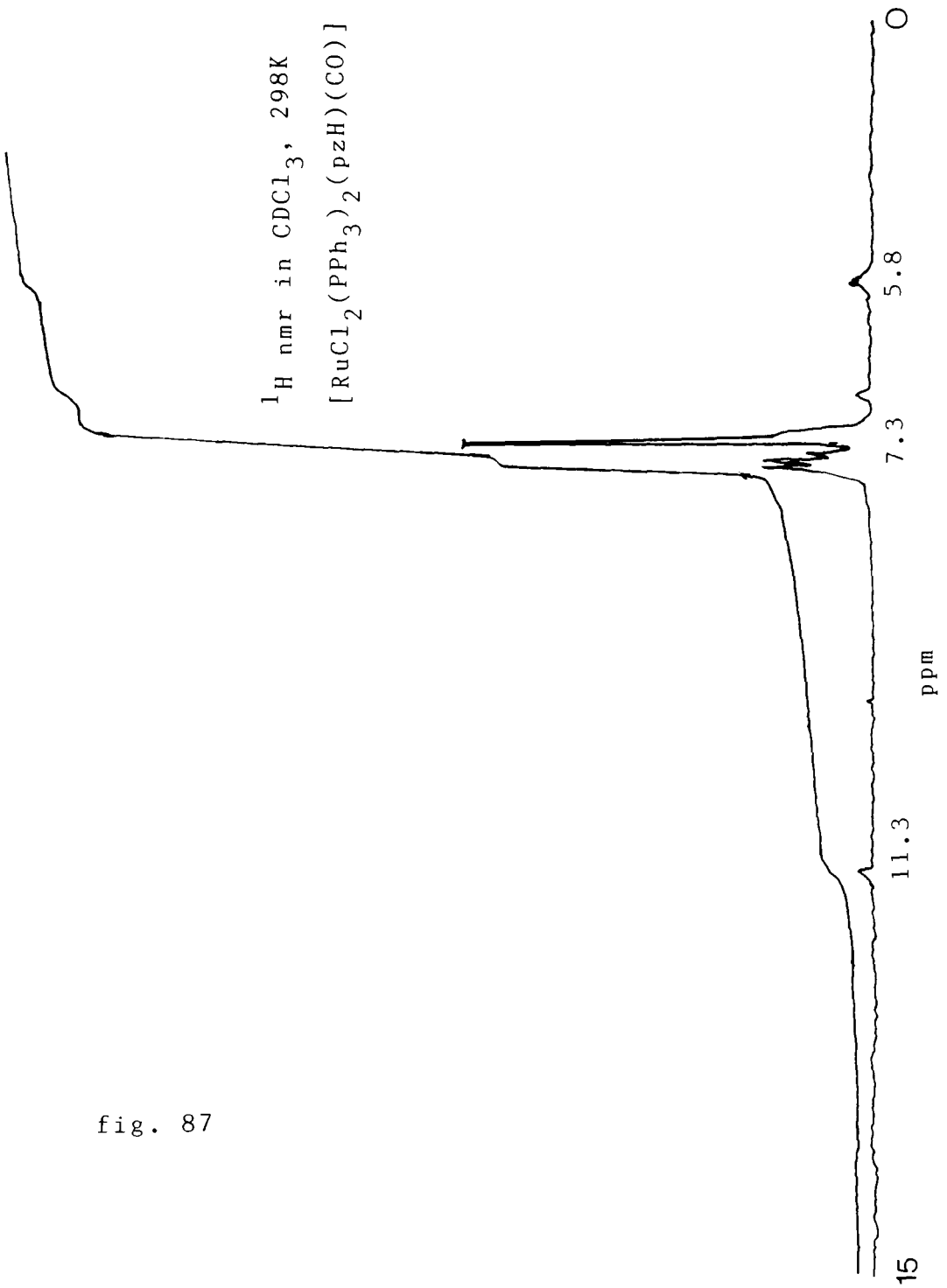

fig. 87

fig.88

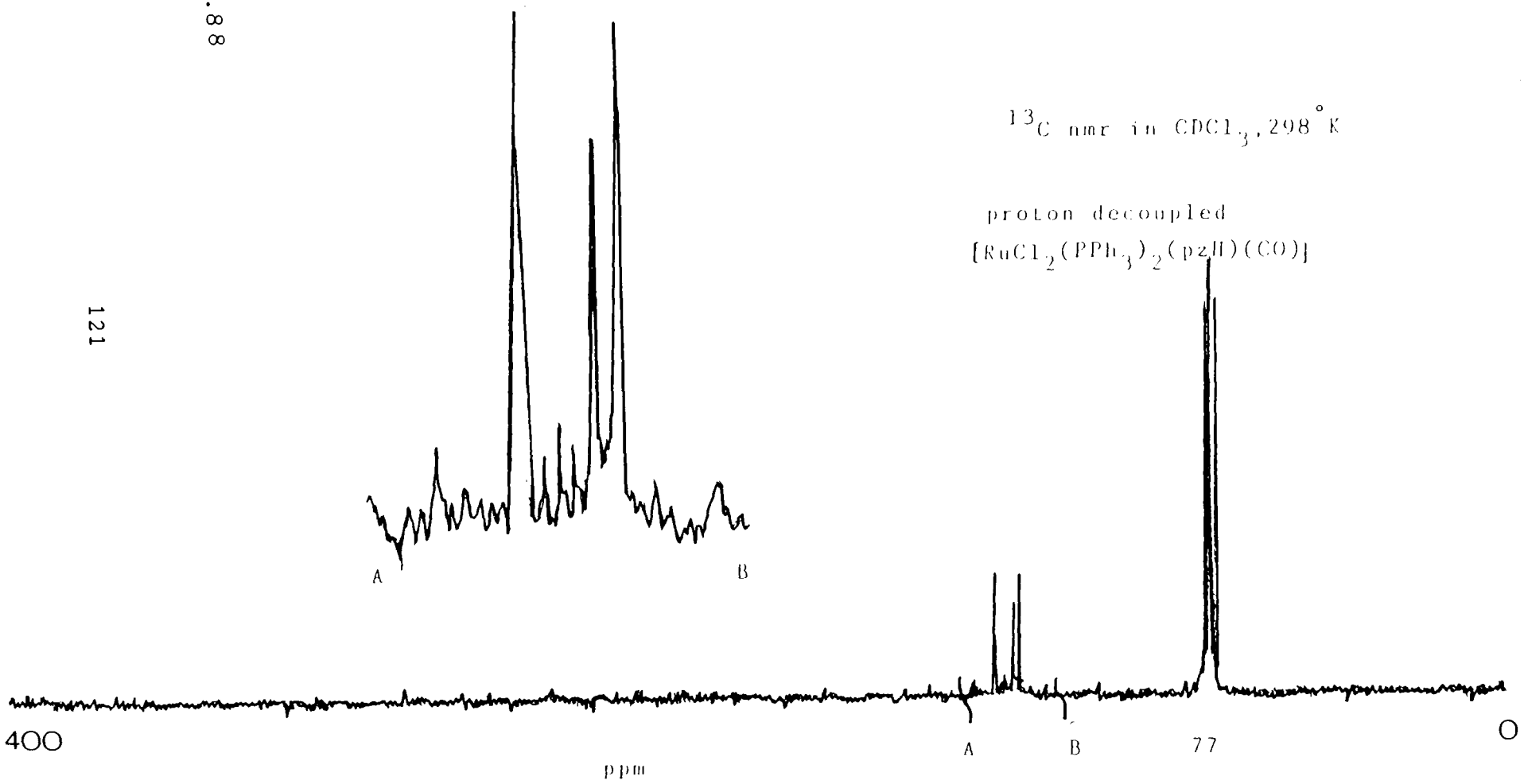
^{13}C nmr in $CDCl_3$, 298° K
proton decoupled
$[RuCl_2(PPh_3)_2(pzH)(CO)]$
A
B
A
B
77
400
O
ppm

fig.89

The ^{13}C nmr spectrum of the same complex is shown in fig. 88. Resonances are shown at 136δ (C3, pyrazole), 130δ (C5, pyrazole) and 128δ (phosphine), with no detectable signal in the region of 106δ for C4, pyrazole. Surprisingly, no resonances are detected in the spectrum at ca. 200 or 250δ, where terminal or bridging carbonyls to ruthenium are detected, although these signals are often weak[109]. The ^{31}P spectrum of the same complex (fig. 89) shows a singlet at -31δ, indicating trans-phosphines, as in the precursor compound.

The formula of the carbonyl complex is therefore suggested to be as in fig. 90 i. e. an octahedral shape with C_{2v} symmetry. Two infra-red active bands would be expected for ν(Ru—Cl) of symmetry $2a_1$ and the broadness of the absorbance in fig. 86, suggests this may be the case.

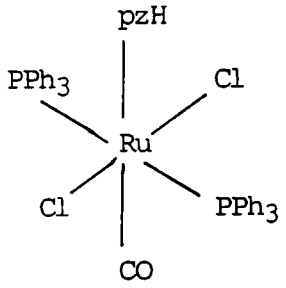

fig. 90 Structure of $[RuCl_2(PPh_3)_2(pzH)(CO)]$

Under more forcing conditions, further substitution appears to occur. When carbon monoxide was bubbled through a previously de-gassed solution of toluene and $[RuCl_2(PPh_3)_2(pzH)_2].\frac{1}{2}C_6H_{14}$ and the mixture refluxed for three hours, it turned pale green. A pale green precipitate was obtained by concentration of the solution and addition of petroleum ether (60/80).

The infra-red spectrum of the pale green precipitate is shown in fig. 91. Three bands are shown in the area expected for terminal carbonyl groups at 1940, 2000 and 2060 cm^{-1}. The intensity of the bands at 1940 cm^{-1} and 3270 cm^{-1} have decreased relative to v(P—aryl) at 1430 cm^{-1}, when compared with those in fig. 85. It is suggested that further substitution of pyrazole has occurred and a mixture of $[RuCl_2(PPh_3)_2(pzH)(CO)]$ and $[RuCl_2(PPh_3)_2(CO)_2]$ is present. Stephenson et al.[80] report one band for trans-$[RuCl_2(PPh_3)_2(CO)_2]$ at 2005 cm^{-1}; Cenini et al.[81] obtained the same band at 2000 cm^{-1}. The species responsible for the band at 2060 cm^{-1} may be a Ru(III) entity (this wavenumber is typical for v(C≡O) in related Ru(III) complexes[80]). More likely, however, is that isomerization of the trans complex has occurred at the elevated temperature to form cis-$[RuCl_2(PPh_3)_2(CO)_2]$ (fig. 92).

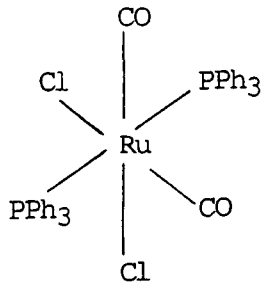

fig. 92 Cis-$[RuCl_2(PPh_3)_2(CO)_2]$

This complex has been found to show bands[80] for v(C≡O) at 2064 cm^{-1} and 2001 cm^{-1}. The colour of the solid mixture under consideration indicated that it contained traces of oxidation product. The far infra-red spectrum of the mixture contains a broad band at 330 cm^{-1} (fig. 93).

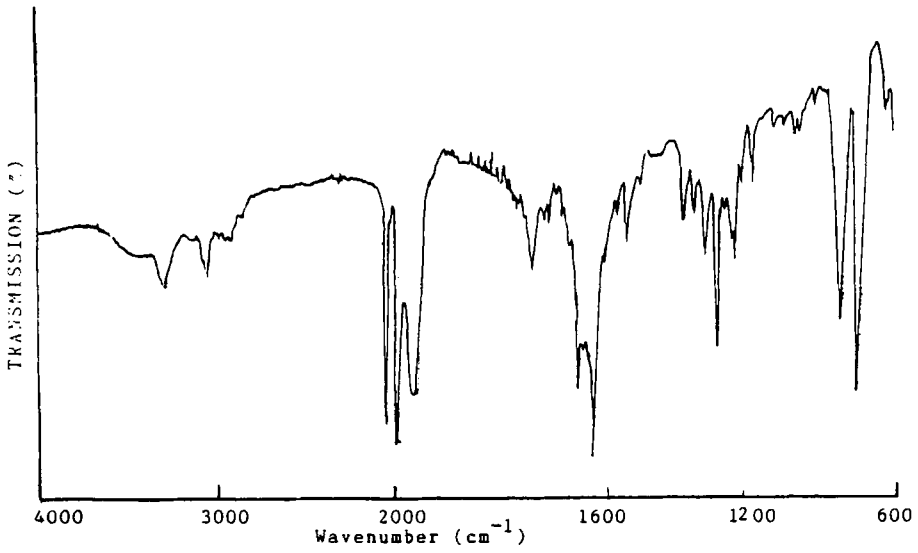

fig. 91 Infra-red Spectrum of Pale Green Precipitate

(KBr disc)

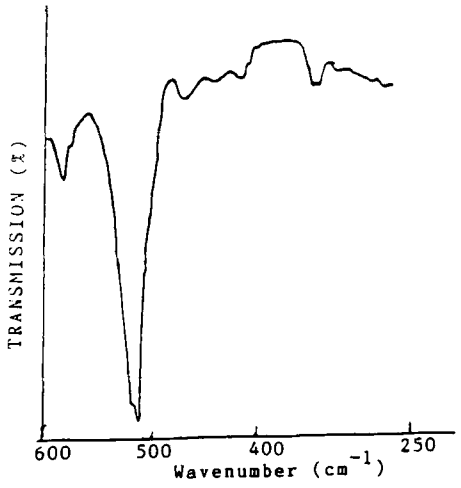

fig. 93 Far infra-red Spectrum of above

(CsI disc)

which could be a combination of bands, again indicating a mixture of products. The band for v(Ru—Cl) in trans-$[RuCl_2(PPh_3)_2(CO)_2]$ is reported[80] at 328 cm^{-1}, whilst the cis complex gives v(Ru—Cl) values at 300 and 275 cm^{-1}. These bands are not apparent in fig. 93, however this part of the spectrum is not well resolved.

The displacement of pyrazole by carbon monoxide can be explained in terms of "Pearsons Principle" [1.8], which classifies Ru^{2+} as a soft base and CO as a soft acid. As previously explained, pyrazole may be regarded as a borderline acid, therefore it is likely that Ru^{2+} preferentially coordinates with CO rather than pyrazole.

(ii) Reaction of $[RuCl_2(PPh_3)_2(DMpzH)]$ with CO

Carbon monoxide was bubbled through $[RuCl_2(PPh_3)_2(DMpzH)]$ in toluene (0.2 mmol in 20 cm^3) for two hours at room temperature and atmospheric pressure. A pale yellow, diamagnetic precipitate was obtained. The precipitate was found to be insoluble in a variety of organic solvents, preventing investigation using nmr. Analysis proved inconclusive, suggesting a mixture of products.

The infra-red and far infra-red spectra of the precipitate are shown in figs. 94 and 95. One terminal carbonyl is suggested by the band found at 1935 cm^{-1}. Other bands to note are those at 1430 cm^{-1} {v(P—aryl)} and the collection of bands around 3250 - 3400 cm^{-1} {v(N—H)}. In fig. 94, there is a broad band around 350 cm^{-1} {v(Ru—Cl)}, with a shoulder extending over 300 cm^{-1}, which is probably v(Ru—Cl) for $[RuCl_2(PPh_3)_2(DMpzH)]$. The spectra suggest that the precipitate obtained was a mixture of $[RuCl_2(PPh_3)_2(DMpzH)]$ and $[RuCl_2(PPh_3)_2(DMpzH)(CO)]$.

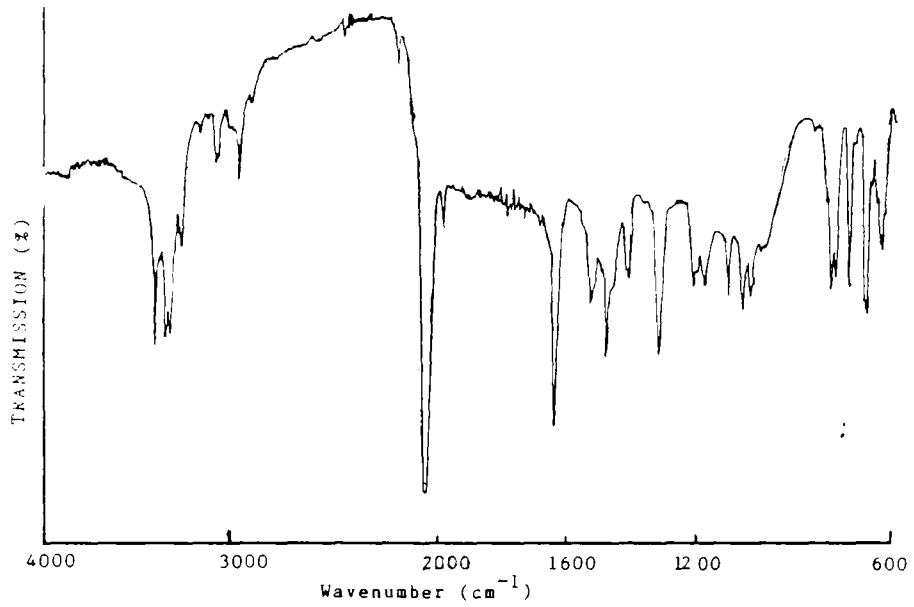

fig. 94 Infra-red Spectrum of Pale Yellow Precipitate (KBr disc)

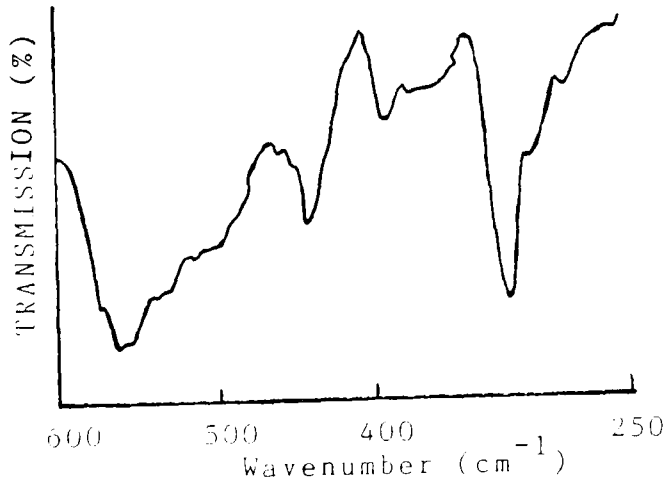

fig. 95 Far infra-red Spectrum of the above sample (CsI disc)

and when nitrogen was bubbled through a toluene suspension of this mixture for two hours and the mixture stirred under nitrogen for a further two days, the precipitate gave an infra-red spectrum identical to that of $[RuCl_2(PPh_3)_2(DMpzH)]$. This indicates that the coordination of carbon monoxide to ruthenium is reversible, presumably the bulky ligands in the aforementioned complex do not encourage coordinative saturation. This effect was not observed after bubbling nitrogen through a toluene solution of $[RuCl_2(PPh_3)_2(pzH)(CO)]$.

(e) Reaction of Ruthenium-Pyrazole Complexes with Hydrogen

The complexes $[RuCl_2(PPh_3)_2(pzH)_2].\frac{1}{2}C_6H_{14}$ and $[RuCl_2(PPh_3)_2(DMpzH)]$ were stirred under hydrogen gas at 1 atmosphere pressure, in a suitable solvent, for 48 h, (ca. 0.2 mmol in 20 cm^3 toluene and acetone respectively). The apparatus is described in [2.2(i)]. The precipitates obtained by concentration of the solution and addition of petroleum ether (60/80), showed no band for v(Ru—H) in their infra-red spectra. The solution spectra were also examined, but no evidence existed for the presence of a hydrido-complex. Both complexes were reacted with oct-1-ene and hyrogen as described in [2.2(ii)], but analysis of the mixture by gas chromatography gave no indication that hydrogenation had taken place. The conditions under which the gas chromatograph was operated were as described in [6.6].

(f) Reaction of Ruthenium-Pyrazole Complexes with Methyl Iodide

(i) Addition of methyl iodide to $RuCl_2(PPh_3)_3$ The complex $RuCl_2(PPh_3)_3$ was stirred with methyl iodide in toluene (0.2 mmol in 20 cm^3, 1:1 molar ratio), under nitrogen, at room temperature for 5 days. Concentration of the brown solution and addition of petroleum ether (60/80) gave a brown precipitate, which was shown by infra-red and nmr spectroscopy to be the starting material, $RuCl_2(PPh_3)_3$. The same result was obtained when the mixture was refluxed for 4 hrs. i.e. no apparent reaction.

(ii) Reaction of $RuCl_2(PPh_3)_3$ with pyrazole and methyl iodide When $RuCl_2(PPh_3)_3$ was strirred with pyrazole and methyl iodide (0.2 mmol in 20 cm^3, 1 : 2 :1 molar ratio), under nitrogen and in toluene, for 2 hr., the solution turned yellow and a white precipitate was formed. The white precipitate was subsequently identified from infra-red and nmr spectroscopy as the quaternary phosphonium halide salt, $MePPh_3^+ I^-$ [4.2(x)]. The precipitate obtained fron concentration of the toluene solution and addition of petroleum ether(60/80), was subsequently identified from spectroscopic measurements as $[RuCl_2(PPh_3)_2(pzH)_2].\frac{1}{2}C_6H_{14}$.

The infra-red and ^1H nmr spectra of the quaternary salt, $MePPh_3^+ I^-$ are shown in figs. 96 and 97. In fig. 96, the P—aryl stretch is shown at 1440 cm^{-1}, whilst the ^1H nmr spectrum in fig. 97 shows a multiplet at 7.9δ (representing the aryl protons) and a doublet at 3.3δ (methyl protons coupled to phosphorus, with $J_{P—H}$ = 15 Hz). The integration ratio is 5: 1 for aryl : methyl protons as expected for $MePPh_3^+ I^-$. The ^{31}P nmr spectrum of the salt gives a single resonance at -21δ.

(iii) Reaction of Methyl iodide with $[RuCl_2(PPh_3)_2(pzH)_2].\frac{1}{2}C_6H_{14}$ The complex $[RuCl_2(PPh_3)_2(pzH)_2].\frac{1}{2}C_6H_{14}$ was stirred with methyl iodide in rigorously de-gassed toluene (0.2 mmol, 1 : 1 molar ratio in 20 cm^3 of solvent) under nitrogen for five days at room temperature, whereupon a dark yellow precipitate formed in the yellow solution. The infra-red, far infra-red and nmr spectra of this diamagnetic precipitate are shown in figs. 98, 99 and 100. The ^1H nmr spectrum shows resonances at 12.2, 8.5, and 6.3δ due to an unidentified species containing pyrazole. The other resonances at 11.6, 8.1 and 6.0δ indicate $[RuCl_2(PPh_3)_2(pzH)_2].\frac{1}{2}C_6H_{14}$. Further clues as to the nature of the species present may be found in the ^{31}P nmr spectrum which has signals at -28 and -53δ. A signal at -53δ is found in the spectrum of the product of the reaction between $[RuI_2(PPh_3)_2]_n$ and pyrazole (fig. 77). This suggests a species of similar structure i.e. probably cationic. The far infra-red spectrum gives a broad band at 350 cm^{-1} {which is taken to be ν(Ru--Cl)}. The band extends to 326 cm^{-1}, the value for $[RuCl_2(PPh_3)_2(pzH)_2].\frac{1}{2}C_6H_{14}$. The infra-red spectrum of the yellow precipitate (4000 - 600 cm^{-1}), gave little information except for the fact that the band attributed to ν(N—H) was split, a possible indication a mixture of species was present. The solid isolated from the solution remaining (by concentration and addition of petroleum ether (60/80), showed some traces of oxidation in that it was pale green in colour and gave broad bands in its ^1H nmr spectrum. It gave two bands for ν(Ru—Cl) in the far infra-red spectrum (600 - 250 cm^{-1}), at 326 and 350 cm^{-1}, indicating a mixture of $[RuCl_2(PPh_3)_2(pzH)_2].\frac{1}{2}C_6H_{14}$ and a new species.

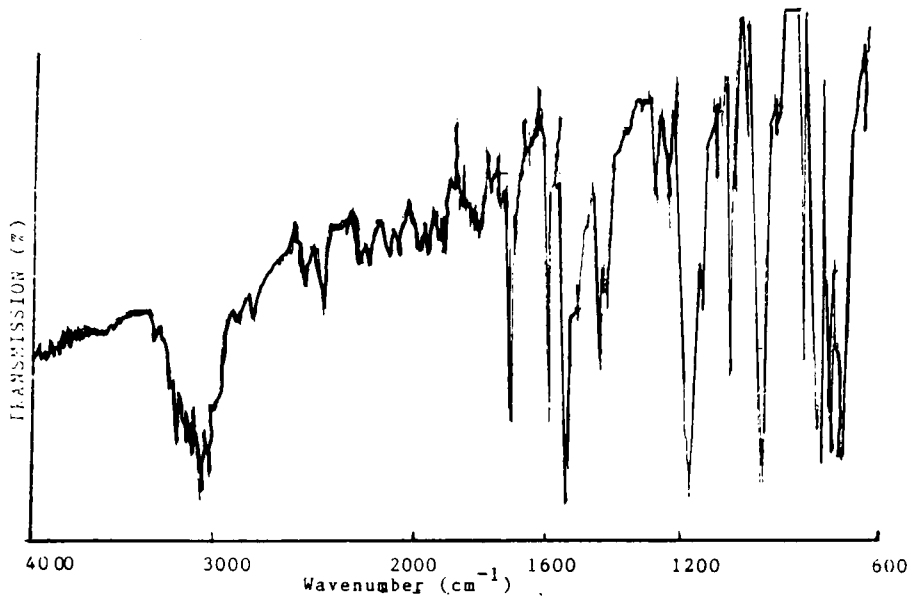

fig. 96 Infra-red Spectrum of $MePPh_3^+I^-$

(KBr disc)

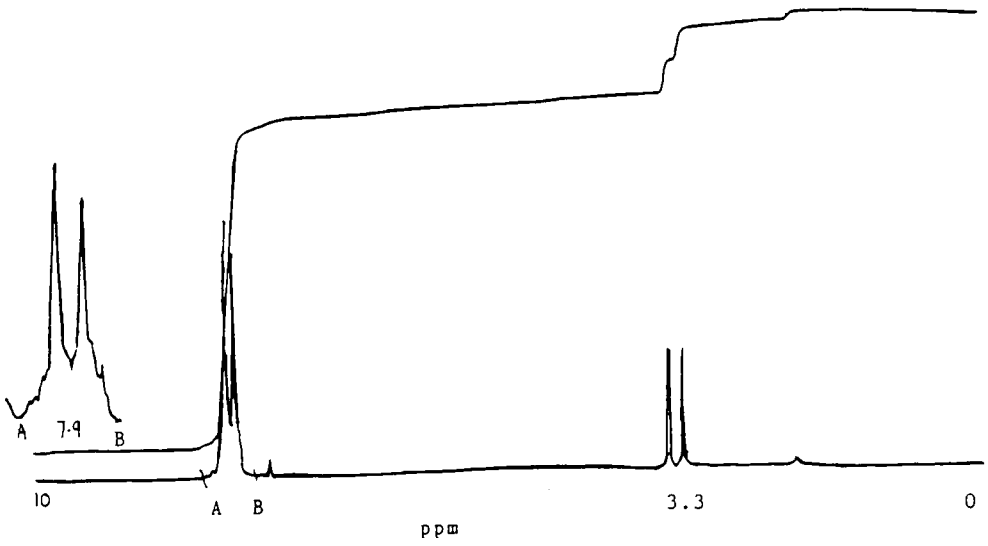

fig. 97 ^1H nmr Spectrum of $MePPh_3^+I^-$

$CDCl_3$, 298K

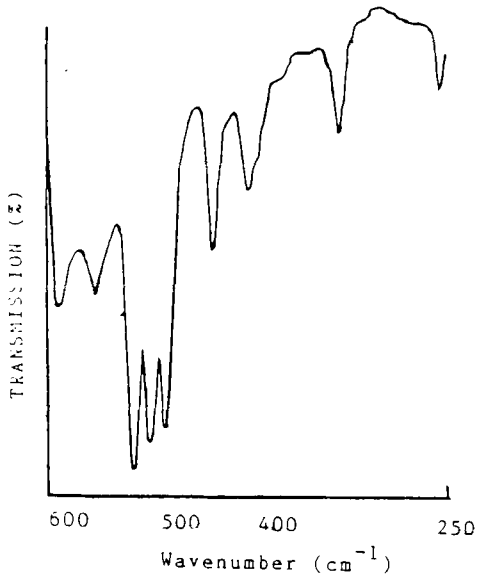

fig. 98 Far infra-red Spectrum of product from $[RuCl_2(PPh_3)_2(pzH)_2]$ and MeI (CsI disc)

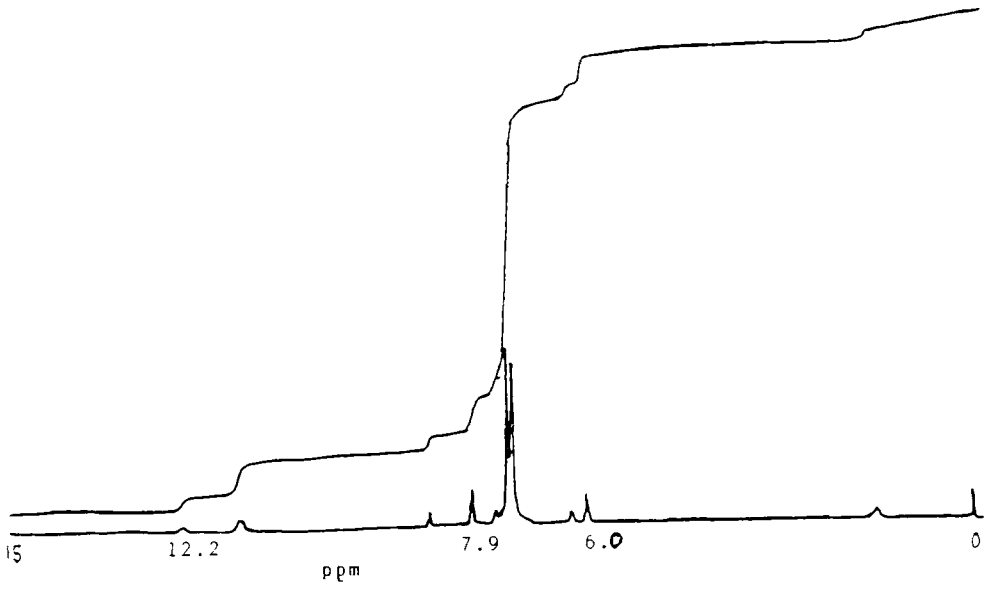

fig. 99 ^1H nmr of above product $CDCl_3$, 298K

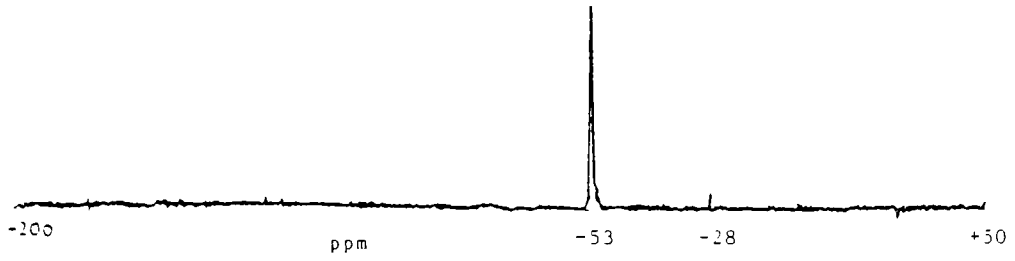

fig. 100 ^{31}P nmr Spectrum of product from $[RuCl_2(PPh_3)_2(pzH)_2]$ and MeI $CDCl_3$, 298K

Group VIII metal complexes have been shown to act as halogen exchange catalysts between alkyl halides[110]. For example, the reaction of MeI with $RuCl_2(PPh_3)_3$ in CH_2Cl_2 gives MeCl and CH_2ICl. The reaction was first thought to involve oxidative-addition of the alkyl halide to the transition metal complex, followed by halide exchange on the metal and reductive elimination of the new alkyl halide. A later paper, however[111], provided evidence that the true catalyst in these reactions is a halide ion generated by the quaternisation of labile phosphines by the alkyl halide. Halogen exchange at the metal centre occurs when Ru(II) or Ru(IV) chloro-complexes are treated with HBr or HI and the halogen exchange is an equilibrium that favours the formation of the longer ruthenium—halogen bond[112]. This is perhaps because the larger halogen has a higher nephelauxetic effect i.e. more ability to decrease interelectronic repulsion, so stabilising the metal ion. The reactions

described occur with coordinatively saturated and unsaturated ruthenium complexes and are not considered to have taken place via an oxidative addition/reductive elimination mechanism. Presumably they proceed by nucleophilic substitution, the high acidity of the hydrogen halide ensuring the availability of halide ions. "Mixed halogen species" are also produced during this reaction.

Because of the similarities in the nmr spectra between the species obtained from the reaction of MeI with $[RuCl_2(PPh_3)_2(pzH)_2].\frac{1}{2}C_6H_{14}$ and that from $[RuI_2(PPh_3)_2]_n$ with pyrazole, it is concluded that in the former reaction some form of halogen exchange has taken place. The quaternary phosphonium salt, $MePPh_3^+I^-$ may provide the source of I^- ions. The salt was formed in quantity in the presence of excess phosphine i.e. reaction (ii), page 129. Although the species was not detected in the spectra arising from reaction (iii), page 130, it has already been suggested* that $[RuCl_2(PPh_3)_2(pzH)_2].\frac{1}{2}C_6H_{14}$ may lose a phosphine in solution and the dissociation constant is small (the presence of the phosphonium salt was not detected in (i), page 129, but $RuCl_2(PPh_3)_3$ catalyses halogen exchange reactions[110]). The formation of the phosphonium salt, followed by nucleophilic substitution could provide a possible mechanism for halogen exchange. The replacement of chlorine by iodine in the complex would increase the bulk of the coordinated ligands, favouring the formation of a cationic species of the type $[RuCl(PPh_3)_2(pzH)_2]^+I^-$. The increase in wavenumber for ν(Ru—Cl) at 350 cm^{-1} indicates a stronger, shorter bond which would be the expected result of the net positive charge delocalised across the cation $[RuCl(PPh_3)_2(pzH)_2]^+$.

---

* see reaction with oxygen [4.4(c)]

It is suggested, therefore that a mixture of $[RuCl_2(PPh_3)_2(pzH)_2].\frac{1}{2}C_6H_{14}$ and $[RuCl(PPh_3)_2(pzH)_2]I^-$. is responsible for the resonances in figs. 99 and 100. Conductivity measurements again proved inconclusive because of the insolubility of these species in suitable solvents. Ruthenium complexes which contain a cationic ruthenium species and iodide as anions have been found in the literature[34] as products of oxidative addition with Ru(I) precursor complexes. The related complex $[RuCl_2(PPh_3)_2(DMpzH)]$, with the much larger pyrazole ligand does not appear to react with MeI under the same conditions, possibly because association of an iodide ion is unfavourable from steric considerations. When $[RuCl_2(PPh_3)_2(pzH)_2].\frac{1}{2}C_6H_{14}$ is stirred with iodine (0.2 mmol, 1:1 molar ratio) in toluene under the same conditions as in reaction (iii), page 130, the spectra of the solid obtained from the reaction mixture indicate that no reaction has taken place. This supports the suggestion that the halide ion is required for halogen exchange and that the reaction does not take place through oxidative-addition.

SECTION FIVE-ATTEMPTS TO PREPARE RUTHENIUM-PYRAZOLYL COMPLEXES WITH μ^2-BRIDGING LIGANDS

5.1 REACTION OF RUTHENIUM-PYRAZOLE COMPLEXES WITH BASE

(a) Under Nitrogen

The complexes $[RuCl_2(PPh_3)_2(pzH)_2].\frac{1}{2}C_6H_{14}$ and $[RuCl_2(PPh_3)_2(DMpzH)]$ were reacted with base in order to investigate the ease of removing the pyrazole protons. The complexes do not possess ideal geometry for generating potential metal - containing ligands (cis coordination of pyrazole ligands would be preferred), however, it is possible that rearrangement of ligands could occur after deprotonation, or possible mono-bridged pyrazole complexes could be created.

Despite refluxing $[RuCl_2(PPh_3)_2(pzH)_2].\frac{1}{2}C_6H_{14}$ with excess base in toluene for some hours, the product obtained by concentration of the solution and addition of petroleum ether (60/80) showed a band in its infra-red spectrum characteristic of the N--H stretch, indicating that the pyrazole proton had not been removed. The bases used were triethylamine and 1,8-bis(dimethylamino)napthalene. A similar result was obtained when $RuCl_2(PPh_3)_3$ was treated with a tenfold molar excess of a mixture of pyrazole and triethylamine in acetone; the infra-red spectrum of the product indicated that $[RuCl_2(PPh_3)_2(pzH)(Me_2CO)]$ had been prepared. The same type of experiments also failed to deprotonate $[RuCl_2(PPh_3)_2(DMpzH)]$. Further attempts to deprotonate $[RuCl_2(PPh_3)_2(pzH)_2].\frac{1}{2}C_6H_{14}$ by reaction with triethylamine in methanol, led to reaction with the solvent, as described in [4.4(b)].

(b) In Air

Sullivan et al.,[30] removed the pyrazole proton from complexes of the type $[(bpy)_2Ru(pzH)_2]^{2+}$ using aqueous potassium hydroxide in a nitrogen atmosphere. For this reason, experiments were conducted in which $[RuCl_2(PPh_3)_2(pzH)_2].\frac{1}{2}C_6H_{14}$ was refluxed in an excess of potassium hydroxide in an acetone/water mixture and under a nitrogen atmosphere. Infra-red spectra of the reaction products indicated that no reaction had taken place and deprotonation had not been achieved. When the same reactants were stirred in air at room temperature, however, the reaction mixture first turned green and then dark blue. This reaction was also carried out in acetone using triethylamine as a base, with a similar result. Although the nature of the base did not seem critical, the intense blue colouration only appeared when three substances were simultaneously present i.e. water/air/base.

(i) Experimental The complex $[RuCl_2(PPh_3)_2(pzH)_2].\frac{1}{2}C_6H_{14}$ (0.30 g, 0.34 mmol) was stirred with excess KOH (0.20 g, 3.40 mmol) in an acetone/water mixture (25 cm^3/5 cm^3), in air, at room temperature for 2 h. The resulting dark blue mixture was filtered and the acetone removed under reduced pressure. Toluene (25 cm^3) was added to dissolve the dark blue product and the mixture washed with three aliquots of water (3 x 5 cm^3). After the final separation of the toluene layer, the layer was dried using anhydrous magnesium sulphate and the mixture filtered. Concentration of the filtrate to ca. 5 cm^3 and addition of hexane gave a dark blue precipitate. The precipitate was filtered off, washed with a small amount of hexane and dried in vacuo. Yield = 0.06 g.

The blue solid obtained was diamagnetic, very soluble in both polar and non-polar organic solvents and contained nitrogen but no chlorine (as shown by Lassaigne fusion tests). The first water aliquot used to wash the toluene layer in the preparation gave a white precipitate of silver chloride when tested with silver nitrate solution. These tests led to the assumption that the chloride ligands were lost during the preparation and passed into solution as potassium chloride. The first water aliquot was often red in colour, turning brown on addition of dilute mineral acid. This seemed to suggest that a "ruthenium red" species was present in solution [4.1(vi)]. However, no product could be isolated from the aqueous solution.

(ii) Infra-red and nmr spectra The infra-red spectrum of the dark blue product is shown in fig. 101. The important features of the spectrum are summarized in table 4.

WAVENUMBER	INTENSITY	ASSIGNMENT
3140	w, br.	O—H stretch, water
3060	w	aromatic C—H stretch
1435	s	P—aryl stretch
1380	m	ring stretch, pyrazole
1360	m	ring stretch, pyrazole
620	w	ring stretch, pyrazole

Table 4 Important Features of Fig. 101

No bands were observed for ν(N—H) in the infra-red spectrum, indicating deprotonation of the pyrazoles. Stobart et al.[37], during the course of

their work with iridium μ^2-pyrazolyl dimers concluded that "We consider absorption in the 1450 - 1500 range to be diagnostic of the bridging ligand." In the present work, such an absorbance is obscured by bands present from the spectrum of coordinated triphenylphosphine. However, pyrazole and pyrazole complexes display an absorbance around 1390 -1350 cm^{-1}. This is due to an in - plane ring stretch. In pyrazole this is at 1390 cm^{-1} (appendix III). For coordinated pyrazole, it generally moves to a lower wavenumber (table 5).

COMPLEX	RING STRETCH (cm^{-1})	REFERENCE
$[RuCl_2(PPh_3)_2(pzH)_2].\frac{1}{2}C_6H_{14}$	1360	fig. 61
trans-$[NiCl_2(pzH)_4]$	1360	fig. 47
$[(COD)Rh(pz)]_2$	1360	12
$[Ni(pz)_2.H_2O]_n$	1390	fig. 53
$[RuBr_2(PPh_3)_2(pzH)_2].\frac{1}{2}C_6H_{14}$	1350	fig. 74
$[Pd(pz)_2(dppe)]$	1360	fig. 106
$[Zn(pz)_2]_n$	1380	60

Table 5 Ring Stretch in Pyrazole Complexes

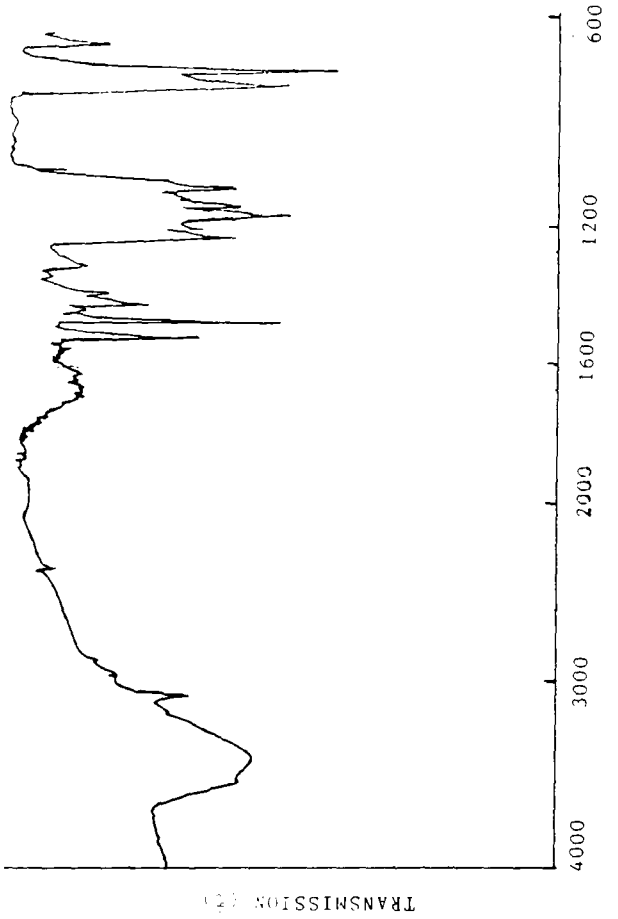

fig. 101 Infra-red Spectrum of dark blue Solid
(KBr disc)

A band in this area can therefore be taken as evidence of coordinated pyrazole, μ^2-pyrazolyl or pyrazolide groups. Two such bands are found in the spectrum of the dark blue product, so it is concluded that the pyrazolide ions in the complex are coordinated in two different ways i.e. bridging and terminal. Coordination of pyrazole shifts the in-plane ring stretch of pyrazole from 1390 to 1360 cm^{-1}; removal of the N--H proton of coordinated pyrazole appears to increase this figure to 1380 cm^{-1}, coordination of a second metal ion would lower this figure again, in this case back to 1360 cm^{-1}. The same spectrum gives evidence of the presence of water from a broad band at 3240 cm^{-1} and a weaker band around 1600 cm^{-1}. The infra-red spectrum showed no band in the region 800 - 900 cm^{-1} indicative of a linear Ru—O—Ru system[93] (see discussion) and no bands in the infra-red or far infra-red regions could be positively assigned to a bent linkage. This is also the case with reported oxo-bridged dimers[88]. The far infra-red spectrum (600 - 250 cm^{-1}, CsI disc), as expected, gave no absorbances between 400 - 250 cm^{-1} in the region expected for v(Ru—Cl).

The ^1H nmr spectrum of the blue solid is shown in fig. 102. A signal representative of phenyl and possibly pyrazole protons exists between 8.4 -7.3δ and there is also a very broad resonance at 1.7δ, assigned to represent water; integration gives an approximate ratio of PPh_3 : $2H_2O$ i.e. 15 : 4. Surprisingly, the spectrum does not display resonances which can be assigned to specific protons contained in the pyrazolide ion, unlike the previous ruthenium-pyrazole complexes discussed, despite the fact that the blue complex was very soluble in $CDCl_3$. Neither increasing the concentration of the solution nor running the spectrum in a solution of acetone-d^6 rectified this situation. The resonances might be included in the region 8.4 - 7.3δ, or slight traces of

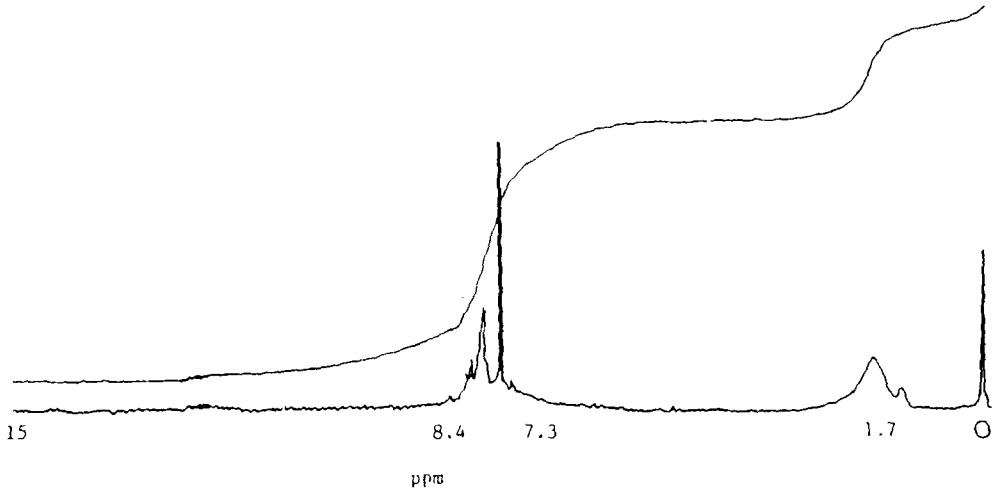

fig. 102 ^{1}H nmr Spectrum of dark blue Solid in $CDCl_3$, 298K

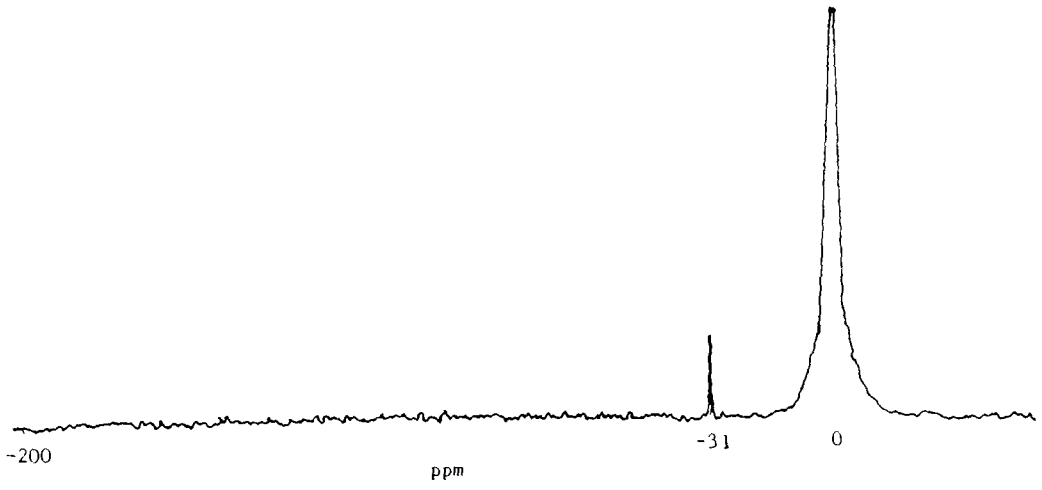

fig. 103 ^{31}P nmr Spectrum of dark blue Solid in $CDCl_3$, 298K

paramagnetic decomposition products may exist in solution which broaden the bands so that they cannot be recognized.

The ^{31}P nmr spectrum is shown in fig. 103. It gives a single resonance at -31δ, with a slight shoulder at -29δ, this resonance may indicate phosphorus in one type of environment. The shoulder could be due to the presence of a small amount of $O{=}PPh_3$. A chemical shift of -31δ does not indicate the possibility of a $Ru(O{=}PPh_3)$ complex [4.1(ii)].

Attempts to prepare the blue complex by reflux, or to recrystallize it from toluene/hexane mixtures resulted in a mixture that gave an insoluble dark powder that could not be identified and a solution that yielded crystals of pure triphenylphosphine oxide. These were obtained by concentration of the solution, then addition of petroleum ether (60/80), followed by cooling. The substance was identified from analysis and its infra - red spectrum (appendix XV), with an absorbance at 1195 cm^{-1} which was identified as the P=O stretch[107,113]. It was also found to give a single resonance in its ^{31}P nmr spectrum at -29δ (appendix VIII). Triphenylphosphine oxide exhibits a strong band at 720 cm^{-1}, this band is weak in the spectrum of the blue complex but is found to increase in intensity in the spectra of samples of different reaction mixtures that have been refluxed for increasing amounts of time. By the same token, a band at 620 cm^{-1} in fig. 102, not found in in the spectrum of $[RuCl_2(PPh_3)_2(pzH)_2].\frac{1}{2}C_6H_{14}$, decreases in intensity in the spectra of the same samples, until it disappears completely. This band is also found in the spectrum of $[Pd(pz)(dppe)_2]$ (fig. 106) and in $[Ni(pz)_2.H_2O]_n$ (630 cm^{-1}, fig. 53). The band is assigned to an absorbance of pyrazole (610 cm^{-1}, appendix III) which moves to a lower wavenumber on coordination to a metal ion and increases to a higher frequency for the coordinated pyrazolide ion. Bands at 1380 and 1360 cm^{-1} in the same

spectra, also decrease until they disappear. These results seem to indicate that the blue complex is unstable and decomposes when heated in solution, with loss of pyrazole and formation of $O{=}{=}PPh_3$.

(iii) Analysis Carbon, hydrogen and nitrogen analysis of the blue solid, although inconsistent, gave an indication of the ratio of ruthenium : phosphorus : pyrazole groups in the complex (1: 1: 2). The non-reproducible results were attributed to the fact that the complex is thermally unstable in solution, triphenylphosphine oxide crystals being formed as a decomposition product. Analysis of these crystals gave C 77.3% H 5.4% P 11.1% (calculated for $C_{18}H_{15}PO$: C 77.7% H 5.4% P 11.2%)

(iv) Visible spectrum The visible spectrum (450 - 750 nm) of a sample of the dark blue product dissolved in acetonitrile is shown in fig. 104. The spectrum shows λ_{max} at 620 nm, which is similar to that shown in the electronic spectrum of previously prepared Ru(III) oxo-bridged dimers in the same solvent [4.1(vi)]. "Mixed valence" Ru(IV)—Ru(III) oxo-bridged dimers show a band that is considerably blue-shifted to 470 nm and attempts at preparing Ru(II) oxo-bridged dimers by reduction of the Ru(III) systems result in decomposition of the dimers into monomeric fragments[88]. The related monomeric Ru(II) and Ru(III) systems do not show this high intensity absorbance. The band observed in fig. 104, therefore, is supportive of a Ru(III)—O—Ru(III) bridge.
Using the formula in fig. 105, the molar extinction coefficent, ϵ could be calculated at ≈ 12,000. The band was found to be less intense than those bands displayed by reported oxo-bridged dimers[88] (17,000 - 25,000). The coefficent dropped to ≈ 3,000 in the spectrum of products that had been prepared by refluxing the reaction mixture for 15 minutes.

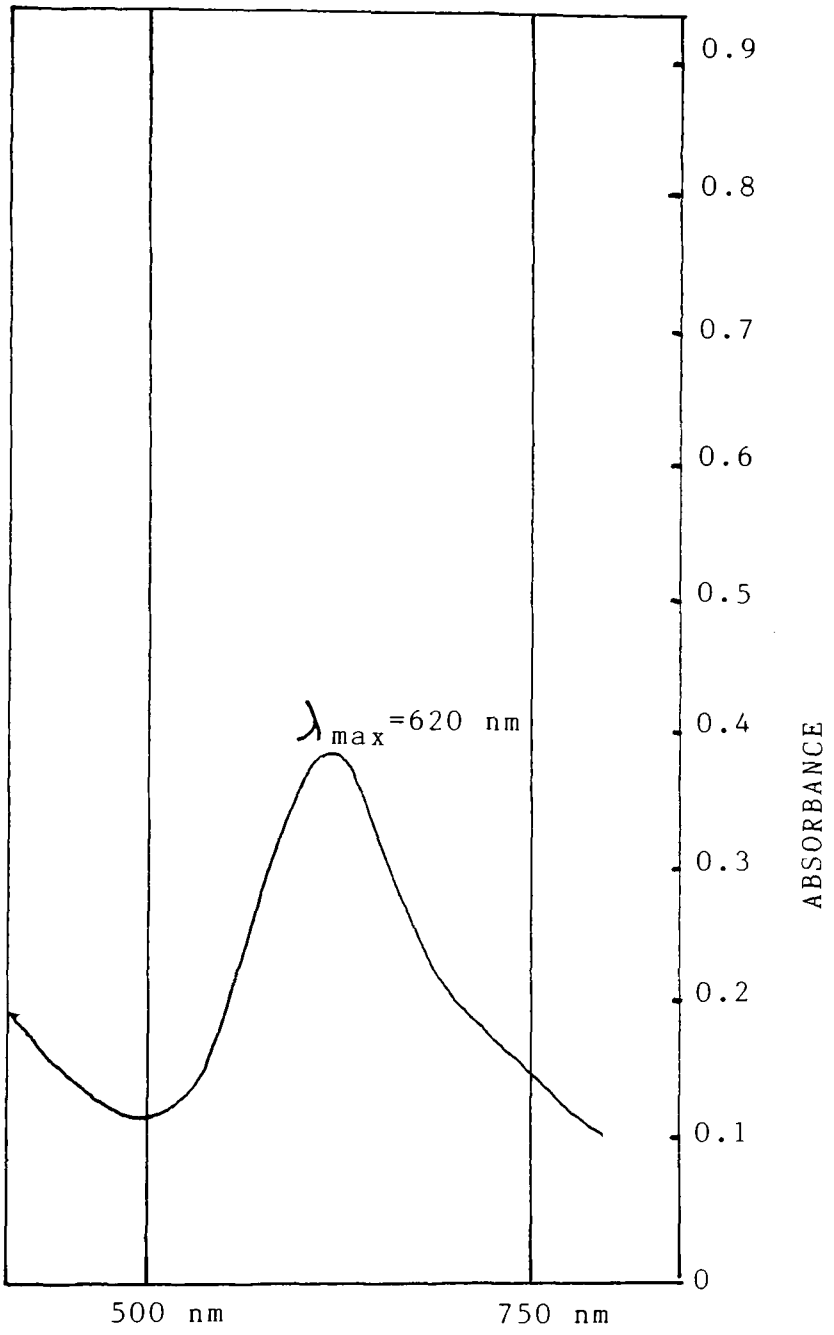

fig. 104 Visible Spectrum of dark blue Solid in Acetonitrile ($0.0400\ g\ dm^{-3}$)

The position of λ_{max} also dropped to below 600 nm . It is suggested that some decomposition had already occurred in the blue solid even when prepared at room temperature; infra-red and ^{31}P nmr spectra gave bands characteristic of triphenylphosphine oxide (720 cm^{-1} and -29δ) in all samples but with varying intensity relative to other bands, according to the length of preparation time and the temperature reached by the reaction mixture.

The visible spectrum in fig. 104 was also monitored over a period of days. After a week the position of λ_{max} had shifted slightly (607 nm), whilst the intensity of the absorbance decreased $\epsilon \approx 6000$, again indicating that the complex is unstable in solution. The complex $[(bpy)_2ClRu—O—Ru(bpy)_2]^{2+}$ is reported as being unstable in solution[88], gradually decomposing into $[Ru(bpy)_2Cl_2]^+$.

(v) Conductivity The conductivity of the blue solid in acetonitrile was measured at 25 °C, using platinum electrodes with a cell constant of 0.1 cm^{-1}. Assuming the blue solid had a molecular mass of $\equiv 10^3$ (fig. 105), its solution conductivity was compared with the conductivity of a known 1 : 1 electrolyte, a solution of lithium perchlorate in acetonitrile. The molar conductivity, Λ_m, of the blue complex was calculated at $\equiv$ 50 S mol^{-1} cm^2 as compared with $\Lambda_m \equiv 200$ S mol^{-1} cm^2 for lithium perchlorate. These results, although not conclusive, suggest that the blue complex is probably molecular rather than ionic. The residual conductivity may well be due to decomposition products in solution - it was noted that a dark precipitate settled at the bottom of the cell, as the experiment proceeded. The molar conductivities of previously prepared oxo-bridged dimers have been reported in the same solvent[88], values are

between 300 - 400 S mol^{-1} cm^2 (Λ_o, 2: 1 electrolytes).

(vi) Discussion The complex is unlikely to contain a bridging O—H entity. The only analogous complex with bridging O—H species found in the literature, with a di-μ^2-hydroxy formulation[114], was subsequently reformulated as a μ^2-oxo species[88].

The diamagnetism of the complex can be explained by a linear Ru(III)—O—Ru(III) linkage. However, the infra-red spectrum suggests this is unlikely. Bending of the linkage decreases the degree of Π-bonding and hence the stability of the system[91], but the stability of the five membered rings formed between the linkage and the pyrazolide ions may compensate for this and allow significant bending - sufficient to bring the ruthenium ions close enough together to allow some form of interaction between them. The pyrazolide ligand has been shown[9] to span distances varying from that attributed to a Ru—Ru bond[34] (2.7Å) to distances where there can be assumed to be no interaction between ruthenium atoms (3.7Å)[92].

On the basis of analytical, magnetic, spectroscopic and conductivity measurements and taking into account the structure of complexes previously prepared by a similar method, the blue product was thought to have a structure of the type shown in fig. 105. Its dark blue colour and method of preparation suggested that it contained a Ru^{III}—O—Ru^{III} linkage, in common with the complexes described in [4.1(vi)]. The complex was also found to be thermally unstable, decomposing into O=PPh_3 and other unidentified products.

The complex in fig. 105, is assumed to be symmetrical on the basis of the observed ^{31}P nmr chemical shift and the fact that previously prepared oxo-bridged dimers have displayed this symmetry, with one exception[89].

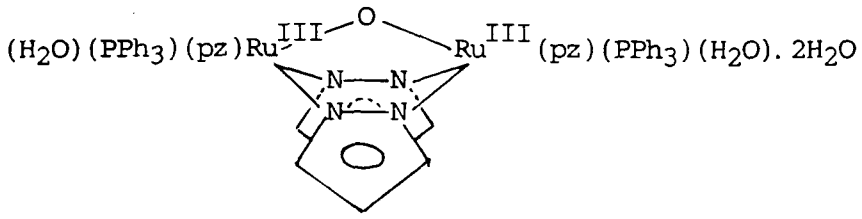

fig. 105 Suggested Formula of Dark Blue Product

The oxo-bridged dimers have demonstrated value as water oxidation catalysts and also effect oxidation of chloride to chlorine[115]. Depending on the pH, oxidation can be accompanied by loss of protons to give hydroxo or oxo complexes, which in the higher oxidation states are stabilised by p -» d_{Π} donation[92]. The higher oxidation state forms of many of these complexes have been found to be versatile stoichiometric and/or catalytic oxidants towards a variety of inorganic and organic substrates[116, 117, 118].

(vii) Deprotonation of ruthenium - pyrazole complexes Removal of the proton of the pyrazole ligand apparently increases the stability of the higher oxidation states of ruthenium[30]. The bound pyrazole group is a relatively weak Π-acceptor ligand, but in its deprotonated form, it has the capacity to act as a Π-donating ligand. The existence of pz^- -» Ru donation stabilises Ru(III) relative to Ru(II), possibly explaining the rapid colour change when oxygen is introduced into the mixture of KOH, H_2O and $[RuCl_2(PPh_3)_2(pzH)_2].\frac{1}{2}C_6H_{14}$.

The failure of triethylamine and 1,8-bis(dimethylamino)napthalene to deprotonate the ruthenium pyrazole complexes in the absence of oxygen was surprising; coordination of pyrazole should increase its acidity[8] and the complex $[(bpy)_2Ru(pzH)_2]^{2+}$ is deprotonated by weak pyridine bases like collidine[30].

SECTION SIX-ATTEMPTS TO SYNTHESIZE μ^1-PYRAZOLYL COMPLEXES CONTAINING PALLADIUM AND ONE OTHER TRANSITION METAL

6.1 PREPARATION OF A PALLADIUM(II) CHELATING LIGAND

The square planar palladium(II) complex $[PdCl_2(dppe)]$[119] reacts with the pyrazolide ion[36] to give $[Pd(pz)_2(dppe)]$ as in equation 6.

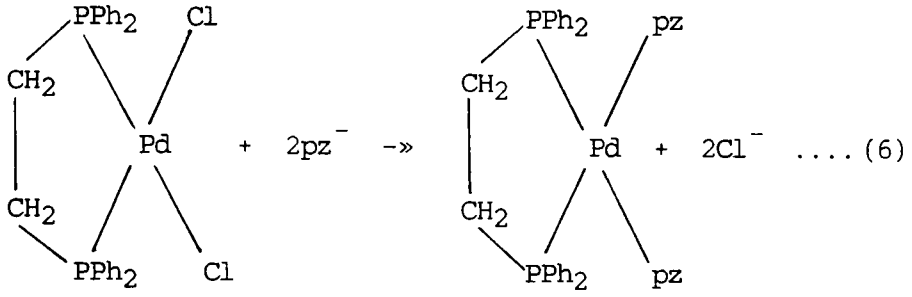

.... (6)

The reaction with the related nickel(II) complex has been shown to result in loss of phosphine [3.6]. The palladium(II) ion, however, is a larger, softer ion than its nickel equivalent and therefore more likely to complex with phosphines as explained by "Pearson's Principle" [1.8]. In this palladium-pyrazolide complex, the pyrazolide ions are unidentate ligands. The whole complex therefore, can act, at least in principle, as a bidentate metal containing ligand which could also behave as a chelating system [1.5]. Reaction of this Lewis base with a complex that is likely to behave as a Lewis acid is a possible method by which heterobimetallic systems can be prepared. For this reason, the complex was reacted with $NiCl_2(PPh_3)_2$ and $RuCl_2(PPh_3)_3$ in attempts to generate mixed-metal complexes.

6.2 EXPERIMENTAL

(i) Preparation of $[PdCl_2(dppe)]$[119] A solution of dppe (0.22 g, 0.55 mmol) in dichloromethane (10 cm^3) and a solution of $K_2[PdCl_4]$ (0.18 g, 0.55 mmol) in water were intimately agitated for 24 h. The aqueous layer slowly lost colour and the organic layer changed to light brown. The aqueous layer was removed and the organic layer and precipitate were washed with copious amounts of water. The organic layer was then filtered to give the product as a buff powder. This was washed with a little ethanol and diethyl ether, then dried at the pump. Yield = 0.18 g (57%)

(ii) Preparation of $[Pd(pz)_2(dppe)]$[36] A methanol solution of pyrazole (0.31 g, 4.56 mmol) and potassium hydroxide (0.26 g, 4.64 mmol) were added to a stirred methanol suspension (80 cm^3) of the complex $[PdCl_2(dppe)]$ (1.28 g, 2.23 mmol). The mixture was refluxed gently and after 4 h, the resulting solution was evaporated to dryness. The residue was extracted with dichloromethane (40 cm^3) and filtered. The solution was then concentrated to ca. 15 cm^3 by evaporation under reduced pressure. Addition of diethyl ether gave a mulberry coloured precipitate. This was filtered, washed with 5 cm^3 ether and dried at the pump. Yield = 0.22 g, (20%).

(iii) Reaction of $[Pd(pz)_2(dppe)]$ with $NiCl_2(PPh_3)_2$ [6.4] Both these complexes were found to be soluble in THF. The palladium complex (0.20g, 0.31 mmol) was reacted with the nickel complex (0.20 g, 0.31 mmol) in THF (25 cm^3) under nitrogen. After reflux for 1 h, the yellow solid that had precipitated was filtered off, washed with THF (5 cm^3) and

dried in vacuo. Yield = 0.04 g.

Analysis

Calculated for $C_6H_6N_4Ni$: C 37.3% H 3.1% N 29.0%

Found: C 36.2% H 3.0% N 28.1%

(iv) Reaction of $[Pd(pz)_2(dppe)]$ with $RuCl_2(PPh_3)_3$ [6.5] The ruthenium complex (0.30 g, 0.31 mmol) was reacted with $[Pd(pz)_2(dppe)]$ (0.20 g, 0.31 mmol) in THF (25 cm^3), under nitrogen. Because of the extreme air - sensitivity of the product of the reaction, air was excluded from the apparatus and freshly distilled solvents used under the most rigorous conditions as described in [2.1]. The dark brown solution obtained after stirring for 15 minutes turned green in the presence of any traces of air. A dark brown air - stable precipitate was obtained by the addition of de-gassed petroleum ether (60/80). The precipitate was filtered off and dried in vacuo. Yield = 0.28g

Analysis

Calculated for $C_{50}H_{45}Cl_2N_4P_3PdRu$: C 56.0% H 4.2% N 5.2%

Found: C 55.8% H 4.2% N 5.6%

A Lassaigne fusion test indicated the presence of chlorine.

6.3 SPECTRA OF $[PdCl_2(dppe)]$ AND $[Pd(pz)_2(dppe)]$

The infra - red spectra of $[PdCl_2(dppe)]$ and $[Pd(pz)_2(dppe)]$ are shown in figs. 106 and 107. The far infra - red spectrum of $[PdCl_2(dppe)]$ is shown in fig. 108. In fig. 106 and 107, the P—aryl stretch from dppe is given at 1440 cm^{-1}. In fig. 107, an in - plane ring stretch of pyrazole is given at 1380 cm^{-1}. The far infra - red spectrum in fig. 108, gives

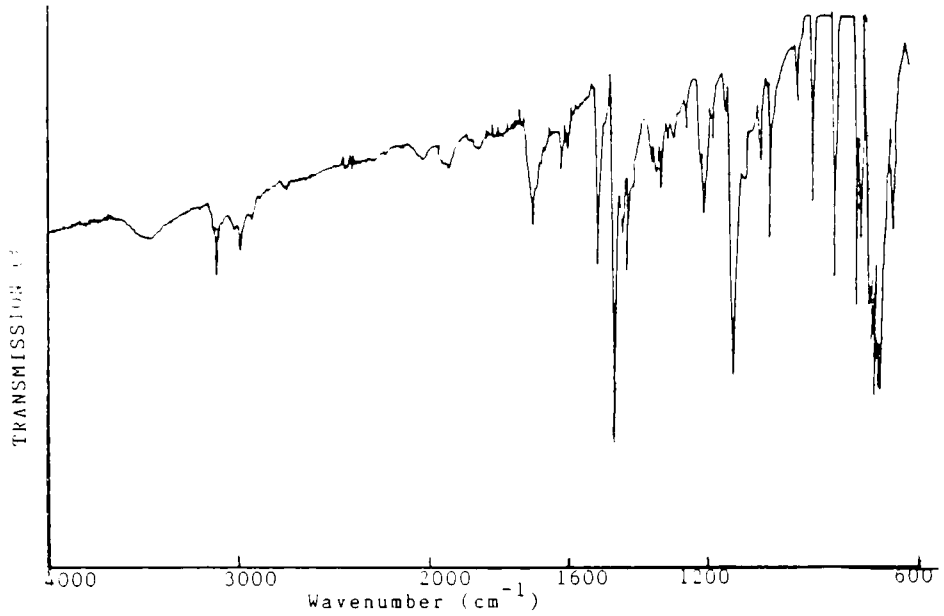

fig. 106 Infra-red Spectrum of $[PdCl_2(dppe)]$

(KBr disc)

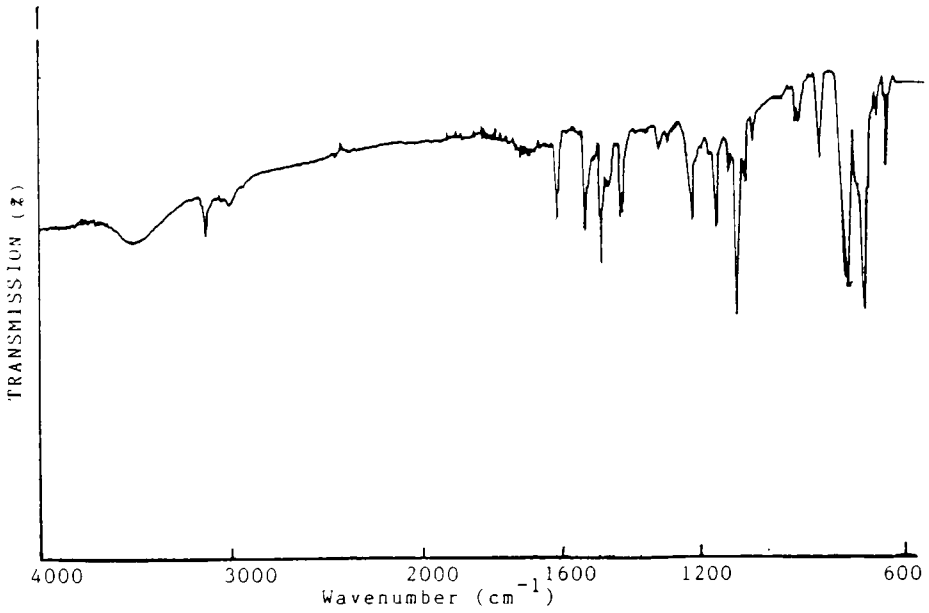

fig. 107 Infra-red Spectrum of $[Pd(pz)_2(dppe)]$

(KBr disc)

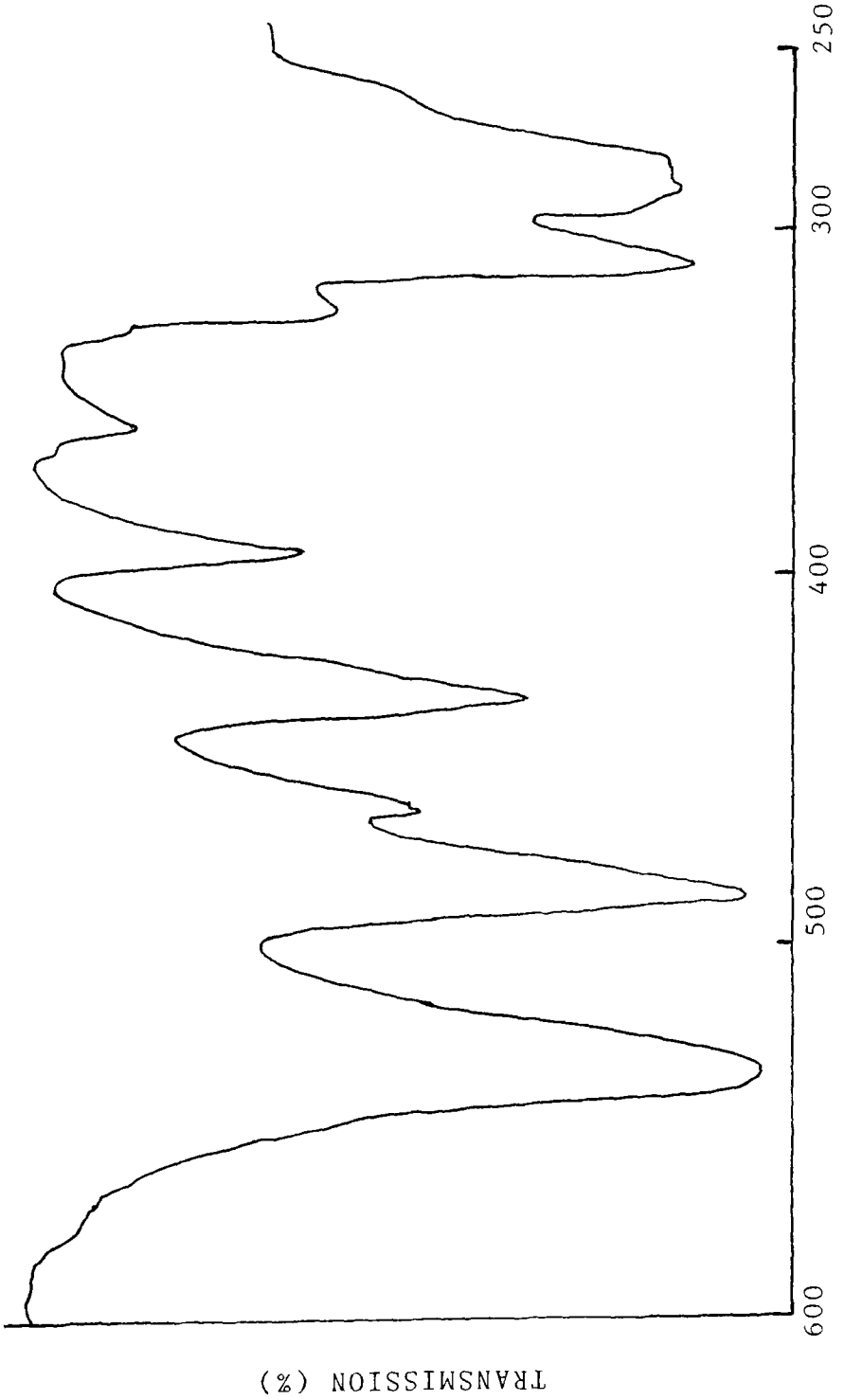

Far infra-red Spectrum of $[PdCl_2(dppe)]$ (CsI disc)

fig. 108

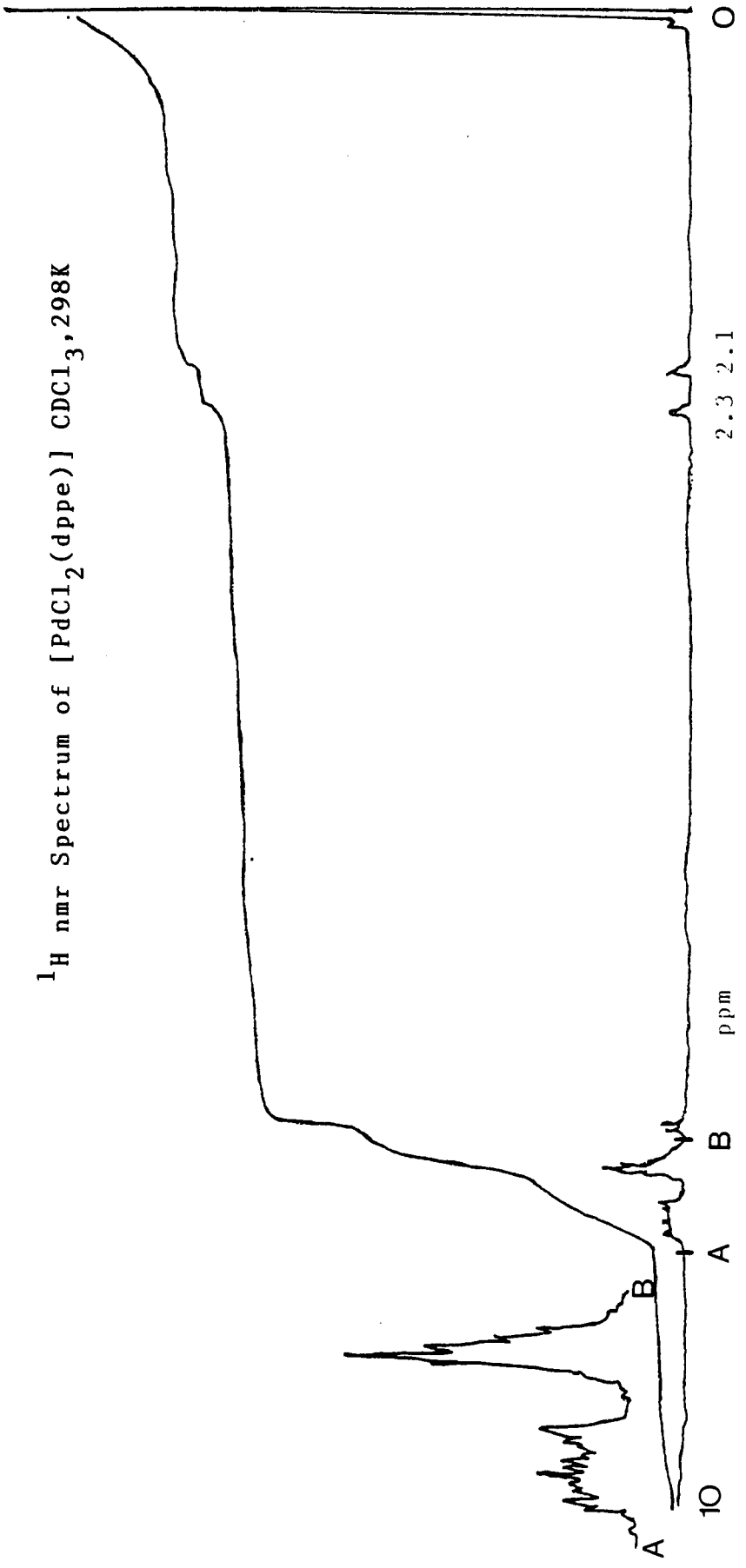

fig. 109

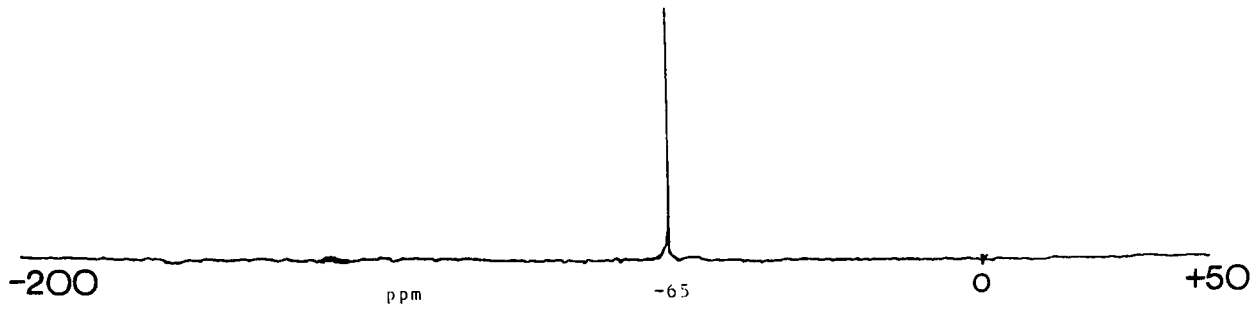

fig. 110 ^{31}P nmr Spectrum of $[PdCl_2(dppe)]$ $CDCl_3$, 298K

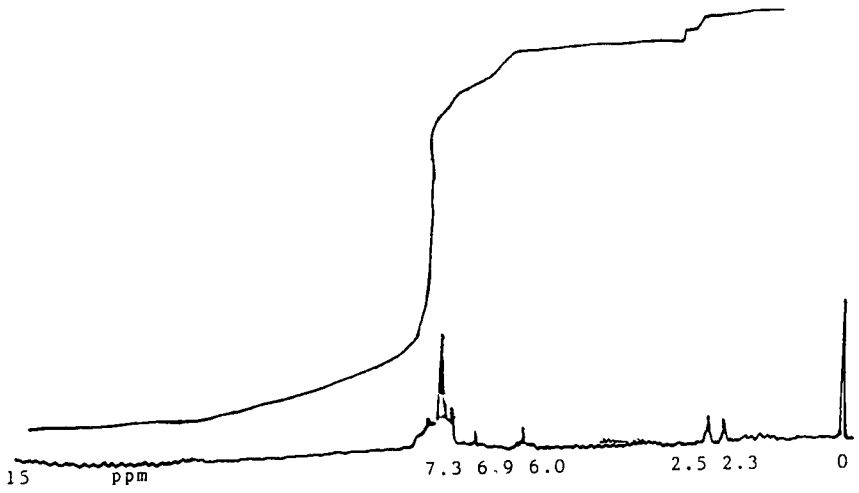

fig. 111 ^{1}H nmr Spectrum of $[Pd(pz)_2(dppe)]$ $CDCl_3$, 298K

fig. 112 ^{31}P nmr Spectrum of $[Pd(pz)_2(dppe)]$ $CDCl_3$, 298K

ν(Pd—Cl) at 288 and 311 cm^{-1} (A_1 + B_1) modes, as quoted in the literature[119]. No bands were found in this area in the corresponding spectrum of $[Pd(pz)_2(dppe)]$.

The ^1H and ^{31}P nmr spectra of $[PdCl_2(dppe)]$ are shown in figs. 109 and 110. The ^1H nmr shows resonances at 2.3 and 2.6δ, which are not well resolved, together with a resonance centered at 7.5δ, which represents the phenyl protons. The ^1H nmr spectrum of dppe (appendix XI), shows the resonance due to the phenyl protons at 7.3δ and a triplet from the alkyl protons at 2.1δ, in an integration ration of 5 : 1. In fig. 109, the integration ratio is 20H : 2H : 2H, showing that two resonances are shown for the alkyl protons on coordination to palladium. The low solubility of this complex has been commented on previously[119] and presumably this accounts for the lack of resolution shown in the spectrum. The ^{31}P nmr spectrum of $[PdCl_2(dppe)]$ gives one resonance

at -65δ, in fair agreement with the literature value (-68δ)[119]. The ^{1}H and ^{31}P nmr spectra of $[Pd(pz)_2(dppe)]$ are shown in figs. 111 and 112. In fig. 111, again, detection of signals is difficult because of the low solubility of the pyrazolide complexes[36]. The ^{1}H nmr spectrum gives signals at 7.5δ (phenyl protons + 2H, C3, pzH), 6.9δ (2H, C5, pzH), 6.0δ (2H, C4, pzH), 2.5δ (CH_2, dppe) and 2.3δ (CH_2, dppe). The ^{31}P nmr spectrum shows one resonance at -32δ. No information regarding the ^{1}H nmr spectrum of $[PdCl_2(dppe)]$ or any nmr studies of $[Pd(pz)_2(dppe)]$ has been found in the published data.

6.4 REACTION OF $[Pd(pz)_2(dppe)]$ WITH $NiCl_2(PPh_3)_2$

As previously mentioned, Ni(II) appears to preferentially coordinate with pyrazole rather than triphenylphosphine [1.8]. It was therefore thought that the reaction of $[Pd(pz)_2(dppe)_2]$ with $NiCl_2(PPh_3)_2$ might result in a pyrazole bridged Ni(II) - Pd(II) species, after displacement of triphenylphosphine by the pyrazolide ions coordinated to palladium. The reaction between these two complexes is described in [6.2(iii)]. The insoluble product was found to be diamagnetic, insoluble in a variety of solvents and to have an infra-red spectrum almost identical with the polymeric $[Ni(pz)_2]_n$ (fig. 53). The analysis of the solid also indicated that it was an impure sample of the nickel complex.

6.5 REACTION OF $[Pd(pz)_2(dppe)]$ WITH $RuCl_2(PPh_3)_3$

The palladium(II) complex was reacted with $RuCl_2(PPh_3)_3$, as in [6.2(iv)], in an attempt to obtain a Pd(II) - Ru(II) mixed metal species in a reaction similar to that of the reaction of $RuCl_2(PPh_3)_3$ with

pyrazole, described in [4.3(a)]. The extreme air-sensitivity of the mixture, made this a difficult reaction to effect; any exposure of the reaction mixture to traces of air resulted in a green product, rather than the brown product, analysed to contain $C_{50}H_{45}Cl_2N_4P_3PdRu$. For convenience, the product is hereafter referred to by its empirical formula.

(i) Spectra of $C_{50}H_{45}Cl_2N_4P_3PdRu$

The infra-red spectra of $C_{50}H_{45}Cl_2N_4P_3PdRu$ and its green (presumably oxidised) product are shown in figs. 113 and 114. The oxidised form was obtained by repeating the preparation [6.2(iv)] in air, or by allowing prepared $C_{50}H_{45}Cl_2N_4P_3PdRu$ to come in contact with the air for a few minutes. The infra-red spectra of products obtained by both these reactions were identical.

Fig. 113 displays the following features: P—aryl stretch (1440 cm^{-1}), ring stretch of pyrazole (1380 cm^{-1}) and C—H aliphatic stretch (2930 cm^{-1}). The spectrum in fig. 114 differs from that in fig. 113 only in that it has additional bands of medium intensity at 1130 and 1060 cm^{-1}. It has already been suggested that the former region may display absorbances due to triphenylphosphine oxide complexed to transition metal cations [4.4(c)], therefore it is proposed that the green product may contain a ruthenium -O=PPh_3 complex. The far infra-red spectrum of $C_{50}H_{45}Cl_2N_4P_3PdRu$ gave no band which could be readily identified as v(Ru—Cl). However, terminal v(Ru—Cl) absorbances can occur[96,97,120] between 300 - 250 cm^{-1}. This area was not well-resolved.

The ^1H nmr spectrum of $C_{50}H_{45}Cl_2N_4P_3PdRu$ gave little information. Despite taking the precautions outlined in [2.1(vi)], broad resonances

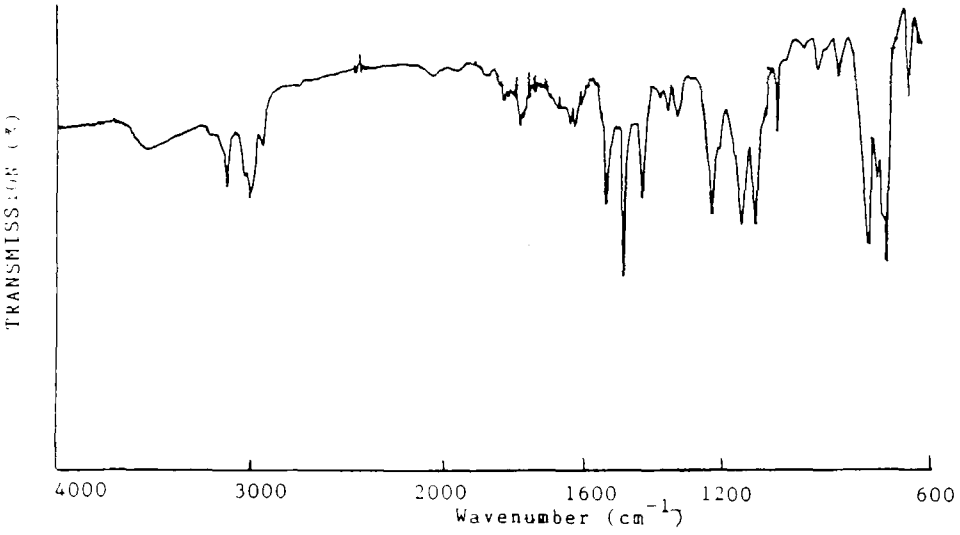

fig. 113 Infra-red Spectrum of $C_{50}H_{45}Cl_2N_4P_3Pd\ Ru$

(KBr disc)

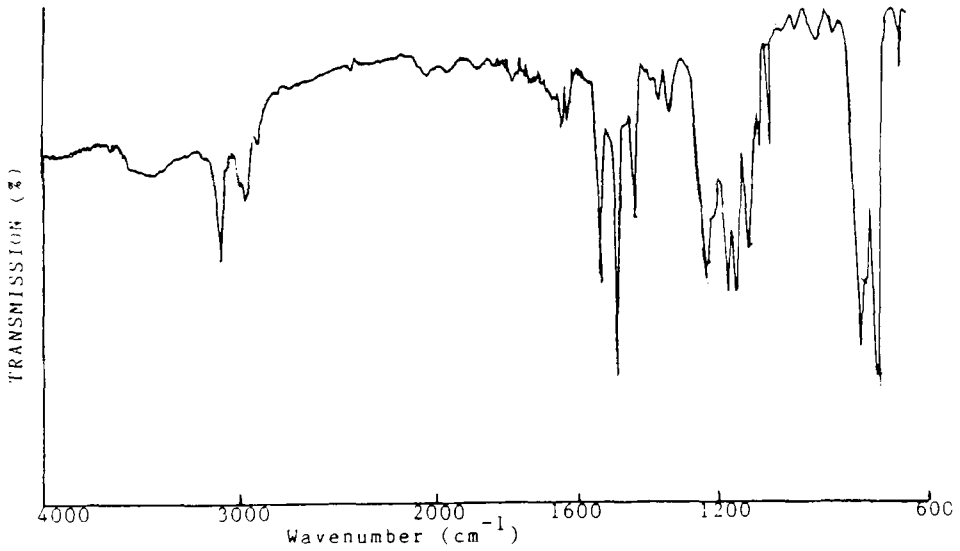

fig. 114 Infra-red Spectrum of the Oxidised Product

(KBr disc)

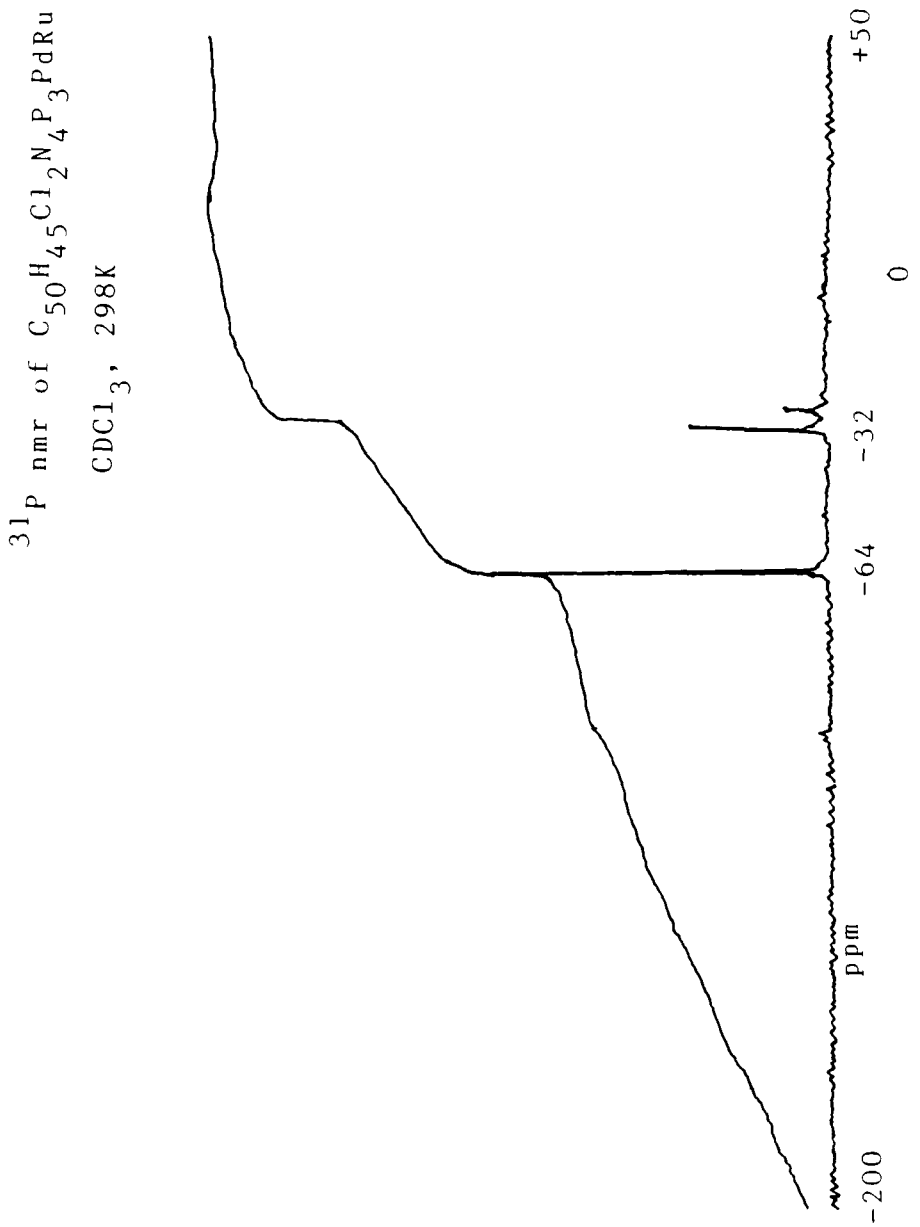

fig. 115

^{31}P nmr Spectrum of the Sample in fig. 116, after another hour $CDCl_3$, 298K

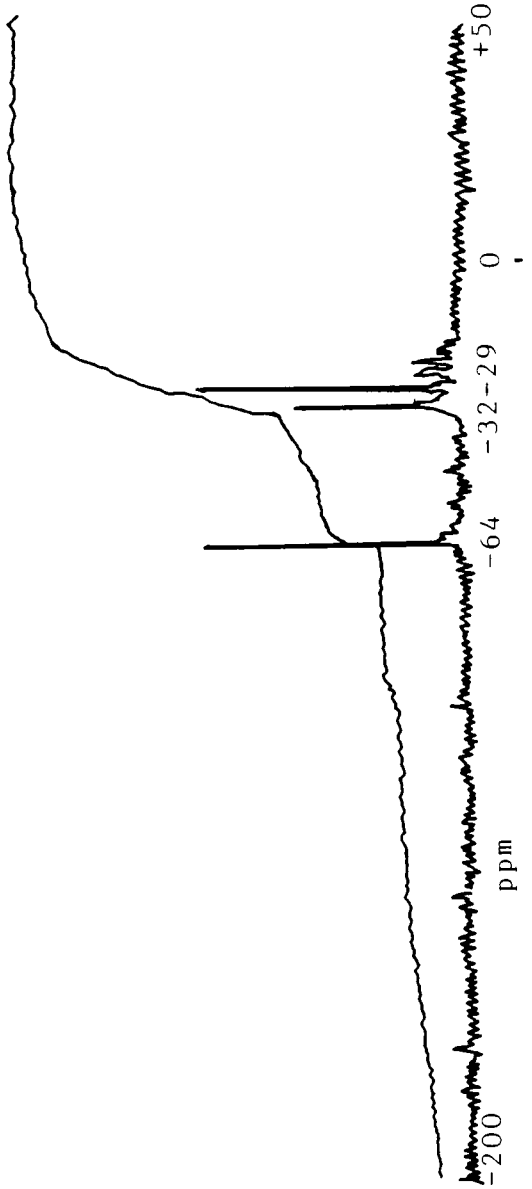

fig. 116

^{31}P nmr of $C_{50}H_{45}Cl_2N_4P_3PdR$
prepared in air $CDCl_3$, 298K

fig. 117

were obtained, again with no identifiable signals for pyrazole protons. Samples prepared for nmr rapidly turned green, indicating reaction with traces of air, presumably the presence of paramagnetic oxidation products in solution prevented interpretation of the spectra. More information was obtained from ^{31}P nmr spectra, in particular from two spectra of the same sample of $C_{50}H_{45}Cl_2N_4P_3PdRu$ taken an hour apart. These are shown in figs. 115 and 116. Three resonances are shown in the former spectrum at -64, -32 and -29δ. They are also the principal signals observed in fig. 116. Integration of both spectra indicate that there is a significant decrease in concentration of the species responsible for the resonance at -64δ as time proceeds, compared with a slight increase and slight decrease of those species which give signals at -29 and -32δ, respectively. This seems to suggest that those species at -32 and -64δ are representative of the unoxidised complex, whilst that at -29δ is due to an oxidation product. No signals are detected at -51 and -40δ, (resonances present in the spectra of $[Pd(pz)_2(dppe]$ and $RuCl_2(PPh_3)_3$[74]) suggesting that a new species has been formed and a mixture of the two precursor complexes is not present.

The ^{31}P spectrum of the green complex, prepared as for $C_{50}H_{45}Cl_2N_4P_3PdRu$ but made in air, is shown in fig. 117. It shows the signals detected in figs. 115 and 116 and additional resonances at -93, -60, -55, -24 and +6δ. The signals at +6 and -29δ are assigned to free triphenylphosphine and its oxide, those at -55 or -60δ could be due to Ru -O=PPh_3 species [4.1(ii)]. No signals are found at +13 or -35δ, which would indicate dissociated dppe or its oxidation product (appendices XII, XIII).

The spectroscopic and analytical evidence, therefore, point to the possible formation of a mixed-metal species, although the difficulties associated with the preparation of $C_{50}H_{45}Cl_2N_4P_3PdRu$ (given its extreme

sensitivity to oxygen) make any formulation tentative.

The solid $C_{50}H_{45}Cl_2N_4P_3PdRu$ was found to be diamagnetic, whilst the green oxidised product showed paramagnetism. The complex $C_{50}H_{45}Cl_2N_4P_3PdRu$ could be a product of the type shown in fig. 118.

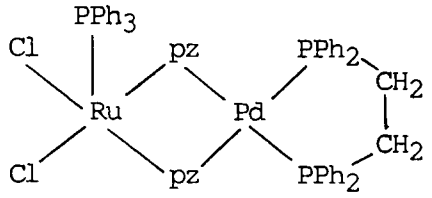

fig. 118 Possible Structure of $C_{50}H_{45}Cl_2N_4P_3PdRu$

This is formulated as a 32 electron complex with ruthenium and palladium both in oxidation state +2. The spectra obtained show bands that are indicative of a complex of the type shown in fig. 118, although definitive evidence for this structure would need to be obtained from well-resolved ^1H nmr spectra.

6.6 CATALYTIC ACTIVITY OF $C_{50}H_{45}Cl_2N_4P_3PdRu$

A mixture of the complex (0.04 g, 0.04 mmol) and oct-1-ene (0.12 g, 1.07 mmol) in chloroform (20 cm^3) was stirred under hydrogen, at ambient temperature, as described in [2.2(ii)]. The mixture turned green after a period of 30 minutes. After twenty four hours, the mixture was filtered and analysed using gas chromatography. The operating conditions of the gas chromatography apparatus together with the resulting chromatograph are shown in fig. 119. The uptake of hydrogen gas was measured at 12 cm^3 (corrected to stp), representing 0.54 mmol of hydrogen. This value was difficult to determine accurately, however, because fluctuations of the level of water in the tube (to approximately $\pm$ 2 cm^3) containing hydrogen were apparent during an initial "settling period" of about 10 minutes after the commencement of the experiment. The peaks with retention times of 3.45, 9.02 and 9.75 min., represent choroform, oct-1-ene and octane respectively. Pure samples of these liquids were passed through the column, prior to analysis of the reaction mixture. Chloroform was used as the solvent, because under the operating conditions used, the retention time of toluene was close to that of the alkane and alkene.

The area under the hydrocarbon peaks shows a conversion of approximately 45% of oct-1-ene to octane. This may be compared with a conversion of ca. 5% in a similar sample run with no introduction of the complex under consideration.

Infra-red and nmr spectra of the green product recovered from the reaction mixture gave no evidence of bands representative of a ruthenium-hydrido complex. This was also true of samples left under hydrogen for twenty four hours without the introduction of the alkene.

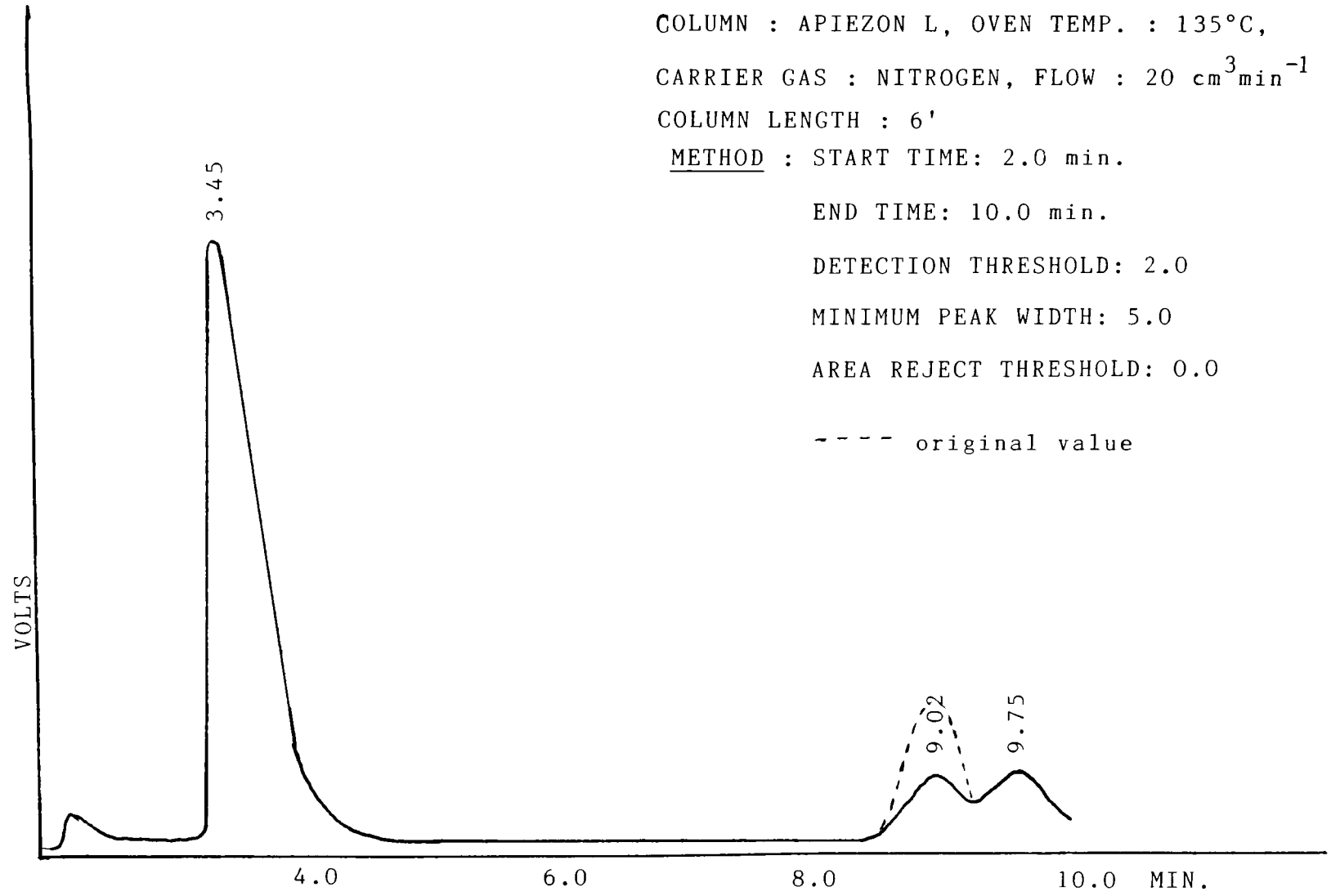
COLUMN : APIEZON L, OVEN TEMP. : 135°C,
CARRIER GAS : NITROGEN, FLOW : 20 cm3min-1
COLUMN LENGTH : 6'
METHOD : START TIME: 2.0 min.
END TIME: 10.0 min.
DETECTION THRESHOLD: 2.0
MINIMUM PEAK WIDTH: 5.0
AREA REJECT THRESHOLD: 0.0
---- original value
VOLTS
3.45
9.02
9.75
4.0
6.0
8.0
10.0 MIN.

fig. 119

The spectra were similar to those of the oxidised complex discussed in [6.5(i)], indicating that oxidation of the complex had again taken place. The results of this experiment would seem to indicate that some form of catalytic action has taken place, although whether this is a result of the unoxidised $C_{50}H_{45}Cl_2N_4P_3PdRu$ or an oxidation product of the complex, remains unclear. No investigation was carried out as to whether any isomerisation of the alk-1-ene had occurred.

The complex $RuCl_2(PPh_3)_3$ is an effective hydrogenation catalyst for terminal alkenes[97]. The solution changes colour to the characteristic deep violet of the hydrido complex [4.1(iii)], which is the true catalyst for the reaction and has been identified by nmr studies of the solution. Solutions of both complexes are exceedingly oxygen-sensitive and form green triphenylphosphine oxide complexes when exposed to air. It is believed that an alkyl complex is first formed, followed by oxidative addition of hydrogen to form a ruthenium(VI) complex which then undergoes rapid reductive elimination of alkane, reforming the initial hydridoruthenium(II) complex (fig. 120).

The catalytic cycle in fig. 120 works well in benzene, toluene and pure alcohols, although its efficiency appears to be severely impeded in chlorinated solvents, such as chloroform[77]. This fact is attributed to the strong solvating behaviour of the solvents.

The absence of any evidence for a hydrido species in the reaction of $C_{50}H_{45}Cl_2N_4P_3PdRu$ with hydrogen, together with the fact that the apparent catalytic hydrogenation of oct-1-ene takes place in a chlorinated solvent, points to the fact that the mechanism of hydrogenation is significantly different from that shown in fig. 120.

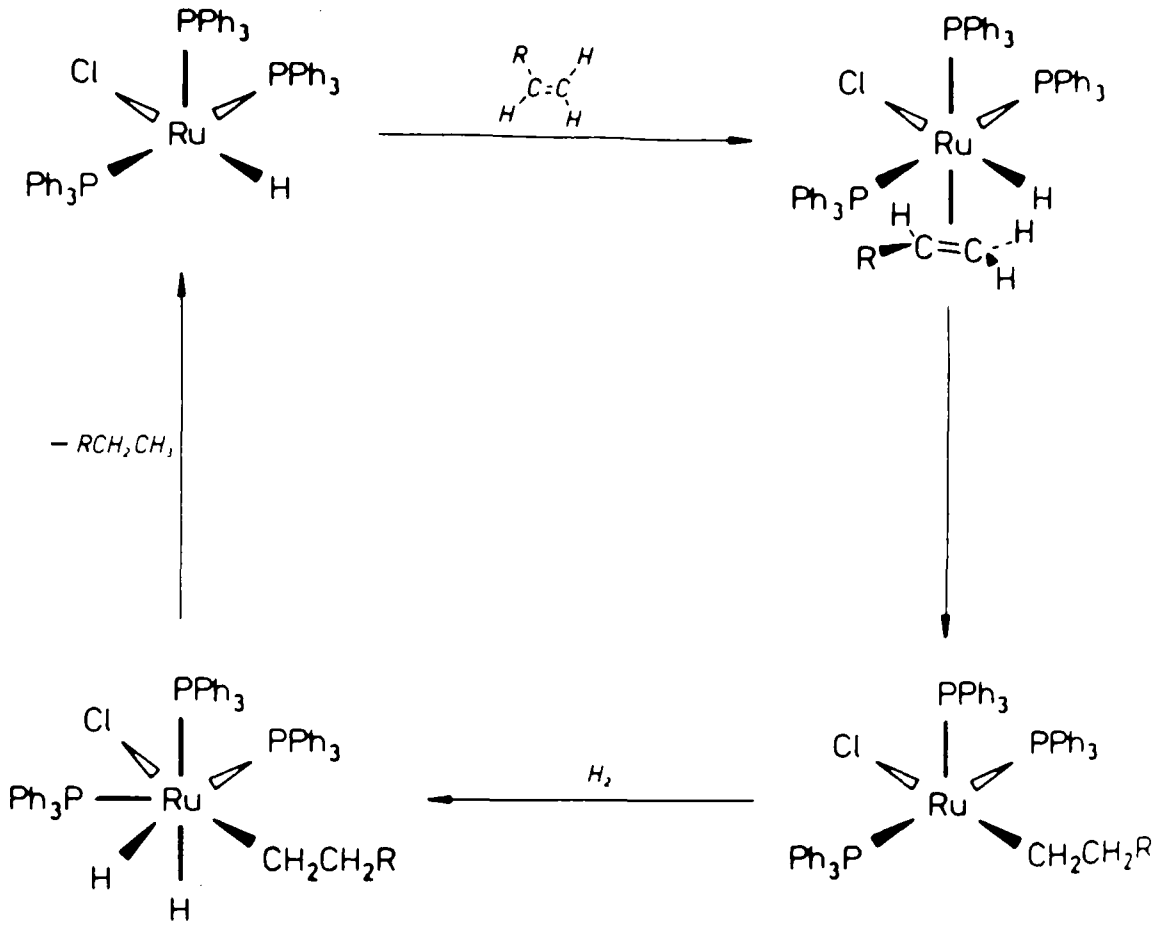

fig. 120 Mechanism of Catalytic Hydrogenation

These preliminary experiments concerned with the product of the reaction between $Pd(pz)_2(dppe)$ and $RuCl_2(PPh_3)_3$, therefore, would seem to indicate that the system has potential for a great deal more study.

CONCLUSIONS AND SUGGESTIONS FOR FURTHER WORK

CONCLUSIONS AND SUGGESTIONS FOR FURTHER WORK

In the section concerned with Ni(II) pyrazole complexes, the results would seem to suggest that the ease of deprotonation of the coordinated pyrazoles (and hence the ease of formation of polymeric species with μ^2-pyrazolyl ligands), is modified by the presence of substituents in the pyrazole ligand. Further investigations could be conducted which would involve the synthesis of Ni(II)/pyrazole complexes in which the ligands contain substituents with different inductive effects e.g. 4-methylpyrazole and 3,5-bis(trifluoromethyl)pyrazole are both commercially available. These complexes could then be reacted with base, in an attempt to synthesize the related polymer. This process would be expected to occur readily in, for example, the pyrazole containing trifluoromethyl substituents because these would be expected to contribute to the acidity of the pyrrole-type proton. A series of experiments of this type, coupled perhaps with condensation-type reactions as mentioned in [3.5(ii)], could establish as to whether the predominant factor affecting the ease of formation of these polymeric species is steric or electronic. The experiments should also lead to the synthesis of a series of novel Ni(II) complexes, both monomeric and polymeric.

Difficulty was encountered in synthesizing a Ni(II) complex that contained both pyrazole and phosphine ligands and the conclusion reached was that Ni(II) preferentially coordinates to pyrazole, as explained by "Pearson's Principle". Complexes of Ni(0), diphosphines and carbonyl groups have been prepared by reacting the ligands with $NiCl_2.6H_2O$ in the presence of a reducing agent such as $NaBH_4$. The products of these

type of reactions have then been utilized to produces Ni(0) - Pt(II) mixed-metal complexes[69]. According to "Pearson's Principle", Ni(O) would be classified as a softer acid than Ni(II) and therefore may be more able to coordinate with both phosphine and pyrazole ligands. The deprotonation of such complexes would provide a route to dimeric and/or polymeric species containing μ^2-pyrazolyl ligands and possibly a means to the synthesis of heterobimetallic species.

The reactions of pyrazole and 3.5-dimethylpyrazole with $RuCl_2(PPh_3)_3$ and the investigation of the properties of the products, particularly with reference to their reactions with base could usefully be extended to other systems (for example the reaction of pyrazole with Wilkinson's Complex, $RhCl(PPh_3)_3$). These reactions should lead to the preparation of novel pyrazole complexes and investigate the feasilbility of routes to synthesizing alternative mixed-metal systems.

The reaction of $Pd(pz)_2(dppe)$ with $RuCl_2(PPh_3)_3$ requires study in greater depth than has been possible in the time available. The exact nature of the product and mechanism of catalytic action, would provide an interesting investigation. The project would require all experimentation to be conducted under strict anaerobic conditions, with rigorous de-gassing of all solvents and reactants concerned with the catalytic activity. The related reaction of $Pt(pz)_2(dppe)$[36] with $RuCl_2(PPh_3)_3$ could also provide a system for further study.

REFERENCES

REFERENCES

1. J. Falbe, H. Barman, J. Chem. Educ. 11 61 (1984)

2. M. M. Habib, W. R. Pretzer, Gulf Research and Development Co., U. S. Patent 4 - 352 - 947

3. M. Inove, M. Kishita, M. Kubo, Inorg. Chem. 4 626 (1965)

4. N. A. Daugherty, J. H. Swisher, Inorg. Chem. 7 1651 (1968)

5. G. Bushnell, K. Dixon, D. Eadie, S. Stobart, Inorg. Chem. 20 1545 (1981)

6. S. Trofimenko, Chem. Rev. 72 (5) 497 (1972)

7. S. Trofimenko, Progress in Inorg. Chem. 34 115 (1986)

8. C. Johnson, W. Henderson, R. Shepherd, Inorg. Chem. 23 2754 (1984)

9. S. Stobart, K. Dixon, D. Eadie, J. Atwood, M. Zarworotko, Angew. Chem. Int. Edn. (Engl.) 19 931 (1980)

10. W. Deese, D. Johnson, A. Ccrdes, Inorg. Chem. 20 1519 (1981)

11. D. Johnson, W. Deese, M. Howe, Inorg. Chem. Nucl. Lett. 16 53 (1980)

12. S. Trofimenko, Inorg. Chem. 10 (7) 1372 (1971)

13. E. Alyea, S. Dias, F. Bonati, Trans. Met. Chem. 6 24 (1981)

14. A. Goel, S. Goel, D. Vanderveer, Inorg. Chim. Acta 82 L9 (1984)

15. F. Bonati, H. C. Clark, Can. J. Chem. 56 2513 (1978)

16. L. Oro, D. Carmona, M. Lamata, M. Apreda, C. Foces-Foces, F. Cano, P. Maitlis, J. Chem. Soc. Dalton Trans. 1823 (1984)

17. K. Beveridge, G. B. Bushnell, K. Dixon, D. Eadie, S. Stobart, J. Am. Chem. Soc. 104 920 (1982)

18. A. Coleman, D. Eadie, S. Stobart, J. Am. Chem. Soc. 104 922 (1982)

19. G. Bushnell, D. Fjeldsted, S. Stobart, M. Zaworotko, J. Chem. Soc. Chem. Commun. 580 (1983)

20. K. Beveridge, G. Bushnell, S. Stobart, J. Atwood, M. Zaworotko, Organometallics 2 1447 (1983)

21. G. Bushnell, S. Stobart, R. Vefghi, M. Zaworotko, J. Chem. Soc. Chem. Commun. 282 (1984)

22. J. Atwood, K. Beveridge, G. Bushnell, K. Dixon, D. Eadie, S. Stobart, M. Zaworotko, Inorg. Chem. 23 4050 (1984)

23. D. Carmona, L. Oro, M. P. Lamata, M. P. Puebla, J. Ruiz, P. M. Maitlis, J. Chem. Soc. Dalton Trans. 639 (1987)

24. F. Barcelo, P. Lahuerta, M. A. Ubeda, Organometallics 7 584 (1988)

25. L. Oro, D. Carmona, J. Reyes, C. Foces-Foces, F. Cano, J. Chem. Soc. Dalton Trans. 31 (1986)

26. C. Claver, P. Kalck, M. Ridmy, A. Thorez, L. Oro, M. T. Pinillos, M. C. Apreda, F. Cano, C. Foces-Foces, J. Chem. Soc. Dalton Trans. 1523 (1988)

27. G. Banditelli, A. L. Bandini, F. Bonati, G. Minghetti, J. Organomet. Chem. 218 229 (1981)

28. R. Uson, L. Oro, M. A. Ciriano, D. Carmona, A. Tirripicchio, M. Tirripicchio-Camellini, J. Organomet. Chem. 206 C14 (1981)

29. R. Uson, L. Oro, M. A. Ciriano, D. Carmona, A. Tirripicchio, M. Tirripicchio-Camellini, J. Organomet. Chem. 224 69 (1982)

30. P. Sullivan, D. Salmon, T. Meyer, J. Peedin, Inorg. Chem. 18 (12) 3369 (1979)

31. T. Ashworth, D. Liles, E. Singleton, J. Chem. Soc. Chem. Commun. 20 1317 (1984)

32. T. Ashworth, D. Liles, E. Singleton, Inorg. Chim. Acta. 98 L65 (1985)

33. J. Shapely, D. Samkoff, C. Bueno, M. Churchill, Inorg. Chem. 21 634 (1982)

34. J. A. Cabeza, C. Landazuri, L. Oro, D. Belletti, A. Tiripicchio, M. Tiripicchio-Camellini, J. Chem. Soc. Dalton Trans. 1093 (1989)

35. W. Deese, D. Johnson, J. Organomet. Chem. 232 325 (1982)

36. G. Minghetti, G. Banditelli, F. Bonati, J. Chem. Soc. Dalton Trans. 1851 (1979)

37. G. Bushnell, D. Kimberley-Fjeldsted, S. Stobart, M. Zaworotko, Organometallics 4 1107 (1985)

38. G. Bushnell, M. Decker, D. Eadie, S. Stobart, R. Vefghi, Organometallics 4 2106 (1985)

39. J. Caspar, H. Gray, J. Am. Chem. Soc. 106 3029 (1984)

40. D. Fjeldsted, S. Stobart, J. Chem. Soc. Chem. Commum. 908 (1985)

41. D. Fjeldsted, S. Stobart, M. Zaworotko, J. Am. Chem. Soc. 107 8258 (1985)

42. R. G. Pearson, J. Am. Chem. Soc. 85 3533 (1963)

43. S. Ahrland, Struct. Bonding 1 207 (1966)

44. J. Chatt, J. Inorg. Nucl. Chem. 8 515 (1958)

45. S. Pitzer, J. Chem. Phys. 23 1735 (1955)

46. J. Chatt, B. L. Shaw, A. E. Field, J. Chem. Soc. 3466 (1964)

47. B. R. James, L. D. Markham, B. C. Hui, G. L. Rempel, J. Chem. Soc. Dalton Trans. 2247 (1973)

48. F. A. Cotton, G. Wilkinson, "Advanced Inorganic Chemistry" 4th Edn. John Wiley and Sons

49. R. L. Carlin, "Transition Metal Chemistry" Vol. 4 Marcel Dekker Inc., New York

50. N. S. Gill, R. S. Nyholm, J. Chem. Soc. 3997 (1959)

51. "Open University Science - A Third Level Course" Summer School Experiment Notes (1986)

52. M. Guichelaar, J. A. M. Van Hest, J. Reedjik, Delft Prog. Report 2 51 (1976)

53. H. T. Witteveen, W. L. C. Rutten, J. Reedjik, J. Inorg. Nucl. Chem. 37 913 (1975)

54. D. Nicholls, B. A. Warburton, J. Inorg. Nucl. Chem. 32 3871 (1970)

55. A. Zecchina, L. Cerruti, S. Coluccia, E. Borello, J. Chem. Soc. B 1363 (1967)

56. D. E. C. Corbridge, J. Appl. Chem. 6 456 (1956)

57. C. W. Reimann, J. Phys. Chem. 74 (3) 561 (1970)

58. M. Goldstein, W. D. Unsworth, Spectrochimica Acta 28A 1297 (1972)

59. J. G. Vos, W. L. Groeneveld, Inorg. Chim. Acta 27 173 (1978)

60. J. G. Vos, W. L. Groeneveld, Inorg. Chim. Acta 24 123 (1977)

61. J. G. Vos, W. L. Groeneveld, Trans. Met. Chem. 4 137 (1979)

62. C. B. Singh, S. Satpathy, B. Sahoo, J. Inorg. Nucl. Chem. 35 3947 (1973)

63. R. W. Alder, P. S. Bowman, W. R. S. Steele, D. R. Winterman, Chem. Commun. 13 723 (1968)

64. J. Reedijk, Rec. Trav. Chim. 91 1373 (1972)

65. K. A. Jensen, Z. Anorg. Allg. Chem. 229 265 (1936)

66. "Transition Metal Complexes of Phosphorus Arsenic and Antimony Ligands" C. A. McCauliffe, Macmillan Press (1973)

67. G. Booth, J. Chatt, J. Chem. Soc. 3238 (1965)

68. C. A. Tolman, Chem. Rev. 77 313 (1977)

69. D. G. Holah, A. N. Highes, V. R. Magnusson, H. A. Mirza, K. O. Parker, Organometallics 7 1233 (1988)

70. P. R. Hoffman, K. G. Caulton, J. Am. Chem. Soc. 97 4221 (1975)

71. S. Cenini, A. Mantovani, A. Fusi, M. Keubler, Gazzetta Chimica Italiana 105 255 (1975)

72. S. Cenini, A. Fusi, G. Capparella, J. Inorg. Nucl. Chem. 33 3576 (1971)

73. P. W. Armit, A. S. F. Boyd, T. A. Stephenson, J. Chem. Soc. Dalton Trans. 1663 (1975)

74. M. T. Atlay, "The Catalysis of Homogeneous Co-oxidation" PhD Thesis Exeter University (1979)

75. Y. Ohkatsu, T. Okuyama, T. Osa, Yukagaku 27 142 (1978)

76. B. W. Graham, K. R. Laing, C. J. O'Connor, W. R. Roper, Chemical Communications 1272 (1970)

77. P. S. Hallman, B. R. McGarvey, G. Wilkinson, J. Chem. Soc. (A) 3143 (1968)

78. R. A. Schunn, E. R. Wonchoba, Inorg. Synth. 13 131 (1972)

79. P. S. Hallman, T. A. Stephenson, G. Wilkinson, Inorg. Synth. 12 237 (1970)

80. T. A. Stephenson, G. Wilkinson, J. Inorg. Nucl. Chem. 28 1945 (1966)

81. S. Cenini, A. Fusi, F. Porta, Gazz. Chim. Ital. 108 109 (1978)

82. J. F. Knifton, J. Mol. Catalysis 11 91 (1981)

83. J. F. Knifton, Chemtech 609 (Oct. 1981)

84. G. Braca, G. Sbrana, G. Valentini, G. Andrich, G. Gregorio, "Fundamental Research in Homogeneous Catalysis" Plenum Press New York 111 221 (1979)

85. G. Braca, G. Sbrana, G. Valentini, G. Andrich, G. Gregorio, J. Am. Chem. Soc. 100 6238 (1978)

86. C. M. Che, K. Wong, T. C. W. Mak, J. Chem. Soc. Chem. Commun. 546 (1985)

87. C. Ho, C. M. Che, T. C. Lau, J. Chem. Soc. Dalton Trans. 967 (1990)

88. T. R. Weaver, T. J. Meyer, S. Adjao Adeyemi, G. M. Brown, R. P. Eckberg, W. E. Hatfield, E. C. Johnson, E. W. Murray, D. Untereker, J. Am. Chem. Soc. 97 3039 (1975)

89. P. Doppelt, T. J. Meyer, Inorg. Chem. 26 2027 (1987)

90. J. E. Earley, T. Fealey, Inorg. Chem. 12 (2) 323 (1973)

91. J. D. Dunitz, L. E. Orgel, J. Chem. Soc. 2594 (1953)

92. J. A. Gilbert, D. S. Eggleston, W. R. Murphy, D. A. Geselowitz, S. W. Gersten, D. J. Hodgson, T. J. Meyer, J. Am. Chem. Soc. 107 3855 (1985)

93. D. J. Hewkin, W. P. Griffith, J. Chem. Soc. (A) 472 (1966)

94. D. Pavia, G. Lampman, G. Kritz, "Introduction to Spectroscopy" Saunders College Publishing (1979)

95. I. L. Finar, "Organic Chemistry" Longmans (1955)

96. J. D. Gilbert, G. Wilkinson, J. Chem. Soc. (A) 1749 (1969)

97. F. H. Jardine "Progress in Inorganic Chemistry" 31 265

98. J. Gilbert, M. C. Baird, G. Wilkinson, J. Chem. Soc. (A) 2198 (1968)

99. K. Shobatake, C. Postmus, J. R. Ferraro, K. Nakamoto, Appl. Spectroscopy 23 12 (1969)

100. B. E. Mann, C. Masters, B. L. Shaw, J. Chem. Soc. (A) 1104 (1971)

101. J. F. Nixon, A. Pidcock, "Annual Review Nmr Spectroscopy" (2) E. F. Mooney, Academic Press (1969)

102. J. R. Thornback, G. Wilkinson, J. Chem. Soc. Dalton Trans. 110 (1978)

103. B. N. Chaudret, D. J. Cole-Hamilton, R. S. Nohr, G. Wilkinson, J. Chem. Soc. Dalton Trans. 16 1546 (1977)

104. J. R. Saunders, J. Chem. Soc. Dalton Trans. 743 (1973)

105. R. K. Poddar, U. Argarwala, Indian Journal Chem. 9 477 (1971)

106. J. A. McGinnety, "Complexes of Nitrogen and Oxygen" MTP International Review of Science (Inorganic Chem. Series-One) Butterworths, London 5 229 (1972)

107. F. A. Cotton, R. D. Barnes, E. Bannister, J. Chem. Soc. 2199 (1960)

108. J. C. Sheldon, S. Y. Tyree, J. Am. Chem. Soc. 80 4775 (1958)

109. J. Mason "Multinuclear Nmr" Plenum Press New York and London 299 (1987)

110. J. E. Lyons, J. Chem. Soc. Chem. Commun. 418 (1975)

111. D. Forster, J. Chem. Soc. Chem. Commun. 917 (1975)

112. H. Nagashima, K. Mukai, Y. Shiota, K. Yamaguchi, K. Ara, T. Fukahori, H. Suzuki, M. Akita, Y. Moro-Oka, K. Itoh, Organometallics 9 799 (1990)

113. M. J. Frazer, W. Gerrard, J. K. Patel, J. Chem. Soc. 726 (1960)

114. F. P. Dwyer, H. A. Goodwin, E. C. Gyarfas, Aust. J. Chem. 16 544 (1963)

115. C. D. Ellis, J. A. Gilbert, R. W. Murphy Jr., T. J. Meyer, J. Am Chem. Soc. 105 4842 (1983)

116. T. J. Meyer, Electrochem. Soc. 7 221C (1984)

117. S. W. Gersten, G. J. Samuels, T. J. Meyer, J. Am. Chem. Soc. 104 4029 (1982)

118. B. A. Moyer, M. S. Thompson, T. J. Meyer, J. Am. Chem. Soc. 102 2310 (1980)

119. A. R. Sanger, J. Chem. Soc. Dalton Trans. 1971 (1977)

120. S. Cenini, A. Fusi, G. Capparella, Inorg. Nucl. Chem. Letters 8 127 (1972)

APPENDIX-REFERENCE SPECTRA

I

Infra-red Spectrum of Triphenylphosphine (KBr disc)

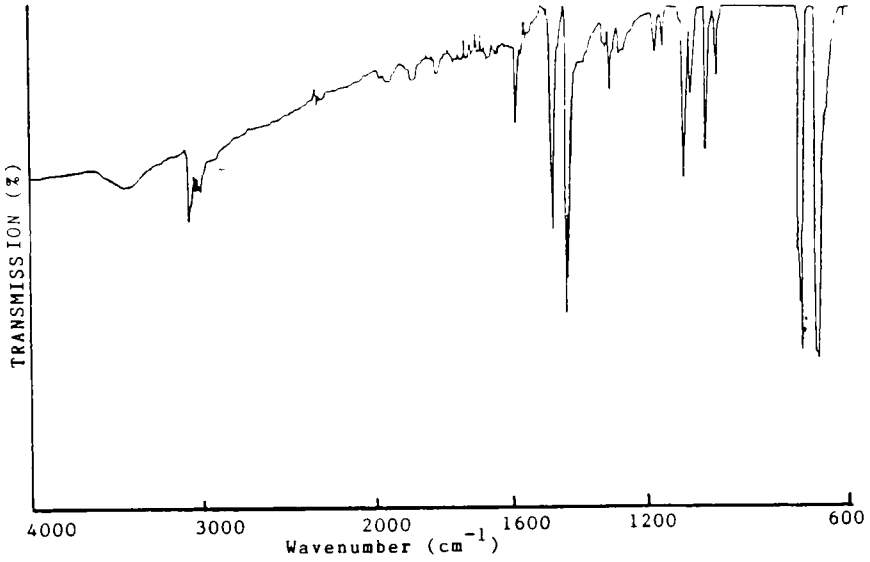

WAVENUMBER (cm^{-1})	INTENSITY	ASSIGNMENT
3060	w	aromatic C—H str.
1585	w	aromatic C=C str.
1480	m	aromatic C—C str.
1440	s	P—aryl str.
1310	w	
1090	m	
1070	w	
1025	m	
1000	w	
740	s	out of plane C—H deformation
690	s	out of plane C—H deformation

^{1}H nmr Triphenylphosphine in $CDCl_3$, 298K

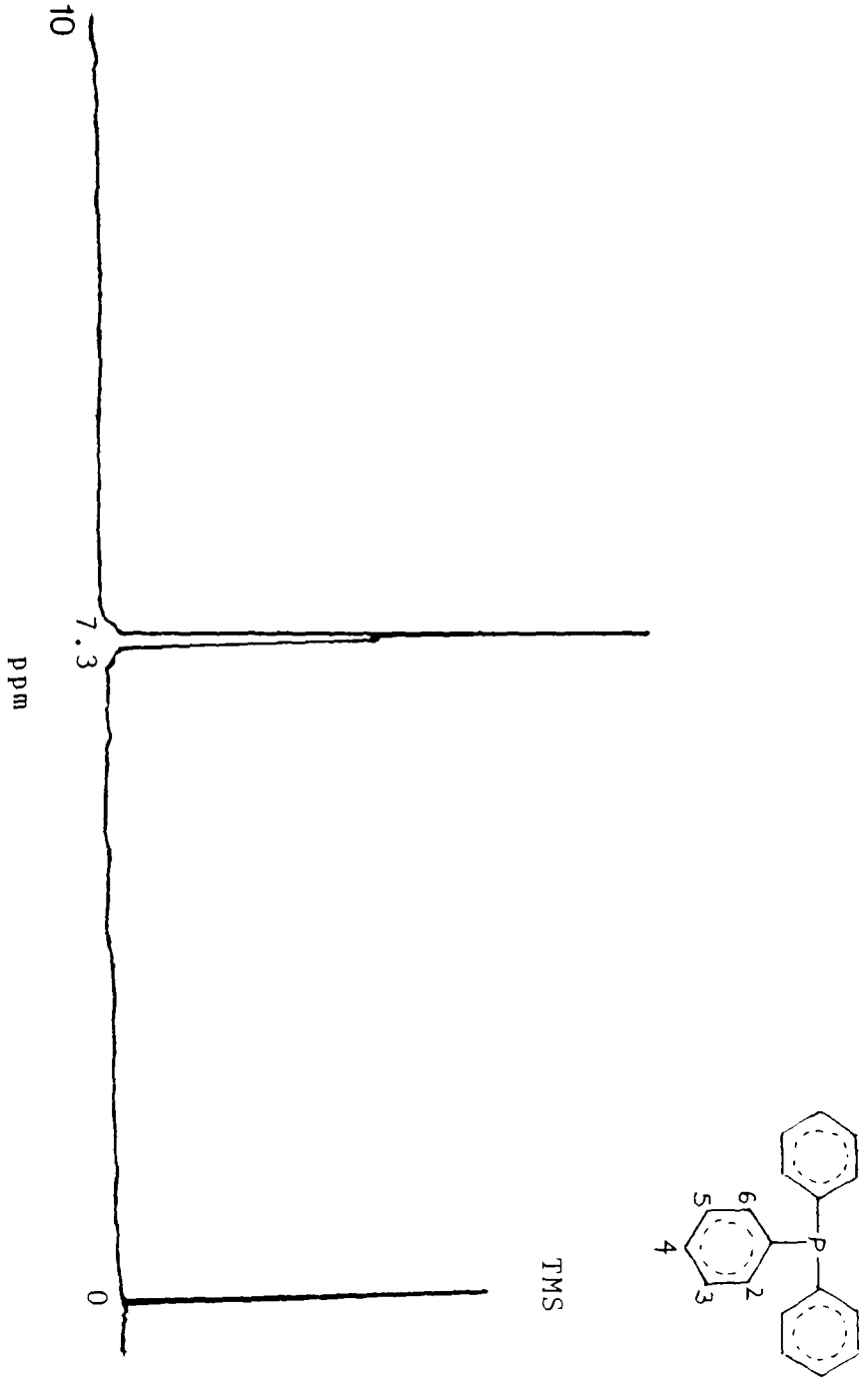

Infra-red Spectrum of Pyrazole (KBr disc)

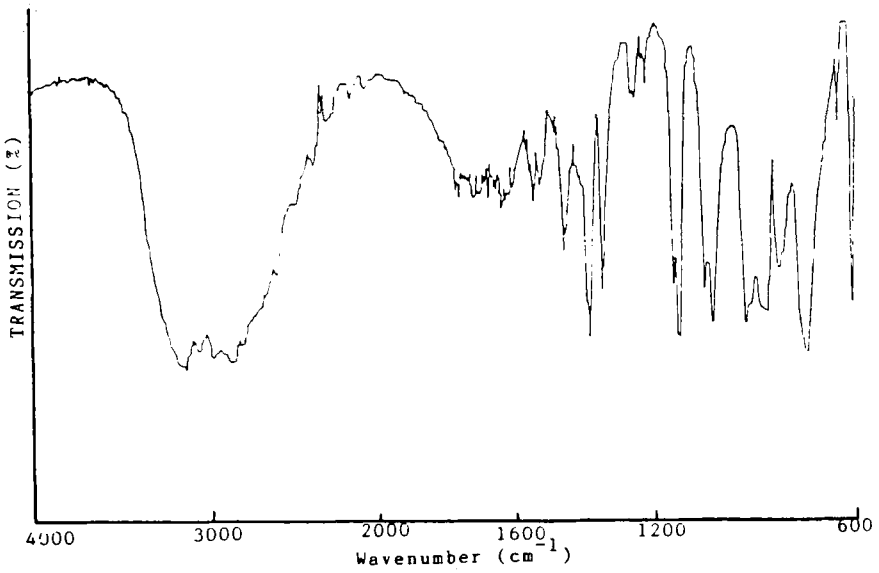

WAVENUMBER (cm^{-1})	INTENSITY	ASSIGNMENT
3500-2320	s(br.)	N—H str.
1460	m	ring str., in plane
1390	s	ring str., in plane
1350	m	ring str., in plane
1140	m	N—H bend, in plane
1130	s	N—H bend, in plane
1050	m	C—H bend, in plane
1020	s	C—H bend, in plane
925	s	ring bend, in plane
870	s	C—H bend, out of plane
825	m	C—H bend, out of plane
750	s	C—H bend, out of plane
640	w	
610	s	

^{1}H nmr Spectrum of Pyrazole in $CDCl_3$, 298K

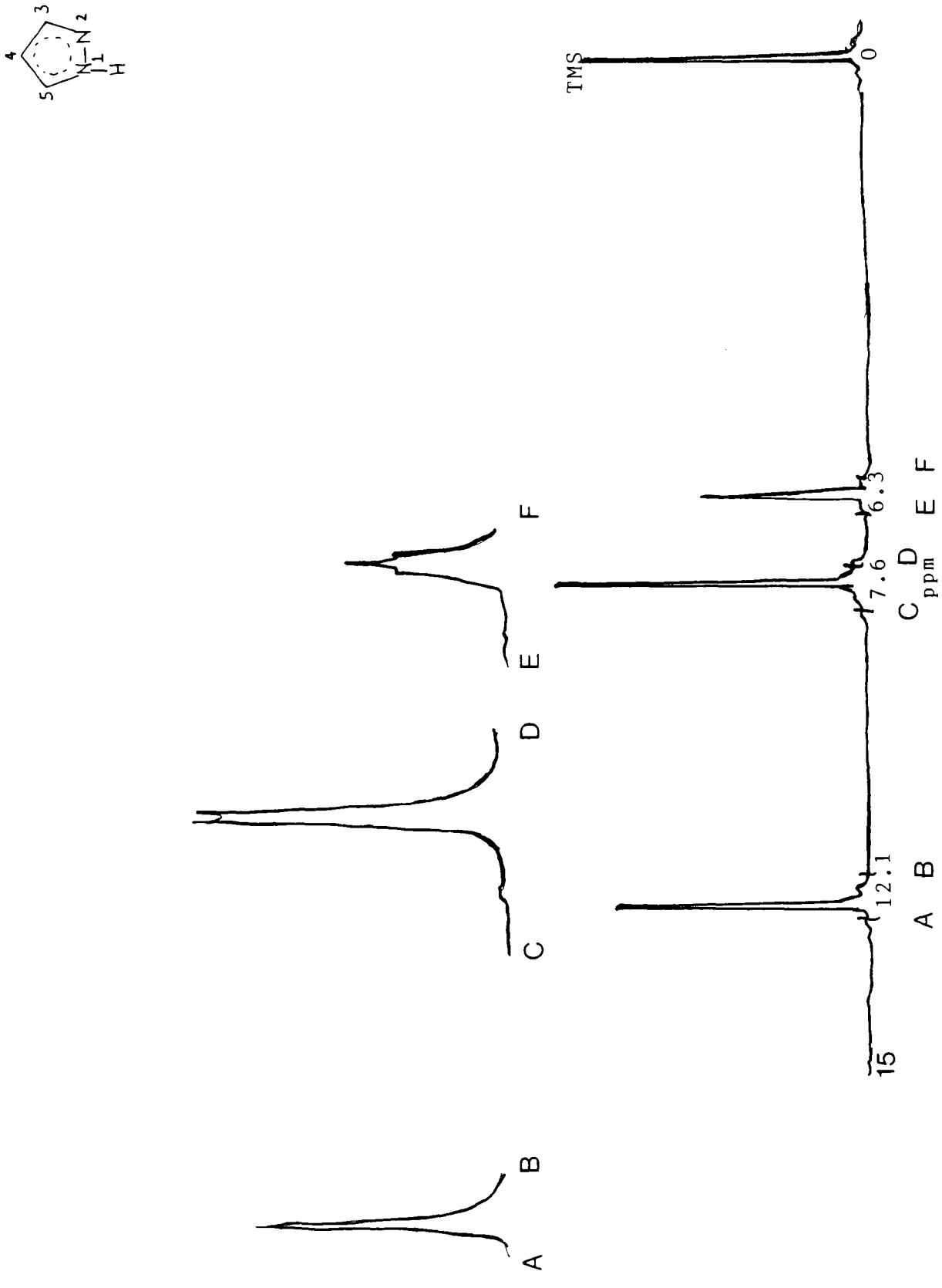

Infra-red Spectrum of 3,5-dimethylpyrazole (KBr disc)

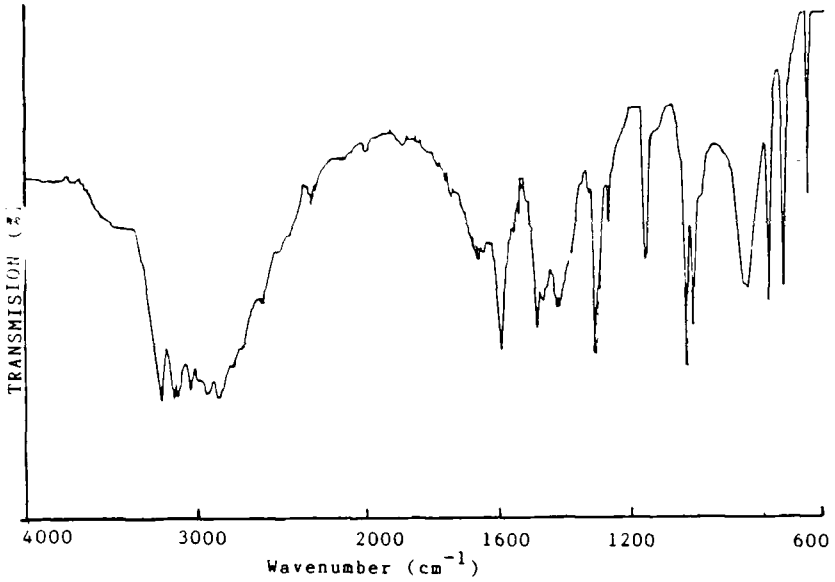

WAVENUMBER (cm^{-1})	INTENSITY	ASSIGNMENT[46]
3200	s	N—H str.
3125	s	C—H str., ring
3100	s	C—H str., ring
3030	s	
2950	s	C—H str., $-CH_3$
2860	s	C—H str., $-CH_3$
1600	m	ring str., in plane
1480	m	ring str., in plane
1460	m	C—H bend, in plane $-CH_3$
1420	m	C—H bend, in plane, $-CH_3$
1300	s	ring str.,in plane
1260	w	C—CH_3 str.
1150	m	N—H bend, in plane
1025	s	

VI

WAVENUMBER(cm^{-1})	INTENSITY	ASSIGNMENT
1010	m	C—H bend, in plane, ring
840	m(br.)	C—H bend, out of plane, ring
780	m	ring bend, in plane
740	m	ring bend, in plane
660	m	ring bend, out of plane

VII

^{1}H nmr Spectrum of 3,5-dimethylpyrazole in $CDCl_3$, 298K

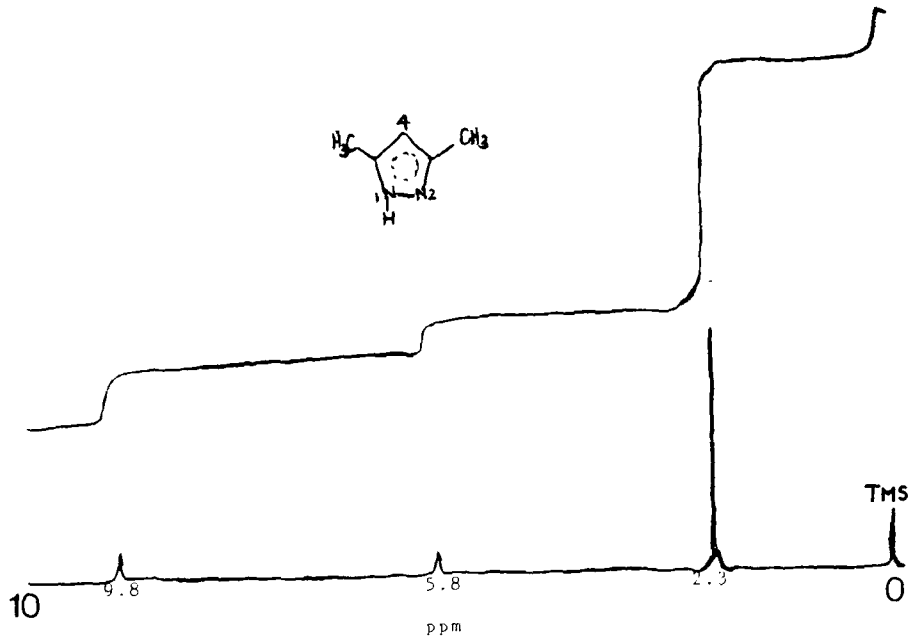

The singlet at 9.8δ represents the proton attached to nitrogen, deshielded because of the high electronegativity of nitrogen. The proton is upfield from the analogous proton in pyrazole, because of the effect of the electron-releasing methyl groups. The singlets at 5.8δ and 2.3δ are attributed to the ring proton at C4 and the methyl protons respectively. Integration gives 1 : 1 : 6 for N1 : C4 : Me protons.

^{31}P nmr Spectrum of Triphenylphosphine oxide in $CDCl_3$, 298K

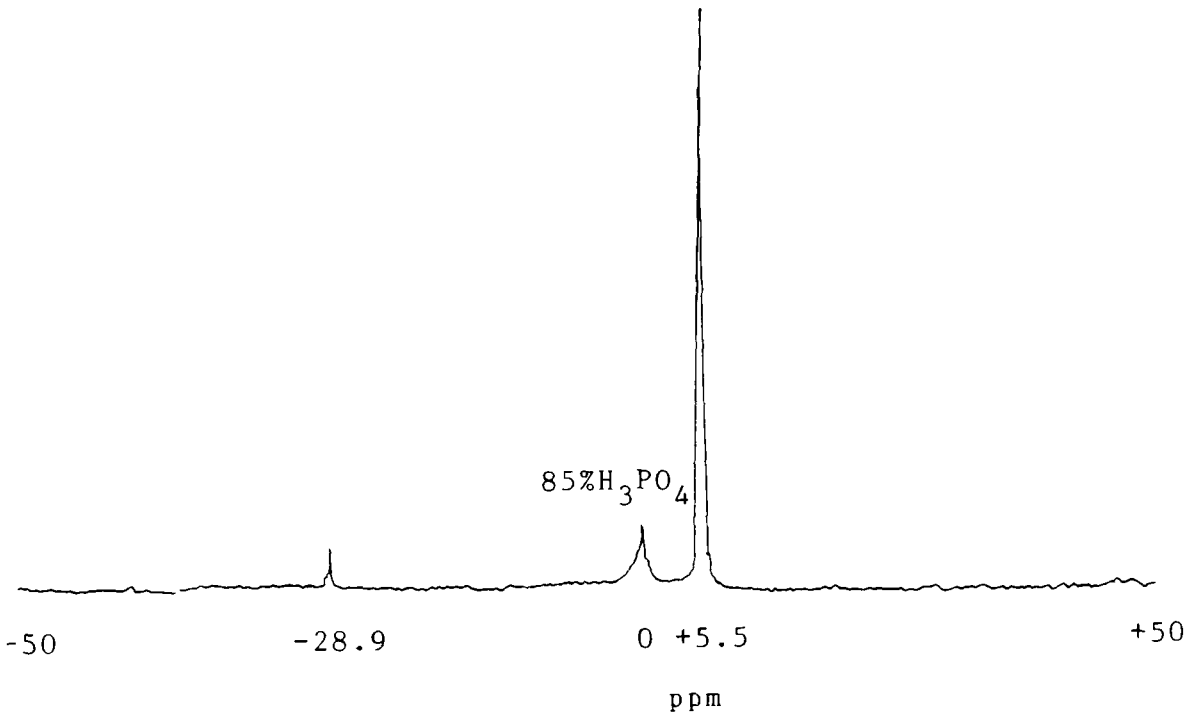

This was prepared by dissolving triphenylphosphine in toluene and leaving the mixture exposed to air for about a week. The mixture was concentrated and a precipitate obtained by adding petroleum ether (60/80). The precipitate was filtered off and dried in vacuo. The white mixture that resulted, was concluded to contain triphenylphosphine oxide, $O{=}PPh_3$, from the presence of a sharp band of medium intensity in its infra-red spectrum[78] (KBr disc). This band, attributed to $\nu(P{=}O)$, is not found in the spectrum of the pure phosphine. The ^{31}P nmr spectrum of the mixture above, gives a resonance at +5.5δ, attributed[77] to PPh_3, whilst the resonance at -28.9δ is taken as representing its oxide.

Infra-red Spectrum of 1,2-bis(diphenylphosphino)ethane [dppe] (KBr disc)

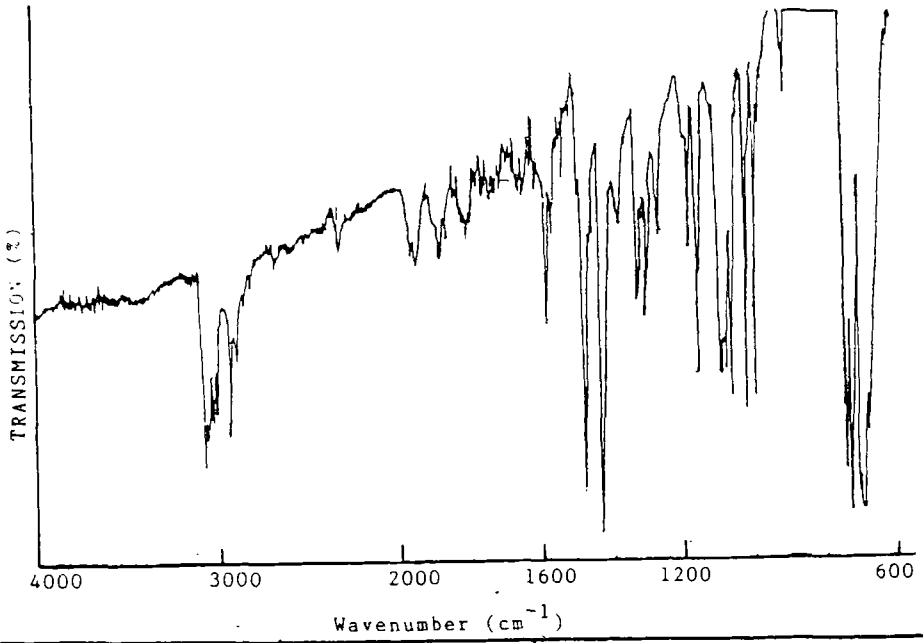

WAVENUMBER(cm^{-1})	INTENSITY	ASSIGNMENT
3060	m	aromatic C—H str.
2940	m	aliphatic C—H str.
1590	m	aromatic C=C str.
1480	s	aromatic C—C str.
1440	s	P—aryl str.[47]
1330	w	aliphatic C—H bend
1310	w	
1280	w	
1190	w	
1160	s	
1100	m	
1080	m	
1070	m	

WAVENUMBER(cm^{-1})	INTENSITY	ASSIGNMENT
1020	s	
1000	s	
750	m	
740	m	out of plane C—H deformation
730	s	
700	s	
680	s	out of plane C—H deformation

^{1}H nmr Spectrum of dppe in $CDCl_3$, 298K

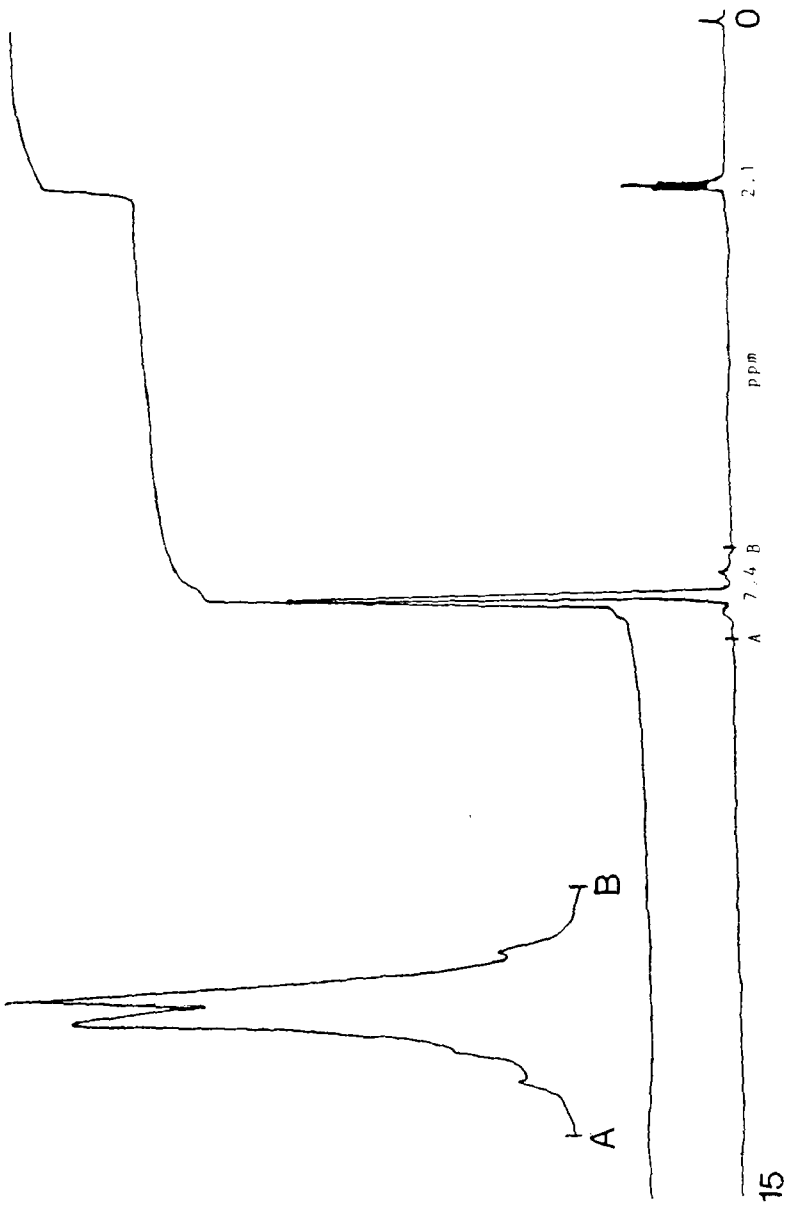

^{31}P nmr Spectrum of dppe in $CDCl_3$, 298K

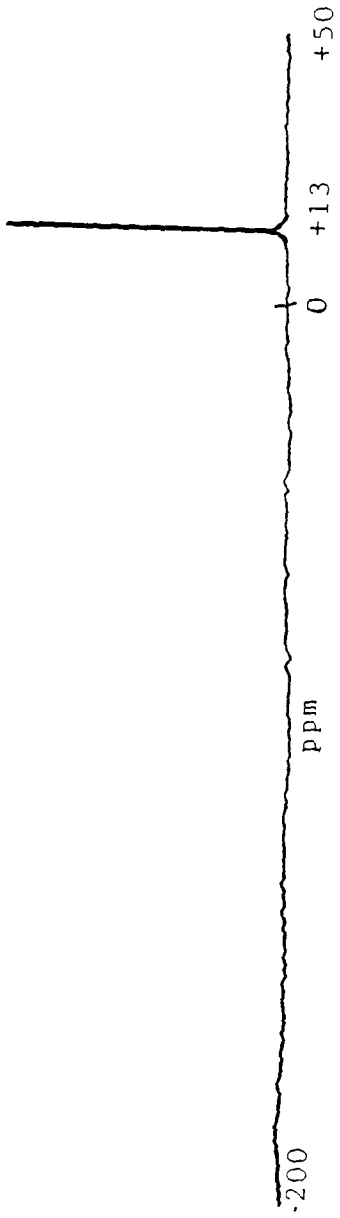

XIII

^{31}P nmr Spectrum of the Oxidation Product of dppe in $CDCl_3$, 298K

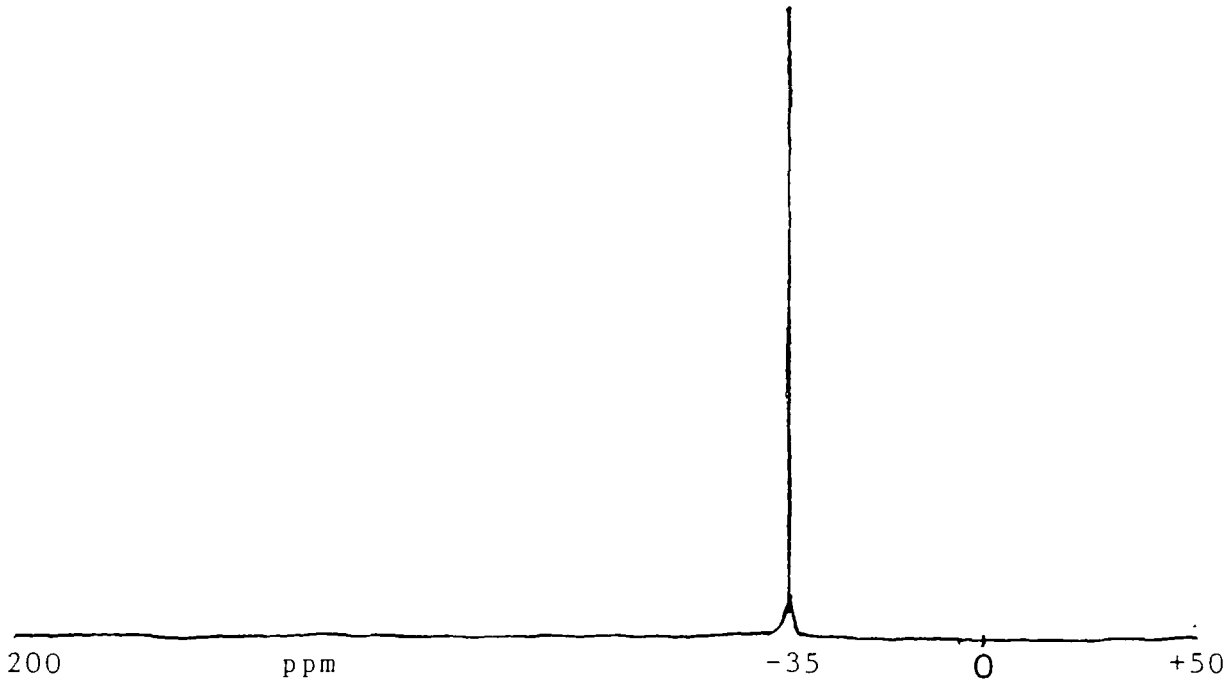

This was prepared by dissolving 1,2-bis(diphenylphosphino)ethane in ethanol, adding hydrogen peroxide (30 wt.%) and leaving the mixture exposed to air for a week. Colourless crystals of the product were obtained, which were washed with ethanol followed by diethyl ether, then dried in vacuo. Complete oxidation of the product to $O{=}PPh_2.C_2H_4.Ph_2P{=}O$ was assumed, because of the presence of just one signal in the above spectrum. Oxidation did not appear to occur when the phospine was treated as in VIII.

^{31}P nmr Spectrum of $[RuI_2(PPh_3)_2]_n$ in $CDCl_3$, 298K

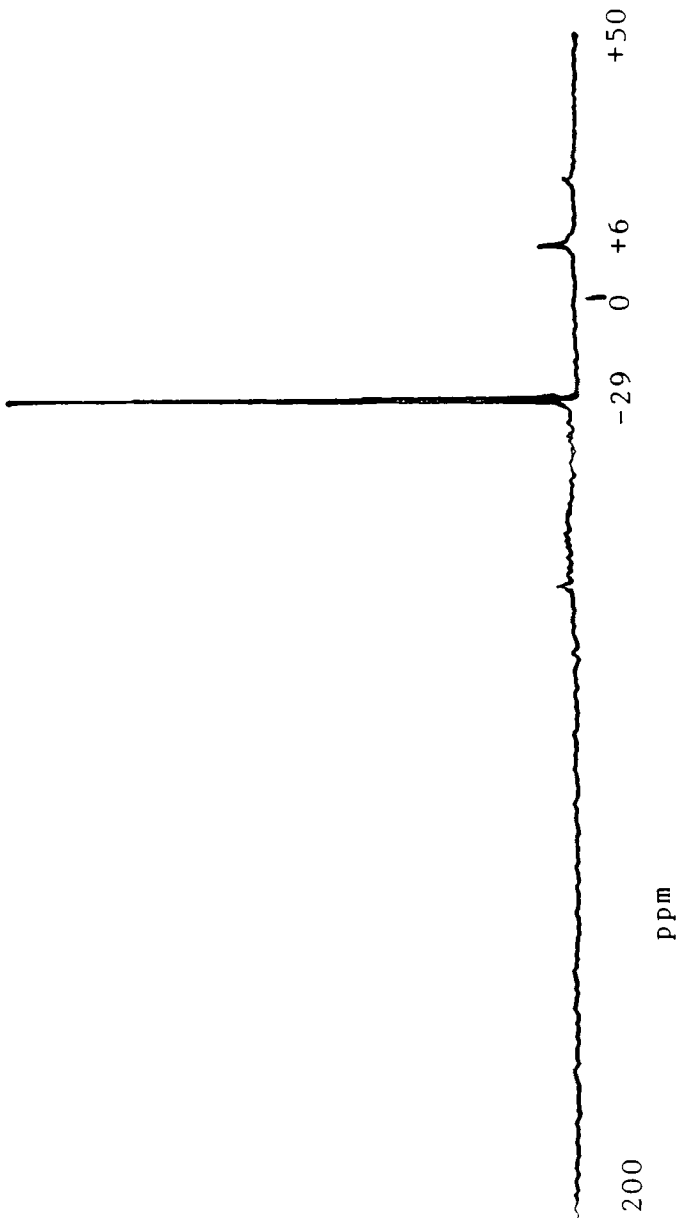

Infra-red Spectrum of Triphenylphosphine Oxide [O==PPh_3] (KBr disc)

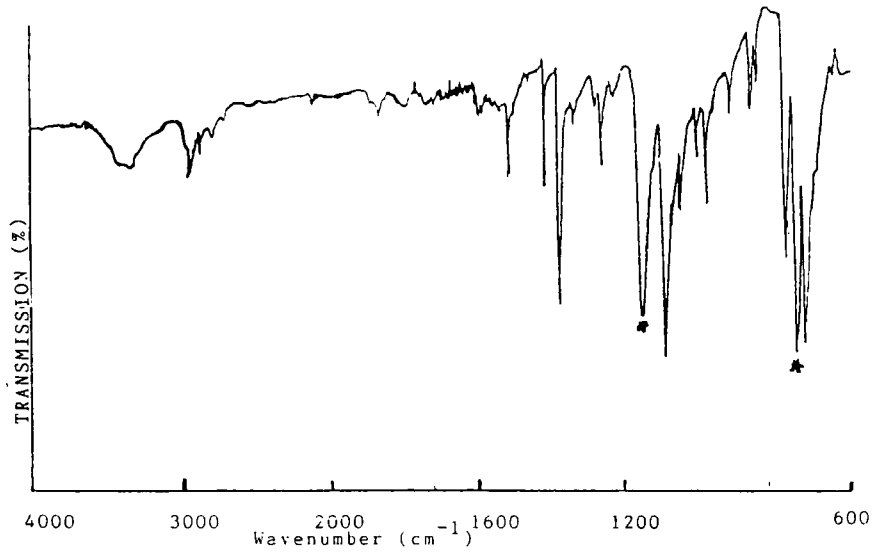

As for PPh_3, additional bands marked * (1195 cm^{-1}, 720 cm^{-1})